博士論文

# Prediction of strength development of surface layer concrete in structure
# （構造体コンクリート表層部の強度発現予測）

孫　博超

## Contents

# Chapter 1 Introduction

## 1.1 Background

The research on mechanical properties is always a common and fundamental problem in concrete research. Effective prediction of concrete compressive strength development has excellent significance for guiding construction progress, ensuring construction safety, and increasing construction efficiency. Many factors are affecting the growth of concrete compressive strength, including the choice of materials such as cement, mix proportion, curing temperature and humidity, etc [1-5]. The prediction of concrete compressive strength growth is also widely studied, especially the influence of curing conditions [6-9]. But so far, most of the research on the prediction of concrete strength growth focus on the influence of curing temperature, and the effect of curing humidity is often neglected. It is undeniable that relative humidity plays a vital role in the hydration of cement and the strength growth of concrete.

From the point of view of engineering, changes in the quality of concrete due to ambient conditions start from its surface immediately after the formwork removed. Whereby the quality of surface layer concrete, particularly strength and durability, is likely to be lower than that of the interior parts. Therefore, the concrete structures were considered of uniform quality both in the surface layer and inside. As if the quality declines, the concrete becomes uneven, and the quality of the surface layer of the concrete becomes extremely low. The surface quality of concrete is important to ensure the durability of concrete structures. The quality of concrete is regarded as important for the durability of concrete structures. On the other hand, inadequate curing will inevitably lead to a low degree of cement hydration, resulting in the formation of more pore structure. Harmful substances such as carbon dioxide and chlorides, can easily erode into the concrete and cause it to deteriorate.

As described by Japanese Architectural Standard Specification[10], the placement time of the formwork are based on different strength requirements according to different structural components and design standards. The formwork placement time for different types of cement at different temperatures as shown in Table 1.1. However, the removal of formwork is based on the strength measurement of the specimens that water curing or sealing curing in the on-site experimental field. In terms of the actual situation of structure, whether the on-site water curing or seal curing of the specimens cannot accurately reflect the development of the actual strength of the structure. This is because the volume of the specimen is small, and its internal temperature is critically affected by the ambient temperature. While the internal temperature of mass concrete is affected by the

hydration heat of cement, which is higher than the actual ambient temperature. On the other hand, different ratios of exposed surface area to depth will reflect different humidity development tendency when curing at humidity unsaturated condition. In addition, water curing cannot be realized in practical engineering, the concrete in actual structure is generally difficult to achieve a sufficient curing. Therefore, considering the safety of the structure and the accuracy of the evaluation, new method should be proposed to predict the strength development directly from the side of the structure and consider the both effect of temperature and relative humidity.

Recently, the method of evaluating the strength development of concrete structures has been applied by setting temperature sensors on formwork to monitor the temperature development of concrete. Through the smart sensor formwork, the concrete surface temperature history permits tracking, on site and in real time, of strength development of concrete. In these ways, the proposed smart sensor formwork system enables a new direction toward higher-level and more sophisticated quality control of concrete structures.

Table 1.1 Age of concrete to determine the location of foundation beams and columns(days)

| | High early strength Portland cement | Ordinary Portland cement<br>Blast furnace cement (Class A)<br>Silica cement(Class A)<br>Fly ash cement(Class A) | Blast furnace cement (Class B)<br>Silica cement(Class B)<br>Fly ash cement(Class B) |
|---|---|---|---|
| T＞20℃ | 2 | 4 | 5 |
| 10℃＜T＜20℃ | 3 | 6 | 8 |

In addition, while the concrete is exposed to air after formwork removal, the evaporation of moisture from the surface of concrete will take away a large amount of internal moisture, resulting in the reduction of internal humidity, which also has a great impact on the strength of concrete. In particular, the relative humidity in the surface layer of concrete is much lower than the internal relative humidity, so the surface layer shows lower strength than that of the deeper layer of concrete. There are many researches on the diffusion and distribution of relative humidity in concrete [11-13]. However, little research is related to the relationship between internal relative humidity and strength to consider the strength development at different depths.

The quality of the cover concrete is very important to the durability of constructions. After pouring, the sides and bottom of the slab of concrete are covered with the formwork and the top surface is covered with a plastic sheet, see as Figure 1.1. In the outdoor concrete environment, due to the sunshine and wind will accelerate the moisture evaporation from the top surface of concrete, the temperature and relative humidity will change accordingly. Therefore, $(T_1, RH_1)$ in Figure 1.1

are varying with time developing. At the bottom, the temperature $T_2$ will change correspondingly due to the heat released by the hydration of cement. While the humidity is always about 100% because there is no loss of moisture, the hydration of cement consumes only a small amount of water. Obviously, the mechanical properties and durability of surface concrete are lower than the bottom.

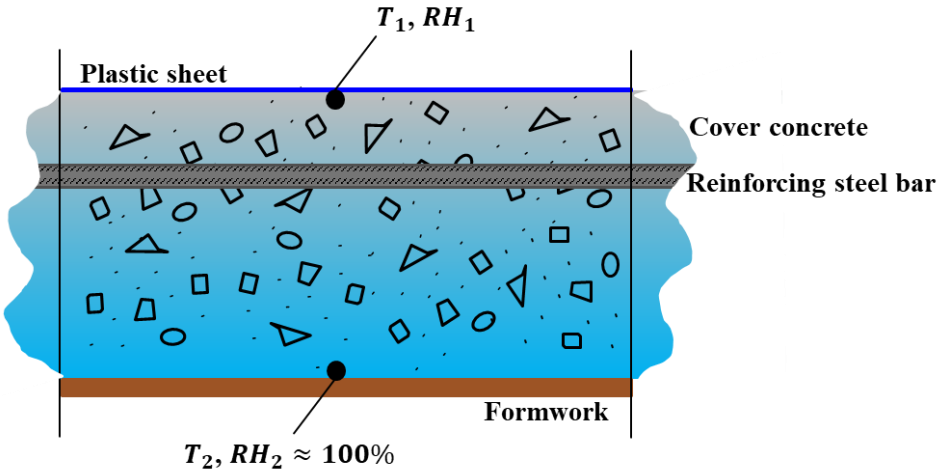


Figure 1.1 Diagram of cast-in-place concrete

On the other hand, the decrease in the moisture content of the surface concrete reducing the hydration rate of the cement. Result to higher porosity and pore diameter are generated in surface layer concrete. In the long term, the cracks caused by drying and steel corrosion will occur gradually. Also, the strength of surface concrete can be used as an essential index to evaluate the durability because high strength inevitably exists high concrete density.

In order to obtain the rule of strength development under the influence of different temperature and relative humidity, it is an appropriate method through calculating the development of equivalent age which allowed to calculate the strength development at a varying temperature and relative humidity curing condition. The equivalent age in this study that corresponds to time would present the degree of reaction (or strength) with different actual temperature and relative humidity conditions relative to the reference temperature($T_r = 20$ °C) and reference relative humidity ($RH_r = 100\%$). As a representation of the concept of concrete maturity, the equivalent age can be shown more intuitively in time. By comparing to the standard curing, the equivalent age under different curing condition can be calculated, and the mold removal time of building concrete under corresponding conditions can be determined based on table 1.1.

In conclusion, concern about the quality of surface concrete, both temperature and relative

humidity have an important impact. How to propose a reasonable and effective method to accurately evaluate the strength growth within the consideration of temperature/relative humidity effect should be a problem need to be solved.

### 1.2 Objective

The objective of this research is to propose a novel method to predict the strength development of the surface layer concrete considering the influence of both temperature and relative humidity.

Firstly, on the basis of the existing prediction model, propose a modified model of the combined influence of temperature and relative humidity through experimental results and theoretical analysis. This part will conduct with the equivalent age function of maturity method and put forward a new relative humidity modified equivalent age function to predict the strength development under the influence of different relative humidity conditions. The significance of the study of this part is to fully consider the impact of various curing factors during the cement reaction process, such as temperature and relative humidity, to achieve a more accurate prediction of the equivalent age development each condition. Then utilize the modified equivalent age function into a strength prediction model to obtain the strength development of each condition.

Secondly, to predict the strength development of surface layer concrete by considering temperature and relative humidity, the development tendency of relative humidity with time of surface layer concrete is necessary to know. Therefore, the internal relative humidity change of surface layer concrete is predicted through the theory of relative humidity diffusion. Then the purpose of evaluating the strength development of surface layer concrete can be achieved by combining with the modified strength prediction model.

This study is obviously of great significance for accurately evaluating the development of concrete strength, guiding the appropriate demolding time in practical construction, and improving production efficiency and safety. However, in addition to the above purposes, the application of the model needs to be satisfied

(1) The proposal of the temperature and relative humidity influenced equivalent age function should be on the basis of science and engineering.
(2) The proposed method should be within a reasonable and accurate prediction range to ensure the safety of engineering applications.
(3) The application of the proposed model should have a certain guiding effect on the actual

construction engineering.

### 1.3 Composition

According to the above research purposes, the specific composition of each chapter of this thesis will be studied in the following details.

Chapter 1 introduces the research background, objectives and the composition of this thesis.

Chapter 2 introduces and summarizes the current research development based on each research aspects concerning the study of this thesis. The literature review mainly includes

- The hydration reaction of the main components of cement and the influence of curing conditions of temperature and relative humidity on the degree of hydration of cement.
- The development and current research of maturity method. Primarily focus on the modification of different temperature and relative humidity.
- The introduction of the widely used strength prediction model.
- Theory of the moisture diffusion in concrete.

Chapter 3, based on the experimental results of the hydration degree of cement powder of different relative humidity and temperature, an equivalent age function at different temperature and relative humidity is derived according to the relation between hydration degree and hydration rate. The proposed function is then validated by comparing the results of other studies.

Chapter4 made the different size cement mortar specimens curing at different temperatures and relative humidity conditions. Then simulated the humidity distribution of the cross-section and predict the strength distribution of each position of the cross-section. Then the prediction strength of the proposed model and experimental strength are verified.

Chapter 5 introduced the variation of internal humidity caused by moisture diffusion and simulated the internal humidity development of concrete in three groups of artificial curing environments. According to the simulated results of humidity diffusion at different depths and the relative humidity modified strength prediction model proposed in chapter 4, the strength development at different depths is predicted. Based on the experimental results of outdoor curing, the strength of concrete under the condition of variable temperature and humidity is predicted, and the strength development at different depths is also predicted.

Chapter 6 summarized the conclusion of each chapter of the thesis and put forward the prospect of future research.

A schematic diagram of each chapter of the thesis is shown in Figure 1.2.

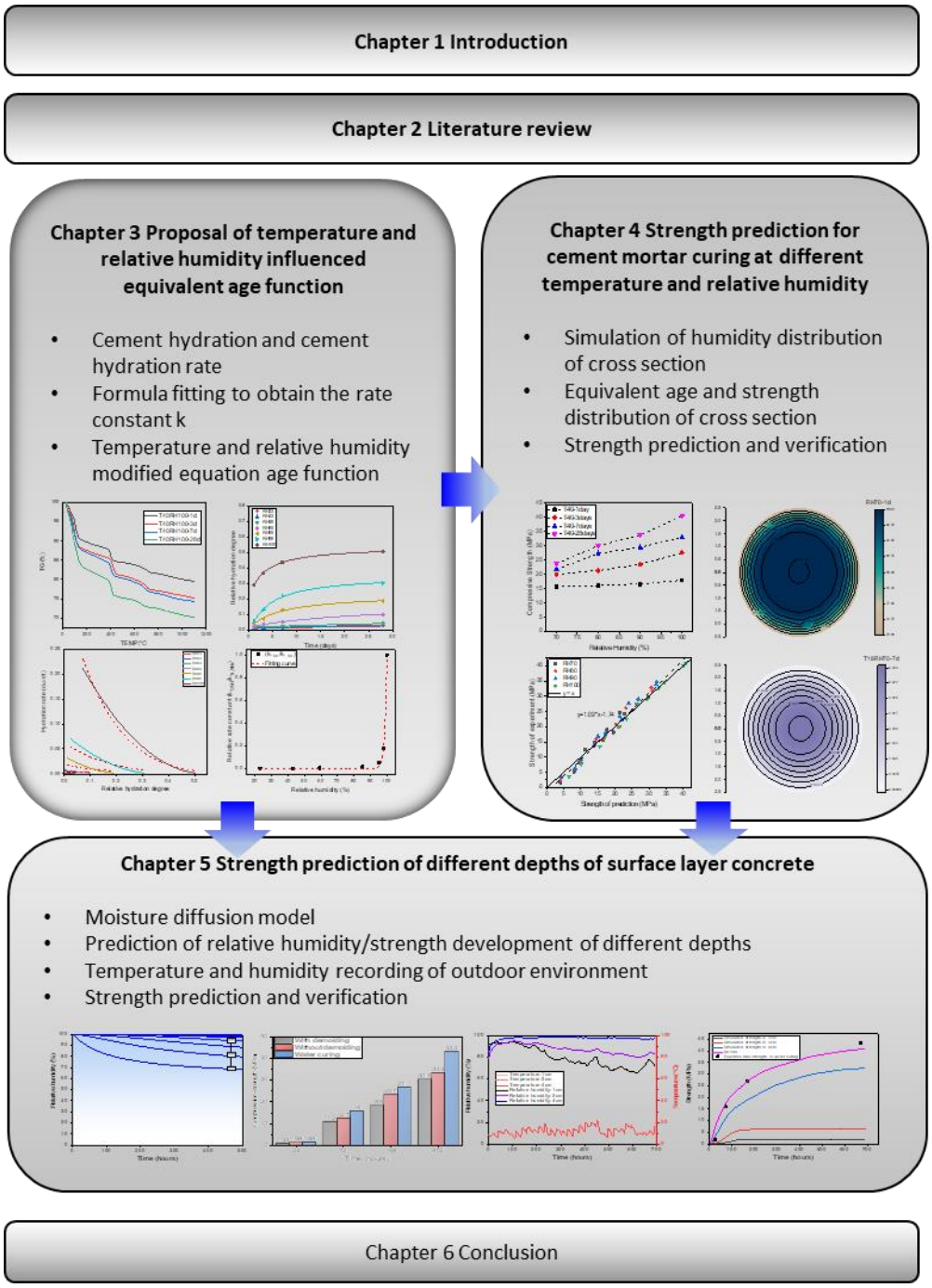


Figure 1.2 Structure of the thesis

## Reference

[1] M. Mazloom, A.A. Ramezanianpour, J.J. Brooks, Effect of silica fume on mechanical properties of high-strength concrete, Cement and Concrete Composites, 26 (2004) 347-357.

[2] S. Tsivilis, G. Parissakis, A mathematical model for the prediction of cement strength, Cement and Concrete Research, 25 (1995) 9-14.

[3] C.S. Poon, Z.H. Shui, L. Lam, H. Fok, S.C. Kou, Influence of moisture states of natural and recycled aggregates on the slump and compressive strength of concrete, Cement and Concrete Research, 34 (2004) 31-36.

[4] A. Oner, S. Akyuz, An experimental study on optimum usage of GGBS for the compressive strength of concrete, Cement and Concrete Composites, 29(6) (2007), 505-514.

[5] A. Oner, S. Akyuz, R. Yildiz, An experimental study on strength development of concrete containing fly ash and optimum usage of fly ash in concrete, Cement and Concrete Research, 35(6) (2005) 1165-1171.

[6] G. A. Khoury, Compressive strength of concrete at high temperatures: a reassessment, Magazine of Concrete Research, 44 (1992) 291-309.

[7] R. Sarshar*, G. A. Khoury, Material and environmental factors influencing the compressive strength of unsealed cement paste and concrete at high temperatures, Magazine of Concrete Research, 45 (1993) 51-61.

[8] S.J. Barnett, M.N. Soutsos, S.G. Millard, J.H. Bungey, Strength development of mortars containing ground granulated blast-furnace slag: Effect of curing temperature and determination of apparent activation energies, Cement and Concrete Research, 36 (2006) 434-440.

[9] J.-K Kim, Y.-H Moon, S.-H Eo, Compressive strength development of concrete with different curing time and temperature, Cement and Concrete Research, 28 (1998) 1761-1773.

[10] 建築工事標準仕様書同解説 JASS 5 鉄筋コンクリート工事, pp. 312

[11] Kenji Sakata, A study on moisture diffusion in drying and drying shrinkage of concrete, Cement and Concrete Research, 13(2) (1983) 216-224.

[12] Yunping Xi, Zdeněk P. Bažant, Larissa Molina, Hamlin M. Jennings, Moisture diffusion in cementitious materials Moisture capacity and diffusivity, Advanced Cement Based Materials, 1(6) (1994) 258-266.

[13] Narayanan Neithalath, Analysis of Moisture Transport in Mortars and Concrete Using Sorption-Diffusion Approach, ACI Materials Journal; 103(3) (2006) 209-217.

# Chapter 2 Literature Review

## 2.1 Cement hydration

Hydration of Portland cement is a very complicated and heterogeneous chemical reaction process[1,2]. From the beginning of water mixing, the hydration reaction of cement will be carried out almost all the time if the curing condition is allowed. The microstructure of cement-based materials will gradually evolve with the hydration reaction of cement. The state of water mixed cement gradually changes from the flow state to the plastic state, and finally to the setting and hardening state.

The hydration process of cement can be summarized as the main clinker material composition(content$\geqslant$95%) alite($C_3S$), belite($C_2S$), tricalcium aluminate($C_3A$) and tetra-calcium aluminoferrite($C_4AF$) have complex hydration reactions, and the main hydration products of calcium silicate hydrate(C-S-H), calcium hydroxide(CH), AFt and AFm, are generated. However, such reaction kinetics is influenced by many factors, such as the mixing method [3,4], the curing temperature "T" [5–11] and the curing relative humidity "RH" [12–18].

Temperature effect on the microstructure porosity and hydration degree in cement pastes are widely reported [19,20]. Several studies have been conducted to illuminate the combined effect of curing age and temperature on mechanical properties involved during cement hydration. Kjellsen et al. [21] studied the microstructure of cement pastes hydrated at temperatures ranging from 5 to 50 °C; a uniform distribution of hydration product for cement can be found when it subjected to low temperatures, against non-uniform hydration products for cement cured at high temperatures. Martínez-Ramírez and Frías [22] showed that the curing temperature plays a fundamental role in the evolution of cement hydration, such that after nine days at 60°C, the same degree of hydration at 90 days and 20°C is obtained. The temperature rise has an adverse effect on the inner and outer microstructure of hydration product particularly in the case of calcium silicate hydrate(C-S-H). Regourd and Gautier [23] reported that the outer C-S-H formed at 80°C was much more fibrous, exhibiting morphology reminiscent of pastes hydrated with calcium chloride accelerators. A comparison of the size of C-S-H particles obtained at 20 and 80°C showed that the size of C-S-H particles in the high-temperature system was about half the size of the particles forming at lower temperatures [24]. Most researchers have shown that exposure to high temperatures at an early age, led to a considerable drop in the long-term strength and an increase of the number of the pores in the cementitious matrix [19,20,25].

In the early stage, after cement mixed with water, cement will continue to hydrate due to sufficient water in the pores. However, due to the evaporation of water from the surface in a drying

environment, a humidity gradient is generated inside the concrete. A number of previous studies have attempted to quantify the effect of environmental relative humidity on Portland cement paste hydration [12-18]. From the report by Powers [12], the rate of hydration declines at reduced relative humidity, and the hydration of cement virtually cased when the relative water vapor pressure in the capillaries drops below about 80%RH. Further studies were conducted based on the compound of cement [13,14], which found that the reactions of alite, belite, and tricalcium aluminate stop hydrating at the relative humidity level of 85%, 90%, and 60%. Another study[15] pointed out that the self-desiccation of cement could not reduce the internal humidity below 80%RH, and belite is the most sensitive to reduced relative humidity. In recent years, few studies focus on the relative humidity effect on the degree of cement hydration. R.J. Flatt [17] gave out the explanation of why alite stops hydrating below 80% relative humidity. M. Wyrzykowski [18] proposed a coefficient describing the reduction of hydration rate as a function of RH for different W/B ratio and different cements.

To link the mechanical properties to the microstructure, the most appropriate method is by Powers' 'gel–space ratio'[26,27], which links compressive strength to the degree of cement hydration and the W/C ratio. The development of mechanical properties of hardening cementitious materials could be quantified by the degree of hydration, shown as Eq. (2.1).

$$f_c = A \cdot X^n \tag{2.1}$$

Where,

$f_c$ is the compressive strength of hardening concrete;

*A* and *n* are the fitting constant,

*X* is the gel/space ration of Portland cement which can be calculated as

$$X = \frac{v(T)(1/\rho)\alpha}{(1/\rho)\alpha + W/C} \tag{2.2}$$

Where,

$v(T)$ is the ration between volume fraction of hydrates over the volume fraction of dissolved cement;

$\rho$ is the density of cement;

$\alpha$ is the hydration degree of cement.

W/C is the inverse of the cement-water ratio.

Gel/space ratio is defined as the ratio of the volumes of the hydrated cement to the sum of the volumes of the hydrated cement and the capillary pore.

## 2.2 Maturity method

The prediction of compressive strength of concrete gain by considering the combined effects of temperature and aging is the most commonly utilized, which is well known as the maturity method [28-30]. This was established on the basis of a well-known principle of maturity concept proposed by Saul [30]. Within this concept, Saul proposed a maturity rule as: "*Concrete of the same mix at the same maturity has approximately the same strength whatever combination of temperature and time go to make up that maturity*". Saul also suggested a linear function to describe the maturity of concrete by considering the relationship with time and temperature, which is shown as Eq. (2.3).

$$M = \sum_{0}^{t} (T - T_0)\Delta t \tag{2.3}$$

Where,

$M$ is the maturity index in °C-hours (or °C-days);

T is the average concrete temperature during the time interval $\Delta t$, (°C);

$T_0$ is the datum temperature (generally taken to be -10°C);

t is the curing time, and $\Delta t$ is the time interval (hours or days).

Based on Arrhenius function, Hansen and Pedersen [31] proposed a new maturity function to evaluate the effect of temperature on strength development of concrete based on the Arrhenius function [32]. Through the function, the actual age of concrete at different temperatures was converted into an equivalent age of the concrete under a reference temperature of 20 ºC.

$$t_e = \sum_{0}^{t} e^{-\frac{E}{R}(\frac{1}{T}-\frac{1}{T_r})} \Delta t \tag{2.4}$$

Where,

$t_e$ is the equivalent age at the reference temperature;

E is the apparent activation energy in J/mol;

$R$ is the universal gas constant, 8.314 $J/mol \cdot K$;

$T$ is the average absolute temperature of concrete during interval $\Delta t$ in Kelvin; $T_r$ is the absolute reference temperature in Kelvin.

This equivalent age function overcame the limitation of Saul's equation because it allowed for a non-linear relationship between the initial rate of strength development and curing temperature. As a representation of the concept of concrete maturity, the equivalent age can be shown more intuitively in the form of time. It also made it possible to calculate the equivalent age through the actual age of concrete, in terms of strength development [33].

A series of studies on the maturity of concrete have been conducted, among which an exponential rate constant function suggested by Tank and Carino [33,34], shows as Eq. (2.5), is usually used.

$$k = A_0 e^{BT} \tag{2.5}$$

Where,

A is the value of rate constant at 0 °C;

B is the temperature sensitivity factor, 1/°C;

T is the temperature of concrete.

Based on the exponential rate constant function of Eq. (2.5), the original equivalent age function Eq. (2.4) can be instead by a new form as

$$t_e = \sum_0^t e^{B(T-T_r)} \Delta t \tag{2.6}$$

Where,

$T$ is the average absolute temperature of concrete during interval $\Delta t$ in Kelvin $T_r$ is the absolute reference temperature in Kelvin.

This equivalent age function is also widely used. To date, most of the assessment methods of strength development of cementitious materials are based upon an independent influence factor of temperature [31,34-38], while the effect of relative humidity (RH) is usually neglected.

Moreover, almost all proposed maturity methods have been devised through assuming concrete/mortar under a standard curing condition with 100%RH (in water), which is much higher than the practical curing RH of most of site-cast concretes. Therefore, the methods only considering curing temperature generally overestimate the strength development of concrete/mortar. It is indispensable to consider the influence of RH on maturity function of concrete/mortar.

In recent years, several maturity models have been proposed for predicting mechanical properties of concrete considering the effect of RH [39,40]. Liao *et al.* [39] proposed a humidity-adjusted maturity function by considering the multi-scale effect of curing temperature and ambient RH, in which a humidity factor was incorporated to describe the temperature dependence based on the exponential rate constant model proposed in reference [33, 34], to evaluate the compressive strength development of early-age concrete. On the other hand, moisture content variation inside concrete during curing is mainly caused by the moisture evaporation on the concrete surface and by a self-desiccation due to the cement hydration of concrete [41]. In most cases of site-cast concrete construction, concrete structures are usually directly exposed to the air after removing their

formwork. This results in a rapid decrease in the moisture content at the superficial layer of concrete, which affects the cement hydration and mechanical properties of this layer, as well as affects the moisture content of the internal concrete layer. According to the literature [42,43], the moisture content inside concrete is also influenced by other factors such as water/cement ratio, environmental temperature and RH, indicating that it should present a distribution at different depths from the concrete surface.

**2.3 Strength prediction model**

Different concrete strength prediction models are utilized by different regions and academic organizations in the world. Mostly, the concrete strength prediction models are function related to compressive strength and time. The 28-day strength is generally used as a primary factor in each model because of the concrete is commonly designed based on the 28-day strength. Among the various strength prediction code, the most used is the fib Model Code for Concrete Structures 2010 (fib MC 2010)[44] and ACI committee 209 (ACI model)[45].

***(1) fib MC 2010***

As described by fib MC 2010 [44], the relevant compressive strength of concrete at various ages $f_{cm}(t)$ could be estimated from:

$$f_{cm}(t) = \beta_{cc}(t) \cdot f_{cm28} \tag{2.7}$$

with:

$$\beta_{cc}(t) = \exp\left\{s \cdot \left[1 - \left(\frac{28}{t_e}\right)^{0.5}\right]\right\} \tag{2.8}$$

where,

$f_{cm}(t)$ is the mean compressive strength in MPa at the age of $t$ days;

$f_{cm28}$ is the mean tested compressive strength of concrete at the age of 28 days; $s$ is a coefficient depending on the strength class of cement.

Coefficient s is given by ranging from 0.20 to 0.38 [44]. As per the Ministry of Land, Infrastructure, Transport and Tourism of Japan [46], the factor $s$ is taken as 0.31 when ordinary Portland cement (OPC) is used as the cementitious material of concrete/mortar.

***(2) ACI model***

ACI model [45] suggested the following model to evaluate the compressive strength evolution of concrete as curing time.

$$f_{cm}(t) = \left[\frac{t}{a + bt}\right] \cdot f_{cm} \tag{2.9}$$

where,

$f_{cm}$ is the mean tested compressive strength of concrete at the age of 28 days;

$a$ and $b$ are coefficients dependent on the type of cement and curing condition of concrete, which were suggested ranging from 0.05 to 9.25 and 0.67 to 0.98 in the code [45], respectively. In this study, the coefficients $a$ and $b$ are taken as 4.0 and 0.85 for OPC concrete, respectively.

**2.4 Moisture diffusion in concrete**

Gases, liquids and dissolved substances are transported due to a constant concentration gradient according to Fick's first law of diffusion, as given in Eq. (2.10):

$$\mathrm{Q} = \mathrm{D}\frac{c_1 - c_2}{l} A \cdot t \tag{2.10}$$

Where,

Q is the amount of substance transported in g;

$c_1 - c_2$ is the difference in concentration in g/m$^3$;

l is the length of the penetrated concrete in m;

A is the penetrated area in m$^2$;

t is the time in s;

D is the diffusion coefficient in m$^2$/s.

In most cases, transient diffusion phenomena occur, that is, the amount of substance diffusing varies with location x and time t. In this case, Fick's second law of diffusion is valid, which describes the change in concentration for an element with time according to Eq. (2.11) considering one-dimensional flow and the diffusion coefficient D to be a constant:

$$\frac{\partial c}{\partial t} = D\frac{\partial^2 c}{\partial x^2} \tag{2.11}$$

Where,

$c$ is the concentration.

Bazant [47] took the relative humidity of concrete as the essential variable and used the diffusion equation to describe the change of relative humidity of concrete in the drying process. This is the most used model to describe the relative diffusion inside the concrete, more information about this model is introduced in Chapter 3.

The transfer, distribution and content change of moisture in concrete have a significant influence on its durability, which can cause steel corrosion, chloride erosion and carbonation in concrete [44,45,48-50]. Moisture transfer between concrete and environment can be divided into two parts: internal and surface water transfer between concrete, and surface water transfer between concrete and environment [47,51,52]. In order to quantitatively describe the characteristics of

moisture transfer in concrete, it is necessary to establish an appropriate model and corresponding boundary and initial conditions. So as to accurately and intuitively show the moisture transfer characteristics, the transfer law of moisture with time and position should be indirectly obtained by means of numerical simulation method based on the calculation parameters[53,54] such as diffusion coefficient[55-61], and surface factor[62-65], initial and boundary conditions of the mathematical model.

**2.5 Conclusion**

Sufficient research has shown that the relative humidity has a significant influence on the development of cement hydration and strength development of cementitious materials. From the point of view of concrete strength prediction, it is necessary to consider the influence of relative humidity and temperature at the same time. However, in practical construction, the only surface of concrete is exposed to the air and affected by the humidity, which leads to the different strength distribution at different depths from the exposure surface. Therefore, it is also necessary to predict the strength development of different depths of concrete.

## Reference

[1] Massazza F, Daimond M, Chemistry of hydration of cements and cementitious systems, In: National council for cement and building materials. Proceedings of ninth international congress on the chemistry of cement. The offsetters, vol. 1. New Delhi, India; 1992. p. 383–48.

[2] Çakır Ö, Aköz F. Effect of curing conditions on the mortars with and without GGBFS. Constr Build Mater 2008;22(3):308–14.

[3] M. Yang, H.M. Jennings, Influences of mixing methods on the microstructure and rheological behavior of cement paste, Adv. Cem. Based Mater. 2 (1995) 70–78.

[4] E.F. Ferraris, Concrete mixing methods and concrete mixers: state of the art, J. Res. Natl. Inst. Stand. Technol. 106 (2001) 391–399.

[5] K.O. Kjellsen, R.J. Detwiler, O.E. Gjørv, Development of microstructures in plain cement pastes hydrated at different temperatures, Cem. Concr. Res. 21 (1991) 179–189.

[6] M. Cervera, R. Faria, J. Olivera, T. Prato, Numerical modelling of concrete curing, regarding hydration and temperature phenomena, Comput. Struct. 80 (2002) 1511–1521.

[7] B. Lothenbach, F. Winnefeld, C. Alder, E. Wieland, P. Lunk, Effect of temperature on the pore solution, microstructure and hydration products of Portland cement pastes, Cem. Concr. Res. 37 (2007) 483–491.

[8] W. Zhang, Y. Zhang, L. Liu, G. Zhang, Z. Liu, Investigation of the influence of curing temperature and silica fume content on setting and hardening process of the blended cement paste by an improved ultrasonic apparatus, Constr. Build. Mater. 33 (2012) 32–40.

[9] K. De Weerdt, M. Ben Haha, G. Le Saout, K.O. Kjellsen, H. Justnes, B. Lothenbach, The effect of temperature on the hydration of composite cements containing limestone powder and fly ash, Mater. Struct. 45 (2012) 1101–1114.

[10] F. Deschner, B. Lothenbach, F. Winnefeld, J. Neubauer, Effect of temperature on the hydration of Portland cement blended with siliceous fly ash, Cem. Concr. Res. 52 (2013) 169–181.

[11] C.C. Castellano, V.L. Bonavetti, H.A. Donza, E.F. Irassar, The effect of w/b and temperature on the hydration and strength of blast furnace slag cements, Constr. Build. Mater. 111 (2016) 679–688.

[12] T.C. Powers, A discussion of cement hydration in relation to the curing of concrete, Proc. Highw. Res. Board 27 (1947) 178–188.

[13] R.G. Patel, D.C. Killoh, L.J. Parrott, W.A. Gutteridge, Influence of curing at different relative humidities upon compound reactions and porosity in Portland cement paste, Mater. Struct. 21 (1988)

192–197.

[14] O.M. Jensen, Thermodynamic limitation of self-desiccation, Cem. Concr. Res. 25 (1995) 157–164.

[15] O.M. Jensen, P.F. Hansen, E.E. Lachowski, F.P. Glasser, Clinker mineral hydration at reduced relative humidities, Cem. Concr. Res. 29 (1999) 1505– 1512.

[16] K.A. Snyder, D.P. Bentz, Suspended hydration and loss of freezable water in cement pastes exposed to 90% relative humidity, Cem. Concr. Res. 34 (11) (2004) 2045–2056.

[17] R.J. Flatt, G.W. Scherer, J.W. Bullard, Why alite stops hydrating below 80% relative humidity, Cem. Concr. Res. 41 (2011) 987–992.

[18] M. Wyrzykowski, P. Lura, Effect of relative humidity decrease due to self- desiccation on the hydration kinetics of cement, Cem. Concr. Res. 85 (Supplement C) (2016) 75–81.

[19] Frías M. The effect of metakaolin on the reaction products and microporosity in blended pastes submitted to long hydration time and high curing temperature. Adv Chem Res 2006;18(1):1–6.

[20] Frías M. Study of hydrated phases present in a MK-lime system cured at 60 °C and 60 months of reaction. Cem Concr Res 2006;36(5):827–31.

[21] Kjellsen KO, Detwiler RJ, Gjorv OE. Pore structure of Plain cement pastes hydrated at different temperatures. Cem Concr Res 1990;20(6):927–33.

[22] Martínez-Ramírez S, Frías M. The effect of curing temperature on white cement hydration. Constr Build Mater 2009;23(3):1344–8.

[23] Regourd M, Gauthier E. Comportement des ciments soumis au durcissement accélère. Béton 1980;387:83–96.

[24] Richardson IG. Tobermorite/jennite – and tobermorite/calcium hydroxide- based models for the structure of C–S–H: applicability to hardened pastes of tricalcium silicate, b-dicalcium silicate, Portland cement, and blends of Portland cement with blastfurnace slag, metakaolin, or silica fume. Cem Conc Res 2004;34(9):1733–77.

[25] Koibuchi K, Yamaguchi H, Kabota K, Ishikawa Y. Hydration and compressive strength development of high strength concrete heated to 60 or 80 °C at the early age. In: Proceedings of Cement and Concrete, vol. 45, Concrete Association of Japan, 1991. p. 204–9.

[26] T.C. Powers, B. T. L., Studies of the Physical Properties of Hardened Portland Cement Paste, ACI J. Proc. 43 (1946) 249–263.

[27] T.C. POWERS, Structure and Physical Properties of Hardened Portland Cement Paste, J. Am. Ceram. Soc. 41 (1958) 1-6.

[28] J. McIntosh, Electrical curing of concrete, Mag. Concr. Res. 1 (1949) 21–28.

[29] R.W. Nurse, Steam curing of concrete. Mag. Concr. Res. 1 (1949) 79-88.

[30] A.G.A. Saul, Principles underlying the steam curing of concrete at atmospheric pressure, Mag. Concr. Res. 2 (1951) 127-40.

[31] P. Freiesleben Hansen, J. Pedersen, Maturity Computer for Controlled Curing and Hardening of Concrete. Nord. Betong. 1 (1977) 21-25.

[32] T.L. Brown, H.E. LeMat, Chemistry: The central science, 4th Ed., Prentice Hall, Englewood Cliffs, NJ, 494-498.

[33] N.J. Carino, H.S. Lew, The maturity method: from theory to application, Proceedings of the 2001 Structures Congress & Exposition, May 21-23, 2001, Washington, D.C., American Society of Civil Engineers, Reston, Virginia.

[34] R.C. Tank, N.J. Carino, Rate constant functions for strength development of concrete, ACI Mater. J. 88 (1991) 74-83.

[35] N.J. Carino, R.C. Tank, Maturity functions for concretes made with various cements and admixtures, ACI Mater. J. 89 (1992) 188-196.

[36] Y.A. Abdel-Jawad, The maturity method: Modifications to improve estimation of concrete strength at later ages, Constr. Build. Mater. 20 (2006) 893-900.

[37] R.C.A. Pinto, A.K. Schindler, Unified modeling of setting and strength development, Cem. Concr. Res. 40 (2010) 58-65.

[38] C. Vázquez-Herrero, I. Martínez-Lage, F. Sánchez-Tembleque, A new procedure to ensure structural safety based on the maturity method and limit state theory, Constr. Build. Mater. 35 (2012) 393-398.

[39] W.C. Liao, B.J. Lee, C.W. Kang, A humidity-adjusted maturity function for the early age strength prediction of concrete, Cem. Concr. Compos. 30 (2008) 515–523.

[40] S.H. Kwon, K.P. Jang, J.W. Bang, J.H. Lee, Y.Y. Kim, Prediction of concrete compressive strength considering humidity and temperature in the construction of nuclear power plants, Nucl. Eng. Des. 275 (2014) 23–29. (2014).

[41] J.K. Kim, C.S. Lee, Moisture diffusion of concrete considering self-desiccation at early ages, Cem. Concr. Res. 29 (1999) 1921–1927.

[42] M. Jooss, H.W. Reinhardt, Permeability and diffusivity of concrete as function of temperature, Cem. Concr. Res. 32 (2002) 1497–1504.

[43] T. Ishida, K. Maekawa, T. Kishi, Enhanced modeling of moisture equilibrium and transport in cementitious materials under arbitrary temperature and relative humidity history, Cem. Concr. Res. 37 (2007) 565–578.

[44] fib Model Code for Concrete Structures 2010, Ernst & Sohn, 2013.

[45] ACI Committee 209, ACI 209.2R-08 Guide for Modeling and Calculating Shrinkage and Creep in Hardened Concrete, (2008).

[46] T. and T. Ministry of Land, Infrastructure, White Paper on Land, Infrastructure, Transport and Tourism in Japan, Http://Www.Mlit.Go.Jp/. (2009).

[47] Z.P. Bazant, L.J. Najjar, Nonlinear water diffusion in nonsaturated concrete, Mater. Struct. 5 (25) (1972) 3–20.

[48] A.K. Tamimi, J.A. Abdalla, Z.I. Sakka, Prediction of Long Term Chloride Diffusion of Concrete in Harsh Environment. Construction and Building Materials, 22 (2008) 829-836.

[49] P.A.M. Basheer, S.E. Chidiact, A.E. Long, Predictive models for deterioration of concrete structures, Constr. Build. Mater. 10 (1) (1996) 27–37.

[50] L. Basheer, J. Kroppb, D.J. Cleland, Assessment of the durability of concrete from its permeation properties: a review, Constr. Build. Mater. 15 (2–3) (2001) 93–103.

[51] J. Zhang, K. Qi, Y. Huang, Calculation of moisture distribution in early-age concrete, J. Eng. Mech. 135 (8) (2009) 871–880.

[52] R.P. West, N. Holmes, Predicting moisture movement during the drying of concrete floors using finite elements, Constr. Build. Mater. 19 (9) (2005) 674–681.

[53] R. J. Gummerson, C. Hall, W. D. Hoff, R. Hawkes, G. N. Holland & W. S. Moore, Unsaturated Water Flow Within Porous Materials Observed by NMR Imaging. Nature, 281 (1979) 56-57.

[54] Kefei Li, Chunqiu Li, Zhaoyuan Chen, Influential depth of moisture transport in concrete subject to drying–wetting cycles, Cement and Concrete Composites, 31 (2009) 693-698.

[55] R. N. Swamy, S. Tanikawa, An External Surface Coating to Protect Concrete and Steel from Aggressive Environments. Materials and Structures, 26 (1993) 465-478.

[56] A. KoninR. FrançoisG. Arliguie, Penetration of Chloride in Relation to the Microcracking State into Reinforced Ordinary and High Strength Concrete. Material and Structures, 31 (1998) 310-316.

[57] A.A. Almusallam, Effect of environmental conditions on the properties of fresh and hardened concrete, Cem. Concr. Compos. 23 (4–5) (2001) 353–361.

[58] M. Du, X. Jin, H. Ye, N. Jin, Y. Tian, A coupled hygro-thermal model of early-age concrete based on micro-pore structure evolution, Constr. Build. Mater. 111 (2016) 689–698.
[59] E.L. Cussler, Diffusion: Mass Transfer in Fluid Systems, Cambridge University Press, New York, 1997.
[60] N.F. Edward, D.S. Paul, G.J. Calvin, A new method for predicition of binary gasphase diffusion coefficients, Ind. Eng. Chem. Res. 58 (5) (1966) 18–27.
[61] J.R. Welty, C.E. Wicks, R.E. Wilson, G.L. Rorrer, Fundamentals of momentum, Heat, and Mass Transfer, Wiley, 2007.
[62] S.F. Wong, T.H. Wee, S. Swaddiwudhipong, S.L. Lee, Study of water movementin concrete, Mag. Concr. Res. 53 (3) (2001) 205–220.
[63] H. Akita, T. Fujiwara, Y. Ozaka, A practical procedure for the analysis of moisture transfer within concrete due to drying, Mag. Concr. Res. 49 (179) (1997) 129–137.
[64] T. Shimomura, K. Maekawa, Analysis of the drying shrinkage behaviour of concrete using a micromechanical model based on the micropore structure of
concrete, Mag. Concr. Res. 49 (181) (1997) 303–322.
[65] K. Sakata, A study on moisture diffusion in drying and drying shrinkage of
concrete, Cem. Concr. Res. 13 (2) (1983) 216–224.

# Chapter 3 Proposal of temperature and relative humidity influenced equivalent age function

### 3.1 Cement hydration degree of various temperature/relative humidity

As described in chapter 2, the hydration degree of cement is a quantity that reflects the reaction amount of mineral composition in cement clinker. Moreover, the hydration reaction of cement is affected by many factors, such as temperature and relative humidity during curing. Within that a fundamental principle is known that the cement will stop hydrating when relative humidity is below 80%, the experimental results of many studies also show the influence of relative humidity on cement hydration [1,2]. Although many cement hydration models have given the effect of temperature and relative humidity on hydration rate, the effect of both on the maturity has not been fully proved to predict the mechanical properties of cementitious products. In order to propose a safe and accurate influence factor of temperature and relative humidity from a point view of engineering to predicted the development of mechanical properties, this chapter based on the hydration degree of cement in the experiment to derived the equivalent age function under the combined effect of temperature and relative humidity.

The cement hydration degree $\alpha_t$, is a function of variables temperature(T), relative humidity(RH) with the dependent on the time t. Then the increase $\Delta\alpha_t$ during the time interval $\Delta t$, characterizing the rate of hydration, is also a function of variables temperature(T), relative humidity(RH) and hydration degree $\alpha_t$. Which can be written as

$$\beta_{T,RH,\alpha_t} = \frac{\Delta\alpha_t}{\Delta t} \tag{3.1}$$

Hence, we can obtain the following calculation of the degree hydration.

$$t_0 = 0, \qquad \alpha_{t_0} = 0$$
$$t_1 = t_0 + \Delta t, \qquad \alpha_{t_1} = \alpha_{t_0} + \Delta t \cdot \beta_{T,RH,\alpha_{t_0}}$$
$$\vdots$$
$$t_n = t_{n-1} + \Delta t, \qquad \alpha_{t_n} = \alpha_{t_{n-1}} + \Delta t \cdot \beta_{T,RH,\alpha_{t_{n-1}}}$$

In summary, at time $t_i$, the cement hydration degree $\alpha_{t_i}$ can be shown as

$$\alpha_{t_i} = \sum_{i=1}^{n} \Delta t \cdot \beta_{T,RH,\alpha_{t_{i-1}}} \tag{3.2}$$

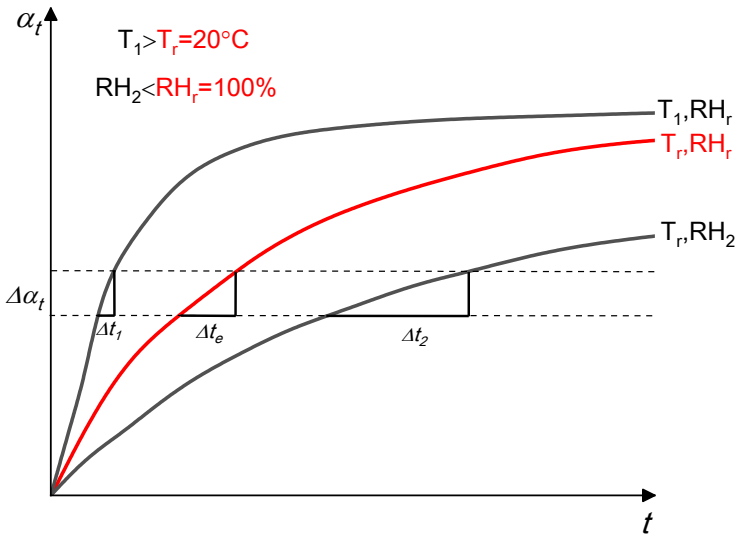


Figure 3.1 Definition of equivalent age at variable temperature and relative humidity

The concept of equivalent age $t_e$ in the current study presents the chemical reaction velocity and its dependence on temperature and relative humidity. The equivalent age $t_e$ that corresponds to time would present the degree of reaction (or strength) with different actual temperature and relative humidity conditions relative to the reference temperature $T_r = 20\,°C$ and reference relative humidity $RH_r = 100\%$. Hence, based on Figure 3.1, the hydration rate of each temperature and humidity condition can be expressed as

$$\beta_{T_1,RH_r,\alpha_t} = \frac{\Delta\alpha_t}{\Delta t_1} \qquad \text{for } T_1, RH_r$$

$$\beta_{T_r,RH_r,\alpha_t} = \frac{\Delta\alpha_t}{\Delta t_e} \qquad \text{for } T_r, RH_r$$

$$\beta_{T_r,RH_2,\alpha_t} = \frac{\Delta\alpha_t}{\Delta t_2} \qquad \text{for } T_r, RH_2$$

By introducing $\Delta\alpha_t$ of $T_r, RH_r$ into the other two conditions, we can express $\Delta t_e$ as

$$\Delta t_e = \frac{\beta_{T_1,RH_r,\alpha_t}}{\beta_{T_r,RH_r,\alpha_t}}\Delta t_1 \qquad \text{for } T_1, RH_r$$

$$\Delta t_e = \frac{\beta_{T_r,RH_2,\alpha_t}}{\beta_{T_r,RH_r,\alpha_t}}\Delta t_2 \qquad \text{for } T_r, RH_2$$

Hereby, the equivalent age of arbitrary variable temperature T and relative humidity RH, the equivalent age can be written as

$$\Delta t_e = \frac{\beta_{T,RH,\alpha_t}}{\beta_{T_r,RH_r,\alpha_t}}\Delta t \qquad or \quad t_e = \sum \frac{\beta_{T,RH,\alpha_t}}{\beta_{T_r,RH_r,\alpha_t}}\Delta t \tag{3.3}$$

The relationship between cement hydration rate $\beta_t$ and cement hydration degree $\alpha_t$ can be found in some cement hydration models[3-6]. In which, Parrot [3] proposed a simple cement hydration model to approximate the rate of reaction of the hydration of the cement clinkers by modeling the formation of hydration products. The following equation expressing the hydration rate as a function is proposed.

$$\beta_t = k(1-\alpha_t)^m \tag{3.4}$$

Where,

$k$ is the rate constant;

$m$ is a correlation coefficient.

This model has been used to verify the characteristics of the reaction rates of each induvial phase of cement clinkers [7,8]. However, to determine the overall hydration reaction rate of cement clinker, it is also applicable. In this study, the hydration reaction rate related to various curing temperature and relative humidity can be derived by the relationship between cement hydration rate and cement hydration degree through the varying of the coefficient $k$. In other words, the rate constant $k$ in Eq. (3.4) is a function of both temperature(T) and relative humidity(RH), therefore, Eq.(3.4) can be expressed as

$$\beta_{T,RH,\alpha_t} = k_{T,RH}(1-\alpha_t)^m \tag{3.5}$$

Where,

$\beta_{T,RH,\alpha_t}$ is the cement hydration rate with the variables of temperature(T), relative humidity(RH) and curing time(t);

$k_{T,RH}$ is the rate constant dominated by temperature(T) and relative humidity(RH).

Considering that at the standard temperature(20ºC) and relative humidity(100%), cement hydration rate in Eq.(3.6) could be calculated as

$$\frac{\beta_{T,RH,\alpha_t}}{\beta_{T_r,RH_r,\alpha_t}} = \frac{k_{T,RH}}{k_{T_r,RH_r}} \tag{3.6}$$

Where,

$\beta_{T_r,RH_r,\alpha_t}$ is the cement hydration rate at reference temperature $T_r$=20ºC and relative humidity $RH_r$=100%;

$k_{T_r,RH_r}$ is the rate constant at reference temperature $T_r$ and relative humidity $RH_r$;

Introducing Eq.(3.6) into Eq.(3.3), the equivalent age influenced by both temperature and relative humidity can be expressed as

$$t_e = \sum \frac{k_{T,RH}}{k_{T_r,RH_r}} \Delta t \tag{3.7}$$

To sum up, the approach in this research to derive the equivalent age function is based on the relationship between hydration rate of cement and hydration degree of cement. Then, by the obtained values of rate constant under various temperature and relative humidity through a cement hydration model, the hydration rate relative to a reference conditions can be derived. Finally, the expression of hydration degree relative to the hydration rate under reference conditions can be expressed, and the equivalent age function of each temperature and humidity relative to reference conditions is obtained.

### 3.2 Experimental process

#### 3.2.1 Thermogravimetric Analysis

The instrument of TG-DTA was carried out by using the Bruker TG-DTA 2000 SA differential thermobalance, as shown in Fig. 3.2a. Cement powder samples cured at the relative humidity of 23%, 43%, 59%, 85%, 95%, 97% of temperature of 20ºC, and cement paste samples cured at relative humidity 100% of temperature of 10ºC, 20ºC and 40ºC are used for the test at the curing age of 1, 3, 7 and 28 days. In addition, a sample of cement clinkers without any curing was also tested for comparative calculation. Before the TG-DTA test, each sample was moved to the acetone solution for soaking for 24 hours, then stored in vacuum at least for 24 hours.

The samples were placed into a nitrogen environment in the thermobalance (nitrogen gas flow ratio = 150 mL/min) during the entire testing process. The samples were heated in the thermobalance from room temperature to 1100℃ at a heating rate of 10℃/min. A temperature plateau of 20 mins at 105℃ was added to the heating process (Fig. 3.2b) to ensure that the free water in the cement paste had evaporated as much as possible. Weight loss of each temperature ranges was calculated by the self-existed software of the instrument.

#### 3.2.2 Calculation of hydration degree

The hydration reactions in cement-based materials or the amount of cement that has reacted with water can be described by examining the degree of hydration as done so in Bhatty [9]. The decomposition of the cement hydrates during thermogravimetric testing was categorized into three stages: dehydration ($Ldh$), dihydroxylation ($Ldx$) and decarbonation ($Ldc$). In this study, these three stages are clearly identified in the plotted thermogravimetric (TG) data of the cement paste samples, see Fig. 3.2, the free water is considered to be totally evaporated during the heating process up to 140℃, and then the loss of the chemically bound water of C-S-H takes place during the dehydration($Ldh$) phase in the temperature range of 140℃ to 400℃. Another peak is found between

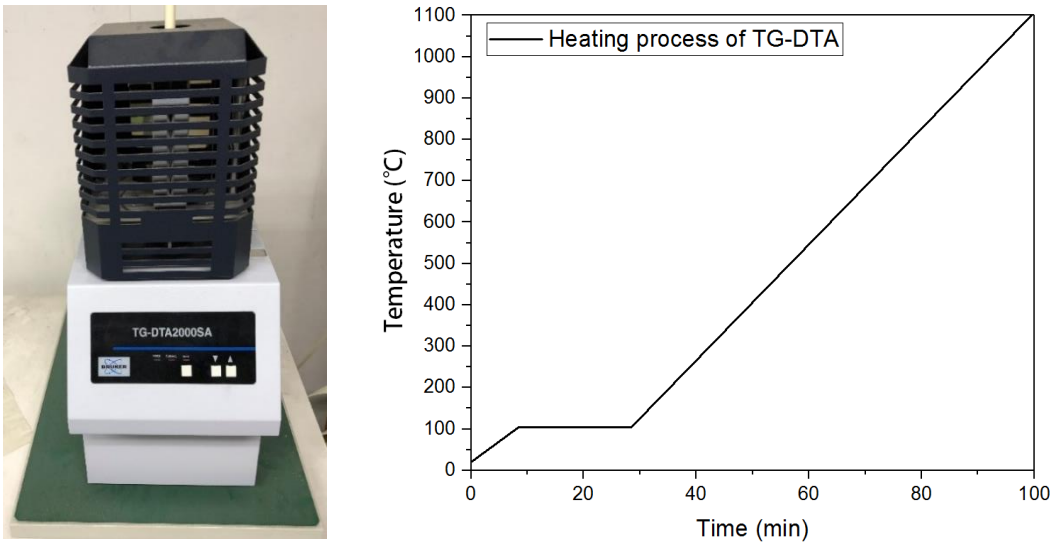


a. Bruker TG-DTA2000SA b. Heating process

Figure 3.2 Bruker TG-DTA2000SA and heating process

400°C and 600°C, which corresponds to the dihydroxylation ($Ldx$) of portlandite. Decarbonation ($Ldc$) occurs due to the decomposition of calcium carbonate (CaCO3) between 600°C and 1100°C. Available methods for calculating the degree of hydration of cement paste by using TGA have been provided by many researchers [9-12]. In this study, the degree of hydration ($\alpha$) is calculated by synthesizing the methods in Bhatty [9] and Monteagudo et al. [12], which can be included as

$$W_B = Ldh + Ldx + 0.41(Ldc - Ldc_a) \tag{3.8}$$

$$\alpha = \frac{W_B}{W_\infty} \times 100 \tag{3.9}$$

Where,

$\alpha$ is the degree of hydration;

$W_B$ is the chemically bound water;

$W_\infty$ is the chemically bound water when $\alpha = 1$;

$Ldh$, $Ldx$ and $Ldc$ are the relative mass loss in the dehydration, dehydroxylation and decarbonation regions, respectively.

$Ldc_a$ is the relative mass loss due to the decarbonation of the anhydrous materials (cement particles in this study).

In Eq. (3.9), $W_\infty$ is taken as 0.24 by the theoretical stoichiometry of cement found that about 0.24 parts of chemically bound water are combined with each part of cement when cement is fully hrdrated[9,13,14].

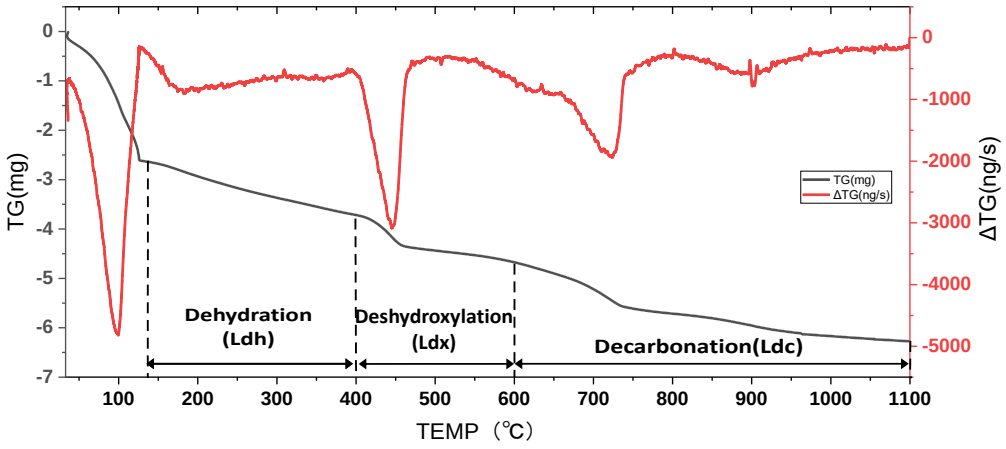


Figure 3.3 Example of weight loss curve

### 3.3 Result and discussion

#### 3.3.1 Hydration degree of various temperature and relative humidity

Fig. 3.3 and Fig 3.4 showed the TG weight loss curves of cement clinker powder cured under different curing relative humidity of the temperature of 20°C and cement paste under different temperature of the relative humidity of 100%. Among them, Fig. 3.3a is the TG curve of cement clinker powder without any conditional curing. It is worth noting that the calcium carbonate contained raw materials is mixed during the cement-producing process, this results in the weight loss due to the decomposition of calcium carbonate ($CaCO_3$) between 600℃ and 1100℃, see Fig. 3.3a. Based on the tested results, this amount is about 1.212% of the total mass of cement clinker. Moreover, as the description of the calculation method of hydration degree in the above section 3.3.2, this amount of decomposition of calcium carbonate should be removed in the calculation, see the $(Ldc - Ldc_a)$ in Eq. (3.9). The remaining calcium carbonate will be treated as carbonation of calcium hydroxide($Ca(OH)_2$) from cement hydration. To consider the carbonation of C-S-H, as the carbonation reactions of C-S-H occur in the natural environment at a prolonged low rate due to the low CO2 concentration in the atmosphere (400 ppm or 0.03-0.04%)[15,16], the carbonation of C-S-H is neglected. For the cement clinker powder curing at each unsaturated relative humidity (Fig. 3.3b-Fig3.3g), different tendencies of TG curves can be found. As the conclusion of other studies in chapter, at a relative humidity of less than 80%, the process of cement hydration almost stops. Therefore, it can be found in Fig. 3.3b-Fig. 3.3d that a similar weight loss of TG curve can be found in the curing condition with the relative humidity of 23%, 43%, 59% during 28-day curing corresponding to the non-cured cement clinker powder. However, when the curing relative humidity is more than 80%, the TG curves of weight loss at different ages show apparent dispersion. It is not

difficult to understand that is caused by hydration of cement. However, substantial weight loss after 600°C can be found due to the decomposition of calcium carbonate that generated from the carbonation of calcium hydroxide(CH). In contrast, cement paste curing at 100%RH (water bath) is much lower calcium carbonate than RH-controlled atmosphere curing, and an evident decomposition of calcium hydroxide can be seen at around 400 °C.

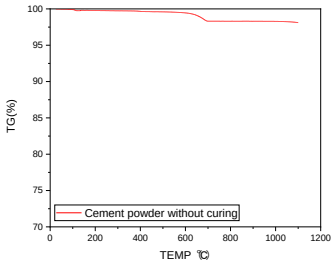


a. Cement powder without curing

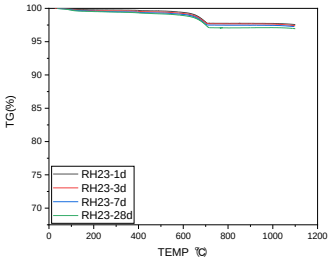


b. Curing at 20°C-23%RH

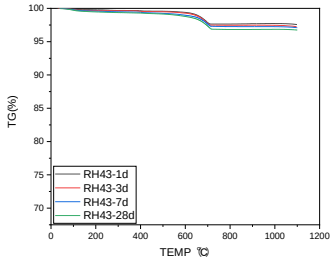


c. Curing at 20°C-43%RH

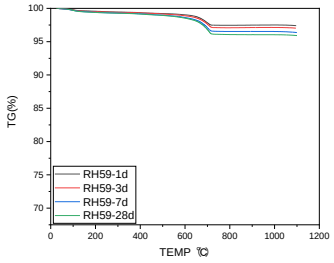


d. Curing at 20°C-59%RH

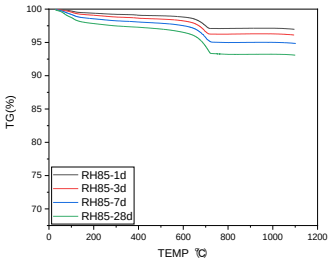


e. Curing at 20°C-85%RH

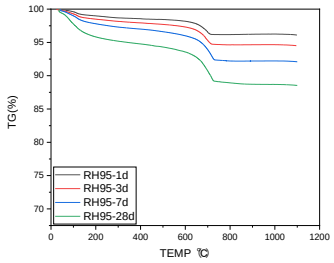


f. Curing at 20°C-95%RH

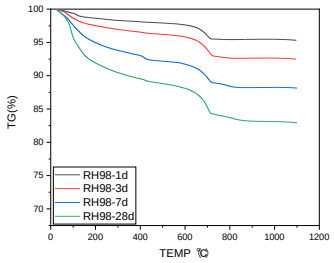


g. Curing at 20°C-98%RH

Figure 3.4 Weight loss curve of TG at various relative humidity of 20°C

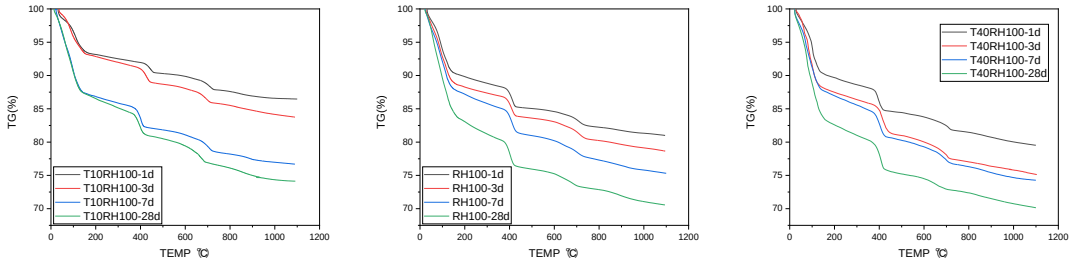


a. Curing at 10°C-100%RH b. Curing at 20°C-100%RH c. Curing at 40°C-100%RH

Figure 3.5 Weight loss curve of TG at various temperature of 100%RH

### 3.3.2 Proposal of temperature-humidity influenced equivalent age function

Fig. 3.6 shows the calculated hydration degree through Eq. (3.9) and Eq. (3.10) and the corresponding approximate curves at various temperature and relative humidity. Shown as Fig. 3.6a, the water bath curing shows a significantly higher level of early-age hydration than the samples cured at unsaturated conditions of relative humidity. With the increase of relative humidity, the hydration degree of cement increases with time at a feasible hydration environment. The hydration degree of 95%RH and 98%RH at 3d curing age is significantly higher than other unsaturated relative humidity. Even though studies have shown that the hydration rate of cement is meager when the humidity is lower than 80%RH, it can be seen from Fig. 3.6a that the hydration degree of 1d and 3d under 85%RH curing is not very different from that of 23%RH, 43%RH and 59%RH, which indicates that the hydration rate is still very slow when the curing humidity is slightly higher than 80%. Due to continuous hydration of cement, the difference in hydration degree between 85%RH and 23%RH, 43%RH and 59%RH becomes evident at the curing ages of 7d and 28d. Besides, regardless of curing age, the samples with curing humidity of 23%RH, 43%RH and 59%RH have a very low degree of hydration, which are lower than 0.045(59%RH at 28 days). For the hydration degree of cement at different temperatures of 100%RH, Fig. 3.6b shows that the hydration degree is faster at higher temperature.

Based on the relationship of cement hydration degree $\alpha_t$ with time in Fig. 3.6, the hydration rate $\beta_t$ of cement under different temperature and relative humidity can be obtained by Eq. (3.2). The relationship between hydration rate and hydration degree of cement under different temperature and relative humidity is shown as the color curves in Fig. 3.7. The red dashed curve is the best fit curve based on Eq. (3.5) for the corresponding hydration rate versus hydration degree curves of each curing conditions. The purpose of function fitting is to obtain values of rate constant k under different temperature and relative humidity conditions. Therefore, the coefficient m value is fixed

here as the best fitting value under the condition of 20°C-100%RH. Consequently, the fitting results are concluded in Table 3.1.

Furthermore, different mineral components of cement, such as $C_2S$, $C_3S$, and $C_3A$, have different reaction rates[17,18]. The reaction rate of $C_3S$ and $C_3A$ is much quicker than $C_2S$ and $C_4AF$, so that the hydration of $C_3S$ and $C_3A$ reaches a steady state much earlier than $C_2S$ and $C_4AF$. Most of $C_3A$ and $C_3S$ have reacted in the first 1000 hours[18]. Due to different types of cement such as high-early strength cement and low heat cement have different content of mineral components, which will lead to different trends in reaction rates. Therefore, the above results of this study can only be applied to ordinary Portland cement or the cement with the same mineral composition.

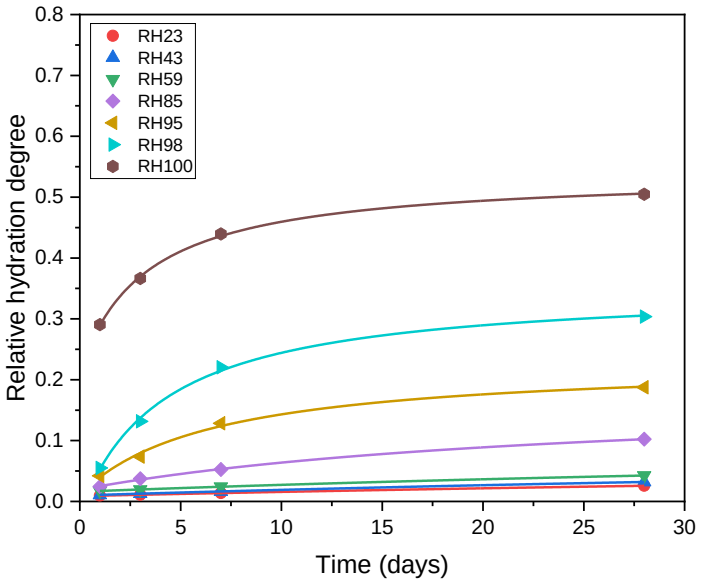


a. Hydration degree at various relative humidity of 20°C

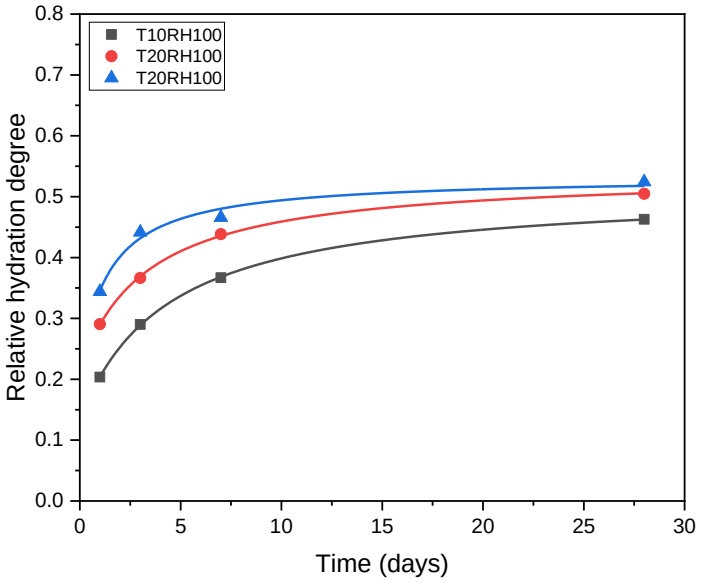


b. Hydration degree at various temperature of 100%RH

Figure 3.5 Hydration degree at various temperature and relative humidity

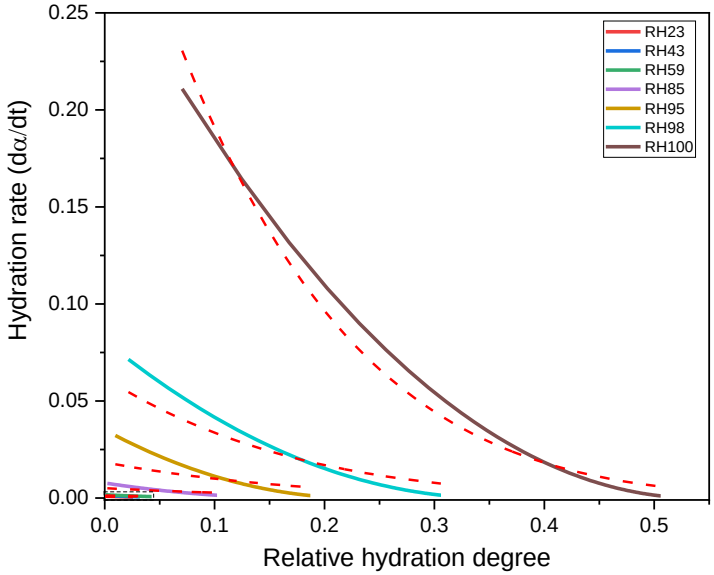


a. Hydration rate versus hydration degree at various relative humidity of 20°C

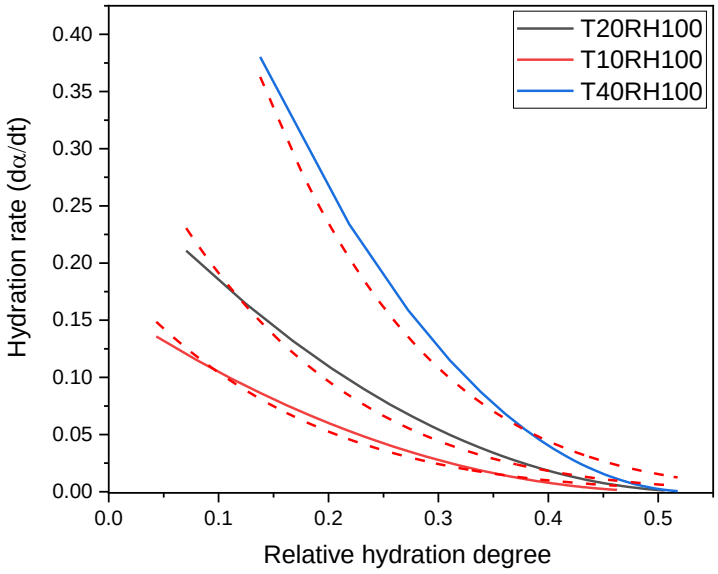


b. Hydration rate versus hydration degree at various temperature of 100%RH

Figure 3.6 Hydration rate versus hydration degree at various temperature and relative humidity

Table 3.1 Results of rate constant $k_{T,RH}$

| Condition | 20°C 23%RH | 20°C 43%RH | 20°C 59%RH | 20°C 85%RH | 20°C 95%RH | 20°C 98%RH | 20°C 100%RH | 10 °C 100% RH | 40 °C 100%RH |
|---|---|---|---|---|---|---|---|---|---|
| $k_{T,RH}$ | 0.0007 | 0.001 | 0.0013 | 0.0051 | 0.0184 | 0.0620 | 0.3525 | 0.1921 | 0.8579 |
| m | | | | | 5.8036 | | | | |
| $\frac{k_{T,RH}}{k_{T_r,RH_r}}$ | 0.0020 | 0.0028 | 0.0037 | 0.0145 | 0.0522 | 0.1759 | 1 | 0.5450 | 2.4338 |

Generally, the temperature effect on the rate constant of chemical reaction is expressed through Arrhenius function by discussing the variation of apparent activation energy $E$ to achieve the rate constant of different conditions. Nevertheless, such a method was simplified by Tank and Carino [19,20] who suggested an exponential form rate constant function can also well expressed the rate constant of different conditions. Which is shown as

$$k_T = Ae^{BT} \tag{3.11}$$

Where,

A is an experimental constant in $\text{day}^{-1}$;

B is the temperature sensitivity factor in 1/°C;

T is the temperature of concrete.

By referring the rate constant equation of Eq. (3.11), the rate constant dominated by both temperature(T) and relative humidity(RH) in this study is written as the following exponential form function.

$$k_{T,RH} = A_1 e^{B_1 T} \cdot \ A_2 e^{B_2 RH} \tag{3.12}$$

Where,

$A_1$, $A_2$ are two constants in $\text{day}^{-1}$,

$B_2$ is the temperature sensitivity factor in 1/°C;

$B_2$ is the relative humidity sensitivity factor in 1/RH.

T and RH are the temperature and relative humidity of concrete.

It should be noted that the proposal of Eq. (3.12) is not only verified by comparing different fitting forms of empirical equations, but also based on the previous research results and model code, references [21-23] utilized the same multiplicative form to express the interaction relationship between temperature and relative humidity and adopted into equivalent age function.

Base on Eq. (3.12), the relative rate constant to a reference temperature($T_r$) and relative humidity($RH_r$) can be expressed as follows and the calculation through the fitting results are also shown within Table 3.1.

$$\frac{k_{T,RH}}{k_{T_r,RH_r}} = e^{B_1(T-T_r)} \cdot e^{B_2(RH-RH_r)} \tag{3.13}$$

Thus, the constants $B_T$ and $B_{RH}$ may obtained from the regression analysis of $\frac{k_{T,RH}}{k_{T_r,RH_r}}$ versus the curing temperature and relative humidity, the fitting results are shown in Fig. 3.7. Regression results of $B_1 = 0.0447$ and $B_2 = 0.8484$ are obtained. Accordingly, by introducing $B_1$ and $B_2$ into Eq. (3.13) and Eq. (3.8), the temperature and relative humidity effected equivalent age function can be expressed as

$$t_{e_{T,RH}} = \sum e^{0.0447(T-20)} \cdot e^{0.8484(RH-100)} \cdot \Delta t \tag{3.14}$$

## 3.4 Conclusion

Based on the hydration degree of cement powder at different temperature and relative humidity, the hydration rate was calculated. Then the relationship between hydration degree and hydration rate can be illustrated. A hydration model was applied to obtain the rate constant at different relative humidity and temperature by regression analysis with the experiment result. Taking 20°C-100%RH as the standard condition, the change of rate constant under different temperature and humidity can be expressed by an exponential function, then the equivalent age equation under the action of temperature and humidity can be obtained. Based on the research, the following aspects can be concluded.

1. The hydration reaction of cement powder is visible under the curing condition of more than 80%RH by the experimental results.
2. The hydration model can describe the nonlinear relationship between hydration degree and hydration rate under different temperature and relative humidity.
3. The proposed exponential function can well fit the value of rate constant under different temperature and relative humidity, and then the modified equivalent age function can be proposed based on it.

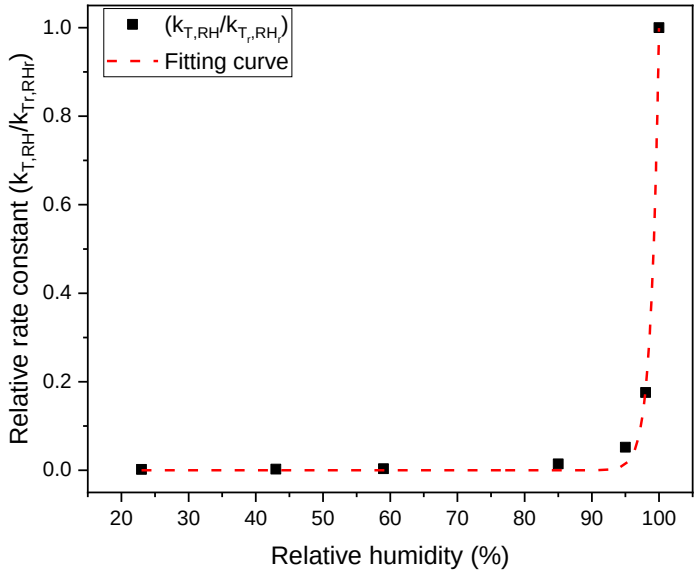


a. Relative rate constant at various relative humidity

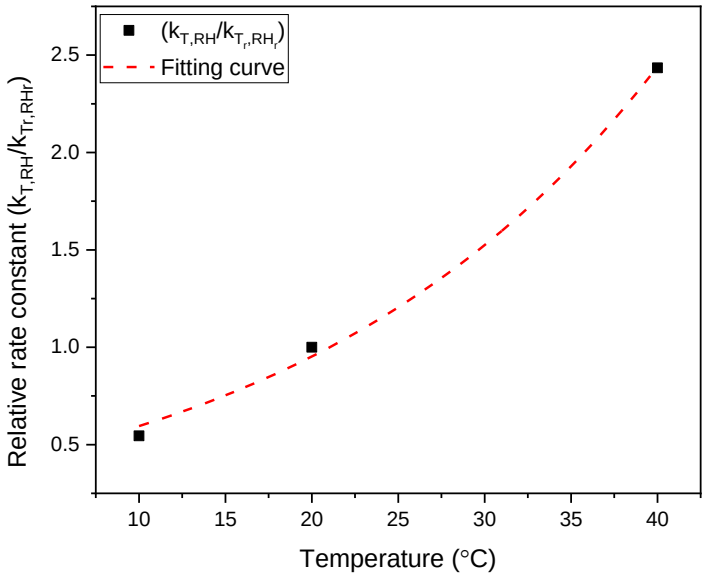


b. Relative rate constant of various temperature

Figure. 3.7 Fitting results of relative rate constant at various temperature and relative humidity

Reference

[1] T.C. Powers, A discussion of cement hydration in relation to the curing of concrete, Proc. Highw. Res. Board 27 (1947) 178–188.

[2] R.G. Patel, D.C. Killoh, L.J. Parrott, W.A. Gutteridge, Influence of curing at different relative humidities upon compound reactions and porosity in Portland cement paste, Mater. Struct. 21 (1988) 192–197.

[3] L.J. Parrot, Modeling of hydration reactions and concrete properties, in: J.P. Skalny (Ed.), Materials Science of Concrete, Westerville, OH, 1989, pp. 181–195.

[4] J.A. Dalziel, W.A. Gutteridge, The influence of pulverized-fuel ash upon the hydration characteristics and certain physical properties of a Portland cement paste, Cement and Concrete Association, Slough, 1986.

[5] T. Kishi, K. Maekawa, Multi-component model for hydration heating of Portland cement, Conc. Lib. JSCE 28 (1996) 97–115.

[6] H.F.W. Taylor, A method for predicting alkali ion concentrations in cement pore solutions, Adv. Cem. Res. 1 (1) (1987) 5–17.

[7] I. Maruyama, T. Matsushita et al., Rate of hydration Alite and Blite in Portland cement, J. Struct. Constr. Eng., AIJ, 75(650)(2010)681-688.

[8] I. Maruyama, T. Matsushita et al., Hydration of 3CaO·Al2O3 and 43CaO·Al2O3·Fe2O3 in Portland cement, J. Struct. Constr. Eng., AIJ, 76(659)(2011)1-8.

[9] Javed I. Bhatty, Hydration versus strength in a portland cement developed from domestic mineral wastes-a comparative study, Thermochimica Acta, Volume 106, 1986, Pages 93-103.

[10] Ahmed Loukili, Abdelhafid Khelidj, Pierre Richard, Hydration kinetics, change of relative humidity, and autogenous shrinkage of ultra-high-strength concrete, Cement and Concrete Research, Volume 29, Issue 4, 1999, Pages 577-584,

[11] Ivindra Pane, Will Hansen, Investigation of blended cement hydration by isothermal calorimetry and thermal analysis, Cement and Concrete Research, Volume 35, Issue 6, 2005, Pages 1155-1164,

[12] M. Monteagudo, A. Moragues, J.C. Gálvez, M.J. Casati, E. Reyes, The degree of hydration assessment of blended cement pastes by differential thermal and thermogravimetric analysis. Morphological evolution of the solid phases, Thermochim. Acta 592 (2014) 37–51.

[13] Mindess, S. and Young, JF, 'Concrete' (Prentice-Hall. Inc., Englewood Cliffs, New Jersey, USA, 1981) 530.

[14] W. Deboucha, N. Leklou, A. Khelidj, M.N. Oudjit. Hydration development of mineral additives blended cement using thermogravimetric analysis (TGA): methodology of calculating the degree of hydration, Constr. Build. Mater., 146 (2017), 687-701,

[15] P. Tans and R. Keeling, Trends in Atmospheric Carbon Dioxide, Earth Syst. Res. Lab. (2015)

[16] W. Ashraf, Carbonation of cement-based materials: challenges and opportunities., Constr. Build. Mater., 120 (2016), 558-570

[17] Wang, Xiao-Yong and Lee, Han-Seung, Evaluation of the mechanical properties of concrete considering the effects of temperature and aging. Constr. Build. Mater., 29(2012), 581-590.

[18] Matsushita T, Hoshino S, Maruyama I, Noguchi T, Yamada K. Effect of curing temperature and water to cement ratio on hydration of cement compounds. In: Proceedings of 12th ICCC, Montreal; 2007. TH2-07.3

[19] R.C. Tank, N.J. Carino, Rate constant functions for strength development of concrete, ACI Mater. J. 88 (1991) 74-83.

[20] N.J. Carino, R.C. Tank, Maturity functions for concretes made with various cements and admixtures, ACI Mater. J. 89, (1992) 188-196.

[21] Z.P. Bazant, L.J. Najjar, Nonlinear water diffusion in nonsaturated concrete, Mater. Struct. 5 (25) (1972) 3–20.

[22] Z.P. Bažant, Constitutive equation for concrete creep and shrinkage based on thermodynamics of multiphase systems, Materials and structures, 1970, 3(1), pp 3–36.

[23] fib Model Code for Concrete Structures 2010, Ernst & Sohn, 2013.

# Chapter 4 Strength prediction for cement mortar curing at different temperature and relative humidity

## 4.1 Theorical introduction

### 4.1.1 Strength prediction model

In the prediction and prediction of concrete strength development, many models are being applied to reflect the relationship between strength development and time. As described in chapter 2, the prediction of strength development under different conditions is basically based on the equivalent age of concrete under standard curing conditions. As a factor to evaluate the maturity of concrete, the equivalent age function is generally established as a function of temperature. Therefore, the research content of this chapter is based on the equivalent age function under the influence of temperature and relative humidity proposed in the previous chapter to evaluate the strength development of cement mortar under different curing conditions. The fib Model Code for Concrete Structures 2010 (fib MC 2010)[1] is used for the strength prediction model.

**fib MC 2010**

As described by fib MC 2010 [1], the relevant compressive strength of concrete at various ages $f_{cm}(t)$ could be estimated from:

$$f_{cm}(t) = \beta_{cc}(t) \cdot f_{cm28} \tag{4.1}$$

with:

$$\beta_{cc}(t) = \exp\left\{s \cdot \left[1 - \left(\frac{28}{t_e}\right)^{0.5}\right]\right\} \tag{4.2}$$

where,

$f_{cm}(t)$ is the mean compressive strength in MPa at the age of $t$ days;

$f_{cm28}$ is the mean tested compressive strength of concrete at the age of 28 days; $s$ is a coefficient depending on the strength class of cement.

Coefficient s is given by ranging from 0.20 to 0.38 [1]. As per the Ministry of Land, Infrastructure, Transport and Tourism of Japan [2], where used the same model as above, has given the factor $s$ as 0.31 when ordinary Portland cement (OPC) is used as the cementitious material.

It is noticed that the $f_{cm28}$ in Eq. (4.1) represents the 28-days compressive strength of concretes/mortars under a reference temperature (20ºC) and reference relative humidity of 100%, which is calculated based on the experimental result of 28-days at 18ºC and 100%RH.

By substituting the equivalent age function under the influence of temperature and humidity, Eq. 3.14, to calculate the development of concrete strength. The above strength prediction can be concluded as

$$\begin{cases} f_{cm}(t) = \exp\left\{s \cdot \left[1 - \left(\frac{28}{t_{e_{T,RH}}}\right)^{0.5}\right]\right\} \cdot f_{cm28} \\ t_{e_{T,RH}} = \sum e^{0.0447(T-20)} \cdot e^{0.8484(RH-100)} \cdot \Delta t \end{cases} \quad (4.3)$$

where,

$f_{cm}(t)$ is the mean compressive strength in MPa at the age of $t$ days;

$f_{cm28}$ is the mean tested compressive strength of concrete at the age of 28 days;

$s$ is a coefficient depending on the strength class of cement, s=0.31;

$t_{e_{T,RH}}$ is the equivalent age effected by temperature and relative humidity;

$T$, $RH$ are the temperature and relative humidity at time interval $\Delta t$.

In this study, the temperature/relative humidity influenced equivalent age function is obtained by analysing the reaction rate of cement hydration. In this chapter, it is utilized to calculate the strength development. During this process, an assumption that hydration reaction and strength developed into a linear rule was applied.

### 4.1.2 Relative humidity change inside cement mortar

The verification procedure of the proposed humidity modified equivalent age function for testing position inside concrete is carried out based on the compressive strength of three size specimens curing at each temperature and relative humidity. The relative humidity distribution with time of each position from the side surface to the core is simulated by the moisture diffusion model. For the cylinder specimens, the relative humidity of the central cross-section is simulated by a one-dimensional diffusion model. For the tube specimens, the humidity change of the central cross-section can be carried out by the two-dimensional diffusion model.

**Moisture diffusion model**

After removing the formwork of concrete in the early days, concrete directly exposed to the air. Water movement inside the concrete occurs due to moisture diffusion by the drying of the surface. At present, Fick's law is generally used to describe the water diffusion of concrete under drying conditions.

The water change inside concrete can be divided into two parts – moisture diffusion and self-desiccation, which can be expressed as follows [1,3-5].

$$\frac{\partial H}{\partial t} = \frac{\partial H_d}{\partial t} + \frac{\partial H_s}{\partial t} \quad (4.4)$$

Where,

$\frac{\partial H}{\partial t}$ is the total variation rate of relative humidity inside concrete;

$\frac{\partial H_d}{\partial t}$ is the variation rate of relative humidity due to moisture diffusion;

$\frac{\partial H_s}{\partial t}$ is the variation rate of relative humidity due to self-desiccation.

The one-dimensional moisture diffusion phenomenon is generally described by Fick's second law, which describes the variation in concentration of an element with time and location. Bazant [3] took the relative humidity of concrete as the essential variable and used the diffusion equation to describe the change of relative humidity of concrete in the drying process. Therefore, the relative humidity change inside concrete due to moisture diffusion can be expressed as

For one-dimensional diffusion

$$\frac{\partial H_d}{\partial t} = \frac{\partial}{\partial x}\left(D(H)\frac{\partial H}{\partial x}\right) \tag{4.5}$$

For two-dimensional diffusion

$$\frac{\partial H_d}{\partial t} = \frac{\partial}{\partial x}\left(D(H)\frac{\partial H}{\partial x}\right) + \frac{\partial}{\partial y}\left(D(H)\frac{\partial H}{\partial y}\right) \tag{4.6}$$

Where,

$D(H)$ is the moisture diffusion coefficient, $m^2/s$;

$\frac{\partial H}{\partial x}$ is the gradient in relative humidity inside concrete of x dimension, $m^{-1}$;

$\frac{\partial H}{\partial y}$ is the gradient in relative humidity inside concrete of y dimension, $m^{-1}$.

The moisture diffusion coefficient $D(H)$ will be influenced by various conditions such as temperature, composition of concrete, proportion of concrete (especially water-cement ratio), hydration degree and so on. At an isothermal condition, the diffusion coefficient can be expressed as a function of the relative humidity inside concrete with a value range of 0<H<1.

$$D(H) = D_1\left[\alpha + \frac{1-\alpha}{1+[(1-H)/(1-H_C)]^n}\right] \tag{4.7}$$

Where,

$D_1$ is the maximum of $D(H)$ in $m^2/s$ for H=1;

$D_0$ is the minimum of $D(H)$ in $m^2/s$ for H=0;

$\alpha$ is the ratio of initial state $D_0$ to $D_1$, $\alpha = D_0/D_1$;

$H_C$ is the relative humidity inside concrete at $D(H) = 0.5D_1$;

$n$ is an exponent;

$H$ is the relative humidity inside concrete.

Up till now, Eq. (4.7) is the most widely used function to calculate the diffusion coefficient with relative humidity of drying concrete. fib model code 2010[1] gives the recommended value of each value with $\alpha = 0.05$, $H_C = 0.8$, $n = 15$. In this study, the value of $D_1$ is determined by referring to the calculation of fib model code 2010 through the compressive strength and order of magnitudes of E-4 is applied for the mortar specimens. It is noted that previous studies have shown that the magnitude of $D(H)$ and $D_1$ ranges widely, often from E-10 to E-4. The input parameters $D_1$ in this chapter are taken by referring fib model code 2010 as for each size specimens.

In addition to the diffusion equation, suitable boundary conditions are needed to solve the moisture change in concrete numerically. Two kinds of boundary conditions are usually used to calculate the drying process of concrete -- the Dirichlet boundary condition and the third boundary condition. The Dirichlet boundary condition can be expressed as

$$H_{sur} = H_e \tag{4.8.1}$$

Where,

$H_{sur}$ is the relative humidity of the exposed surface of concrete;

$H_e$ is the environmental relative humidity.

The expression of the third boundary condition is shown as

$$-D(H)\frac{\partial H}{\partial x} = f(H_{sur} - H_e) \tag{4.8.2}$$

Where,

$f$ is the surface factor.

Bazant [3] dealt with this problem by assuming an additional thickness to the specimen (that is, the equivalent surface thickness). Comparing analytical results with experimental ones, Bazant and Najjar reported that the value of the equivalent surface thickness is 0.75 mm. The experiment in this chapter is performed in the curing room with a constant curing condition, relative stable boundary condition can be measured by setting a temperature/relative humidity sensor on the surface of concrete, therefore, the boundary condition applied in the numerical calculation is taken as the measured relative humidity at the stable state.

### 4.1.3 Numerical analysis

As a general solution method, finite difference method (FDM) is usually used to solve linear or nonlinear differential equations of engineering problems. It has the advantages of simple formula,

flexible geometry operation, easy learning and application. The basic principle of finite difference method can be included as: to approximate the differential equations and definite solution conditions of continuous variables by using the difference equations with a finite number of unknowns after discretization. The operation steps of the finite difference method to solve partial differential equations can be summarized as follows.

a) Determine the basic equations and definite solutions problems;

b) Discretize the continuous solution region into finite grids;

c) Reply the continuous variable function of the solution domain by the discrete variable function on the grid node;

d) Determine the difference scheme of the difference method.

e) Solve the differential equation.

- **One-dimensional diffusion problem**

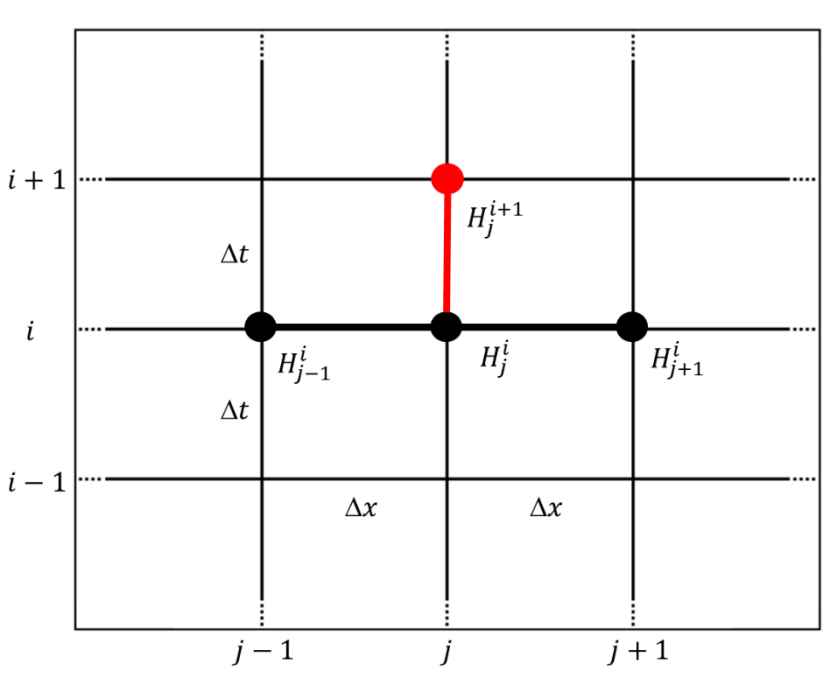


Figure 4.1 The finite difference mesh squares with FTCS scheme of 1D-moisture diffusion equation

On account of the dominant equation of one-dimensional diffusion problem is a second-order nonlinear partial differential equation, this study utilizes the difference scheme of "Forward difference in time, central difference in space (FTCS)" to solve the current problem. Assuming that on a grid of $i \times j$, which divided by $i$ steps in the time domain and $j$ steps in the space domain,

the corresponding scheme of FTCS can be summarized within Fig. 4.1. At step $i$, the unknow node $H_j^{i+1}$ can be calculated from nodes $H_{j-1}^i$, $H_j^i$ and $H_{j+1}^i$.

Discretize the moisture diffusion equation of Eq. (4.5) by FTCS method, the following differential form of the first and second-order nonlinear partial differential equations of diffusion function can be obtained.

$$\frac{\partial H}{\partial t} = \frac{H_j^{i+1} - H_j^i}{\Delta t} \tag{4.9}$$

$$\frac{\partial}{\partial x}\left(D(H)\frac{\partial H}{\partial x}\right) = \frac{D\left(H_{j+\frac{1}{2}}^i\right)\left(H_{j+1}^i - H_j^i\right) - D\left(H_{j-\frac{1}{2}}^i\right)\left(H_j^i - H_{j-1}^i\right)}{\Delta x^2} \tag{4.10}$$

Where,

$H_j^i$ represents the relative humidity at node $(i, j)$, and so on;

$\Delta t$ is the step length in time;

$\Delta x$ is the step length in space;

The $H_{j+\frac{1}{2}}^i$ and $H_{j-\frac{1}{2}}^i$ in Eq. (4.10) can be expressed as

$$H_{j+\frac{1}{2}}^i = \frac{H_j^i + H_{j+1}^i}{2} \tag{4.11}$$

$$H_{j-\frac{1}{2}}^i = \frac{H_j^i + H_{j-1}^i}{2} \tag{4.12}$$

To sum up, the difference equation of 1D-moisture diffusion function can be expressed as Eq. (4.13).

$$H_j^{i+1} = H_j^i + \frac{\Delta t}{\Delta x^2}\left[D\left(H_{j+\frac{1}{2}}^i\right)\left(H_{j+1}^i - H_j^i\right) - D\left(H_{j-\frac{1}{2}}^i\right)\left(H_j^i - H_{j-1}^i\right)\right] \tag{4.13}$$

- **Two-dimensional diffusion problem**

Similar to the one-dimensional diffusion problem, the two-dimensional diffusion problem is also a second-order nonlinear partial differential equation with two variable parameters (x and y). The difference scheme of "Forward difference in time, central difference in space (FTCS)" is also suitable to solve two-dimensional diffusion problem. Assuming that on a grid of $i \times j$, which divided by $i$ steps in the time domain and $j_x$ , $j_y$ steps of the x, y dimension in the space domain, the corresponding scheme of FTCS can be summarized within Fig. 4.2. At step $i$, the unknow node $H_{j_x,j_y}^{i+1}$ can be calculated from nodes $H_{j_x-1,j_y}^i$, $H_{j_x,j_y-1}^i$, $H_{j_x,j_y}^i$, $H_{j_x+1,j_y}^i$ and $H_{j_x,j_y+1}^i$.

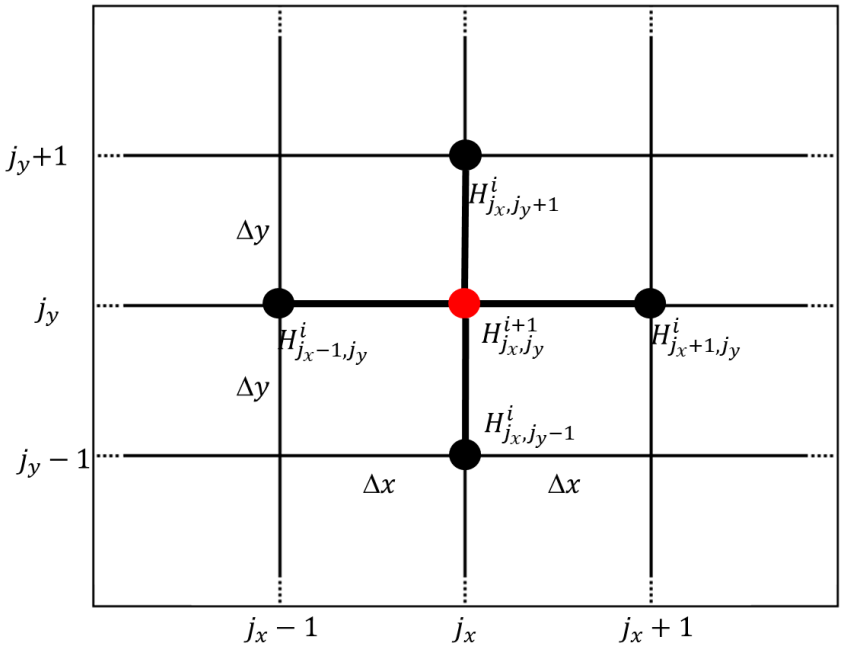


Figure 4.2 The finite difference mesh squares with FTCS scheme of 2D-moisture diffusion equation

Discretize the 2D-moisture diffusion equation of Eq. (4.6) by FTCS method, the following differential form of the right side of the equation can be obtained.

$$\frac{\partial}{\partial x}\left(D(H)\frac{\partial H}{\partial x}\right)+\frac{\partial}{\partial y}\left(D(H)\frac{\partial H}{\partial y}\right)$$

$$=\frac{D\left(H^i_{j_x+\frac{1}{2},j_y}\right)\left(H^i_{j_x+1,j_y}-H^i_{j_x,j_y}\right)-D\left(H^i_{j_x-\frac{1}{2}j_y}\right)\left(H^i_{j_x,j_y}-H^i_{j_x-1,j_y}\right)}{\Delta x^2}$$

$$+\frac{D\left(H^i_{j_x,j_y+\frac{1}{2}}\right)\left(H^i_{j_x,j_y+1}-H^i_{j_x,j_y}\right)-D\left(H^i_{j_x,j_y-\frac{1}{2}}\right)\left(H^i_{j_x,j_y}-H^i_{j_x,j_y-1}\right)}{\Delta y^2} \qquad (4.14)$$

Where,

$H^i_j$ represents the relative humidity at node $(i,j)$, and so on;

$\Delta t$ is the step length in time;

$\Delta x$ and $\Delta y$ are the step length of x and y dimension in space;

The $H^i_{j_x+\frac{1}{2},j_y}$, $H^i_{j_x-\frac{1}{2},j_y}$, $H^i_{j_x,j_y+\frac{1}{2}}$ and $H^i_{j_x,j_y-\frac{1}{2}}$ in Eq. (4.14) can be calculated by referring Eq. (4.11) and Eq. (4.12), similar expression can be inferred. To sum up, the difference equation of 2D-moisture diffusion function can be expressed as the following equation.

$$H_{j_x,\,j_y}^{i+1} = H_{j_x,\,j_y}^{i} + \Delta t \left[ \frac{D\left(H^{i}_{j_x+\frac{1}{2},\,j_y}\right)\left(H^{i}_{j_x+1,\,j_y} - H^{i}_{j_x,\,j_y}\right) - D\left(H^{i}_{j_x-\frac{1}{2},\,j_y}\right)\left(H^{i}_{j_x,\,j_y} - H^{i}_{j_x-1,\,j_y}\right)}{\Delta x^2} \right.$$
$$\left. + \frac{D\left(H^{i}_{j_x,\,j_y+\frac{1}{2}}\right)\left(H^{i}_{j_x,\,j_y+1} - H^{i}_{j_x,\,j_y}\right) - D\left(H^{i}_{j_x,\,j_y-\frac{1}{2}}\right)\left(H^{i}_{j_x,\,j_y} - H^{i}_{j_x,\,j_y-1}\right)}{\Delta y^2} \right] \quad (4.15)$$

It should be noted that diffusion models to simulate the development of moisture in concrete are only a means of digitizing the phenomenon. The results of the mathematical model will be close to but not quite equal to the actual situation. Because of the irregular porous structure inside the concrete, the development of relative humidity inside the concrete will show differential development rules. This also leads to a certain deviation between the development of internal humidity obtained by mathematical model simulation and the actual situation. These deviations are inevitable and are often ignored in the simulation.

The diffusion coefficient is influenced by several factors, such as temperature, relative humidity, concrete internal structure, surface situation or other extral factors[6-8]. As for the aspect of concrete, the key factors are represented by the effects of moisture and temperature. The effect of moisture content on the moisture diffusion coefficient was investigated thoroughly in the past and it was shown that the moisture diffusion coefficient is significantly dependent on moisture content[9,10]. Therefore, modern computational tools need to involve the effect of moisture content on the moisture diffusion coefficient in order to produce satisfactory results.

In this study, referring to fib Model Code 2010, the diffusion coefficient $D(H)$ is calculated as Eq. (4.7) with the consideration of relative humidity. The involved parameter $D_1$ is determined through the compressive strength of the mortar specimens instead of considering the effect of temperature on it. The research related to parameter $D_1$ shows that it is dependent on temperature and shows an increased tendency with the increasing temperature[11,12]. In contrast, the determine method of $D_1$ in fib Model Code 2010 neglected the temperature effect on the diffusion, which will lead to a higher estimation of moisture content. Such a result should be noticed when preforming the following procedure of evaluating the equivalent age and strength development.

## 4.2 Experimental investigation

### 4.2.1 Materials

A series of cement mortars under different curing conditions were tested in this study, in which the chemical composition of used OPC and the properties of cement and river sands are listed in Table 4.1 and Table 4.2. All materials were provided by local companies.

Table 4.1 Chemical composition of cement (% by mass).

| | $C_3S$ | $C_2S$ | $C_3A$ | $C_4AF$ | MgO | $SO_3$ | $Cl^-$ | $Na_2O$ | LOI |
|---|---|---|---|---|---|---|---|---|---|
| Cement | 56 | 18 | 9 | 9 | 1.41 | 2.10 | 0.015 | 0.50 | 2.26 |

Table 4.2 Properties of cement and sand

| Ordinary Portland Cement (OPC) | | Sand | |
|---|---|---|---|
| Density (g/cm$^3$) | 1.41 | Absolutely density (g/cm$^3$) | 2.54 |
| Specific surface area (cm$^2$/g) | 3340 | Surface dry density (g/cm$^3$) | 2.59 |
| Initial setting time (min) | 135 | Absorption (%) | 2.03 |
| Final setting time (min) | 200 | Fineness modulus | 2.65 |

### 4.2.2 Mix preparation of specimens

The water-cement ratio of the tested mortars was 0.50, while the unit weight of cement was 564.6 kg/m$^3$. The detail of the mix proportion is shown in Table 4.3. Three types of mortar specimens with different dimensions were used, including cubic specimens (1cm×1cm×1cm) and two kinds of cylindrical specimens (diameter×height: ø5cm×10cm and ø10cm×20cm) (see Fig. 4.3), to study the effect of relative humidity on the development of the compressive strength of the cement mortars. Each branch of specimens was cured under the same chamber with a constant temperature and relative humidity. Three levels of temperature (10ºC, 18ºC and 40ºC) and four different relative humidity (70%, 80%, 90% and 100%) were designed in this study. Water bath curing was used for specimens under 100% RH. According to the test standard JIS A1108 [13], the mean measured values of compressive strength of each mortar was used for the study obtained by the measured values of three corresponding specimens. The specimens with different temperature and relative humidity were named as T*x*-RH*y* meaning that the specimen was cured under *x* ºC of temperature and *y*% of relative humidity.

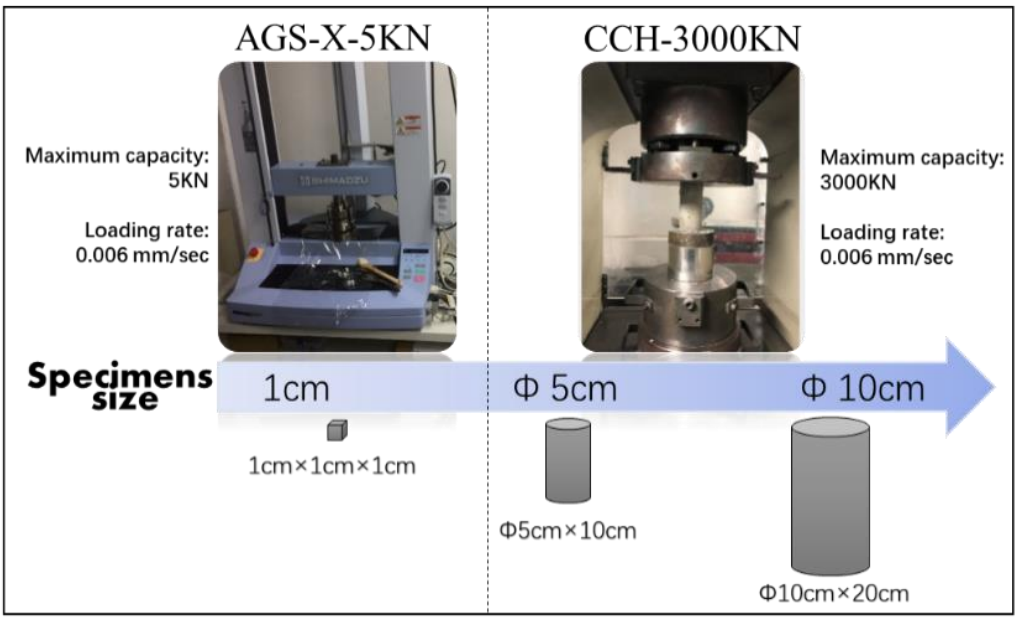


Figure 4.3 Compressive strength testing machines and corresponding specimens sizes

Table 4.3 Mix proportion

| W/C | Unit Weight (kg/m$^3$) | | |
|---|---|---|---|
| | Water | Cement | Sand |
| 0.5 | 282.3 | 564.6 | 1552.7 |

### 4.2.3 Test method

To obtain high accuracy test results of specimens with different sizes, two different compressive strength testing machines with different maximum load capacity (AGS-X-5KN and CCH-3000KN) were used, as shown in Fig. 4.3. Moreover, in order to reflect the effect of curing temperature and relative humidity on the specimens at a very early age, all specimens were directly moved to their corresponding curing chambers after casting. Demolding of the specimens was performed after 12-15 hours after casting depending on the degree of hardening of the specimens. Subsequently, all specimens were absolutely exposed and maintained in designed temperature and relative humidity environment up to their designed curing time.

### 4.3 Test results and Discussion

#### 4.3.1 Compressive strength of each curing temperature and relative humidity

It was well known that environmental temperature has a noteworthy influence on the development of compressive strength of concrete/mortar. In this research, all mortar specimens were placed directly to the corresponding curing environment after their casting. Table 4.4 lists the whole compressive strength results for the specimens with different temperature, relative humidity, and specimen size. As shown in Fig. 4.4, when curing temperature varies from 10°C to 40°C, the compressive strengths of the cement mortars at low temperature are obviously lower than that at high temperatures, especially when they are under a low relative humidity. For example, the compressive strength of mortars under 70% relative humidity and 10 °C of temperature were significantly lower than the levels of other specimens, regardless of their curing age. The difference of compressive strength of the mortars caused by curing temperature increased as curing age, as shown in Fig. 4.4. The 28-days compressive strength of the mortars at 18 °C of temperature was close to or higher than the one at 40 °C under the same relative humidity. This is explained by the "crossover effect" which illustrates that a higher temperature at an early age can result in concretes present a higher initial strength and lower long-term strength[14]. Based on the results of the present study, this "cross" behavior is also applicable to concretes under different relative humidity.

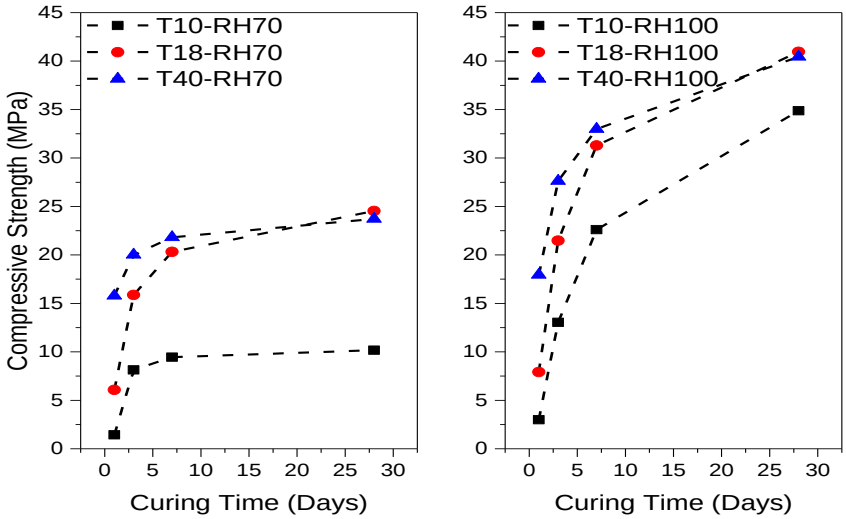


Figure 4.4 Compressive strengths of ø5cm cylindrical specimens as curing age

Table 4.4 Experimental compressive strength

| Size | T (ºC) | Relative humidity (%) | Compressive strength (MPa) | | | |
|---|---|---|---|---|---|---|
| | | | 1 day | 3 days | 7 days | 28 days |
| 1 $cm^3$ | 10 | 70 | 2.90 | 4.04 | 5.20 | 6.81 |
| | | 80 | 3.27 | 5.72 | 6.50 | 8.96 |
| | | 90 | 3.35 | 5.99 | 9.89 | 15.03 |
| | | 100 | 3.91 | 13.61 | 21.34 | 30.06 |
| | 18 | 70 | 9.35 | 17.42 | 18.10 | 21.45 |
| | | 80 | 10.35 | 18.55 | 22.88 | 28.88 |
| | | 90 | 10.63 | 19.66 | 27.26 | 33.00 |
| | | 100 | 11.05 | 22.78 | 29.25 | 40.26 |
| | 40 | 70 | 16.19 | 20.81 | 21.34 | 22.87 |
| | | 80 | 17.57 | 22.20 | 25.16 | 29.11 |
| | | 90 | 17.58 | 24.13 | 26.97 | 32.23 |
| | | 100 | 19.66 | 27.81 | 32.81 | 39.97 |
| ø5×10cm | 10 | 70 | 1.44 | 8.14 | 9.67 | 10.17 |
| | | 80 | 2.14 | 9.58 | 12.45 | 12.80 |
| | | 90 | 2.51 | 10.88 | 13.76 | 17.18 |
| | | 100 | 3.00 | 13.05 | 22.61 | 34.88 |
| | 18 | 70 | 6.08 | 15.87 | 20.32 | 24.54 |
| | | 80 | 6.91 | 17.44 | 24.26 | 29.70 |
| | | 90 | 7.28 | 18.35 | 27.38 | 33.20 |
| | | 100 | 7.92 | 21.48 | 31.30 | 40.96 |
| | 40 | 70 | 15.79 | 20.01 | 21.81 | 23.72 |
| | | 80 | 16.10 | 21.37 | 27.39 | 30.11 |
| | | 90 | 16.68 | 23.49 | 29.47 | 33.77 |
| | | 100 | 17.95 | 27.63 | 32.99 | 40.44 |
| Ø10×20cm | 10 | 70 | 1.72 | 8.11 | 14.78 | 18.18 |
| | | 80 | 2.54 | 8.68 | 15.88 | 20.76 |
| | | 90 | 3.23 | 9.13 | 16.88 | 23.37 |
| | | 100 | 3.55 | 13.40 | 22.44 | 34.51 |
| | 18 | 70 | 5.25 | 15.51 | 24.26 | 29.79 |
| | | 80 | 6.32 | 16.11 | 26.08 | 32.91 |
| | | 90 | 6.32 | 18.02 | 27.63 | 34.79 |
| | | 100 | 7.72 | 19.87 | 29.01 | 40.86 |
| | 40 | 70 | 12.49 | 18.95 | 24.53 | 25.57 |
| | | 80 | 13.69 | 20.05 | 27.41 | 31.74 |
| | | 90 | 14.38 | 22.14 | 29.07 | 33.97 |
| | | 100 | 16.81 | 27.38 | 32.90 | 40.17 |

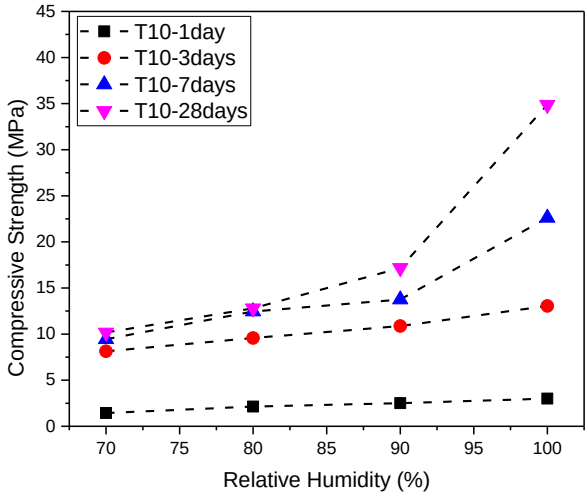


a. curing at 10 °C

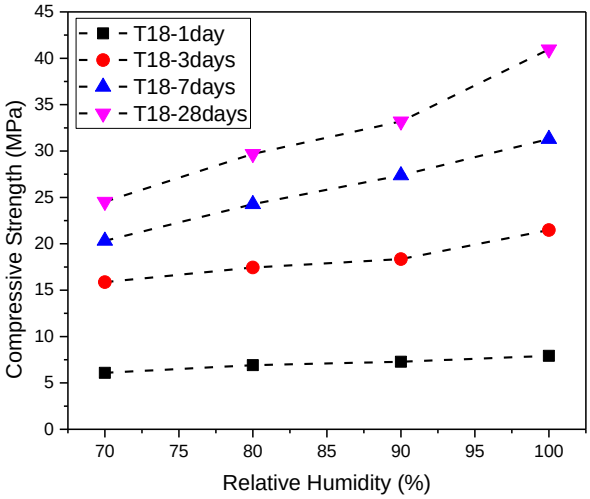


b. curing at 18 °C

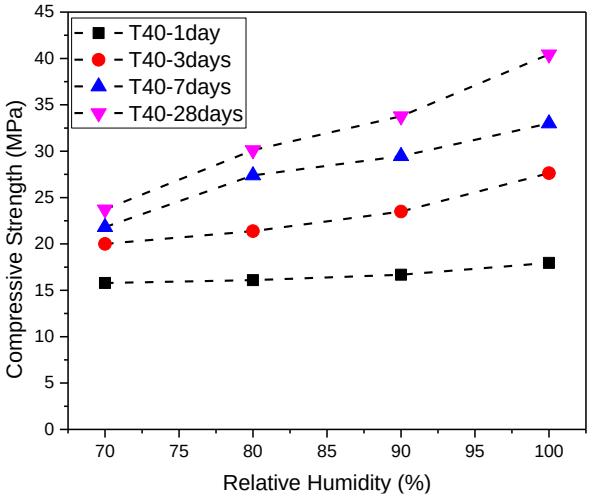


c. curing at 40 °C

Figure 4.5 Compressive strength of ø5cm cylindrical specimens with RH

Fig. 4.5 shows the development of compressive strength of ø5cm specimens with different relative humidity under different temperature and with various curing ages. Results show that relative humidity has a significant effect on the development of compressive strength of the mortars regardless of the level of curing temperature. In an unsaturated relative humidity state, as shown in Fig. 4.5 the evaporation of water inside mortar occurred when the ambient relative humidity was lower than 100%. The mortars presented a low compressive strength when it was under a low relative humidity, especially at the later age of curing. This is attributed to that more and more moistures were transferred from the surface of mortars to the air as time goes on, which had been similarly reported by other researchers [15-17].

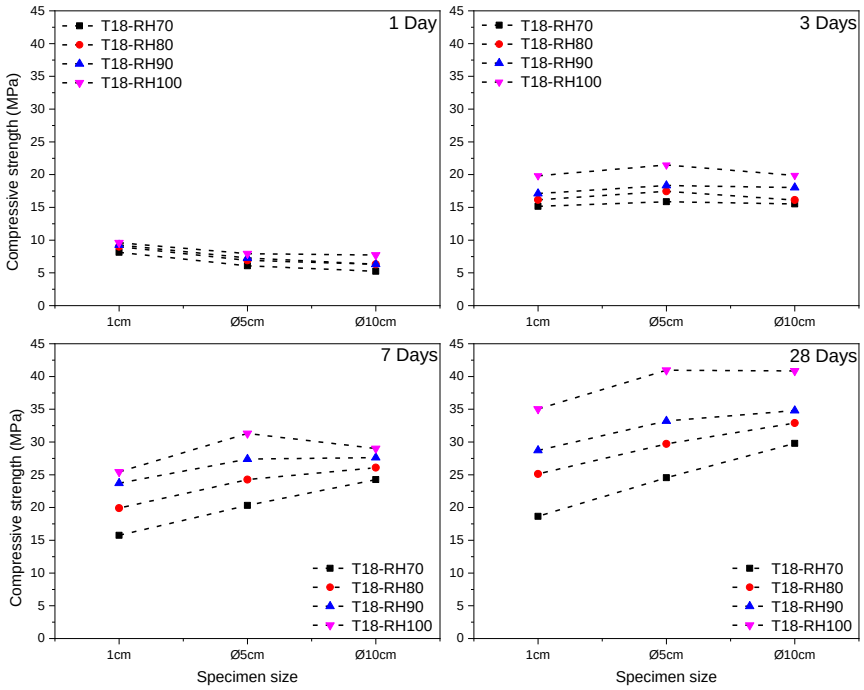


Figure 4.6 Compressive strength development of specimens under various curing conditions

Fig. 4.6 shows the test results of different size specimens at various relative humidity and curing ages. At the early age of 1 day and 3 days, the compressive strengths of large-size mortars were lower than those of small-size specimens. At the ages of 7 days and 28 days, however, the compressive strengths of ø10cm mortar specimens were slightly higher than others', except for Specimen T18-RH100 at 7 days of curing that may cause by tested problems. Under the same curing condition, the rate of water consumption of mortars caused by the inside cement hydration activity should be the same regardless of the size of specimens. However, the moisture evaporation from the surface of specimens led to a decrease of the relative humidity inside the mortar. The affected depth should be the same for the specimens with the same size. In theory, the impact of curing relative

humidity on moisture loss as well as on mortar compressive strength should decrease as the distance from the center to the mortar surface. Fig. 4.7 shows a schematic of the internal humidity distribution of ø5cm and ø10cm specimens after a period of moisture evaporation. In this state, the section on the right of each diagram shows the humidity distribution of the section. Here, the internal humidity is divided into two parts, hydratable zone (RH＞80%) and non-hydratable zone (RH＜80%). After a period of exposure, the moisture on the periphery of the specimen evaporates and the humidity drops below 80%. According to the minimum humidity required for cement hydration, the cement will no longer hydrate. At the same time, the cement with more than 80%RH (hydratable zone) is able to continuously hydrated. The compressive strength of ø10cm should be higher than ø5cm according to the proportion of the hydratable zone of the section.

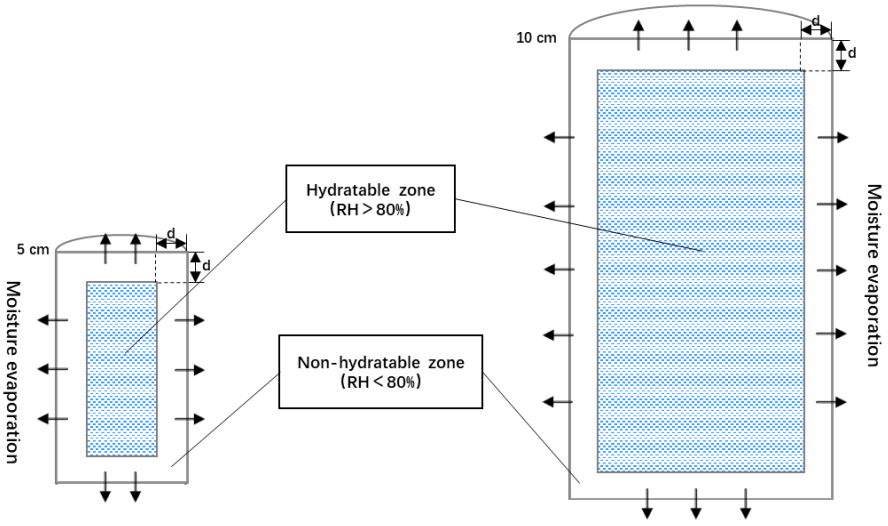


Figure 4.7 Internal moisture distribution and main surface evaporation zones of mortars

### 4.3.2 Simulation of relative humidity distribution

After the simulation, the internal relative humidity distribution at 18°C of cross-section of each size specimens are shown from Fig. 4.8 to Fig. 4.10. Since similar relative humidity distribution trends can be found at different temperatures, the only curing condition of each specimen size was carried out when curing at 18 °C. Figure 4.8a, b and c respectively shows the change of cross-section humidity of specimens with the size of $1\,cm^3$ under curing humidity of 70%RH, 80%RH, and 90%RH. With the curing time goes on, the relative humidity content of the cross-section gradually decreases due to the moisture evaporation. For each size specimen, relative humidity at the edge of the cross-section is close to the environmental humidity, this is due to the setting of boundary conditions of the simulation. Since a shallow depth that affected by humidity of the specimens of

$1\,cm^3$, the environmental humidity will soon affect the central position of the section, so the humidity at the central position of the section will gradually decrease with the passage of curing ages, see in Fig. 4.8. Moreover, the internal relative humidity distribution of specimens with different cross-section shapes is different, which is mainly determined by different simulation methods based on different moisture diffusion system. Therefore, non-uniform relative humidity distribution is found between the corner position and the central position on a cubic cross-section($1\,cm^3$ specimen), contrastively, which is more uniform distribution on a circular cross-section (Ø5cm and Ø10cm specimen). By comparing the cross-section relative humidity of the specimen with different sizes, the same curing temperature and relative humidity in Fig. 4.8 to Fig. 4.10, it is evidence that different ambient relative humidity has different effects on specimens of different sizes. The specimens with large cross-sectional areas are less affected by the ambient relative humidity, which leads to a high relative humidity content on the cross-section of the bigger size specimen.

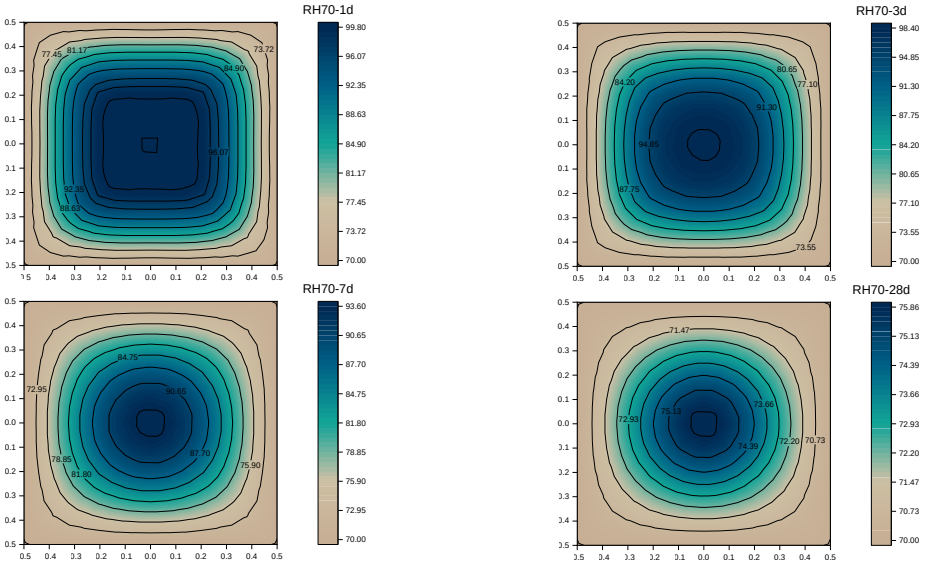


a. Curing at 18ºC-70%RH

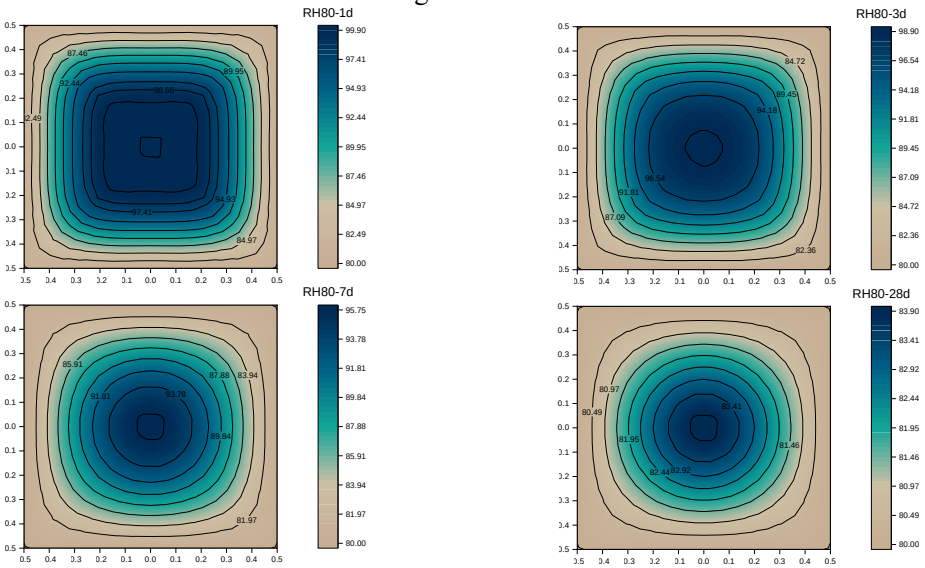


b. Curing at 18ºC-80%RH

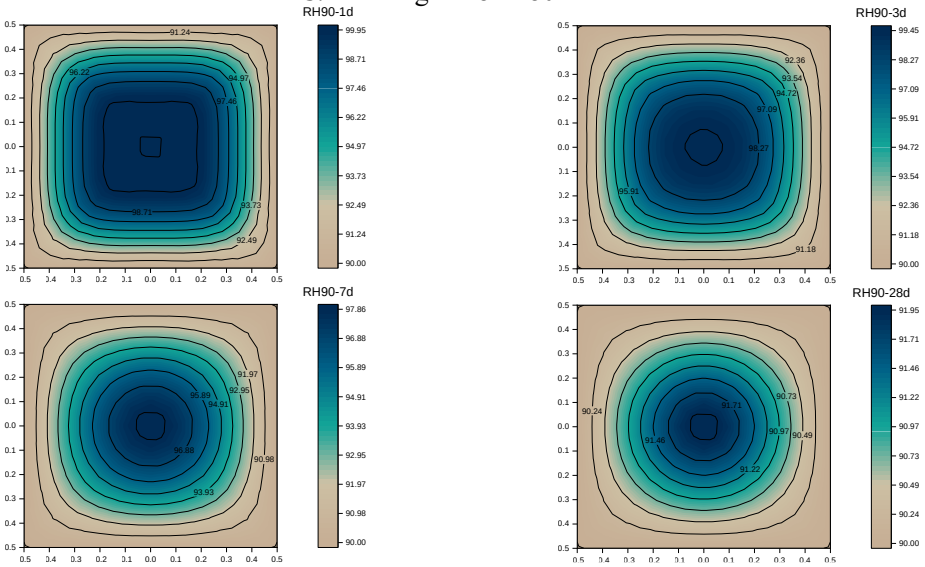


c. Curing at18ºC-90%RH

Figure 4.8 Relative humidity distribution of specimen size 1cm$^3$ (in %RH)

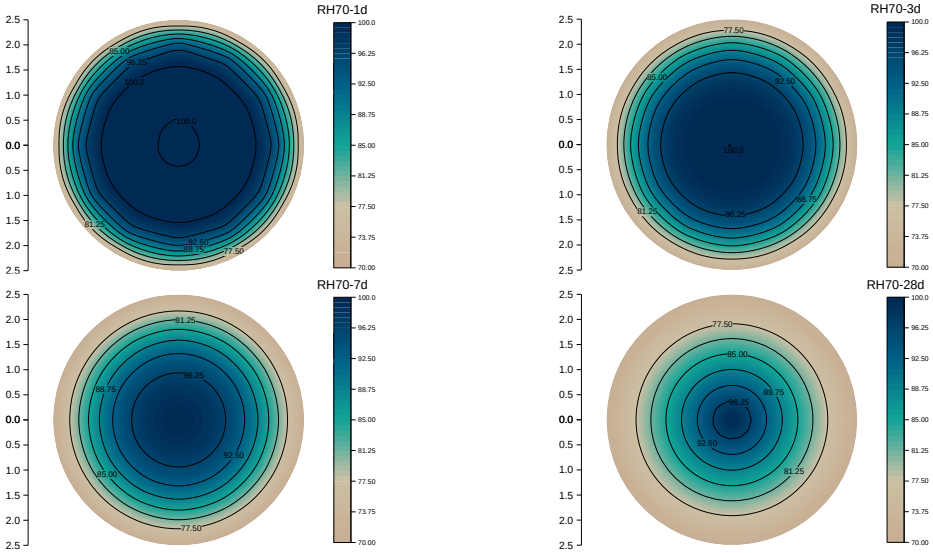


a. Curing at 18ºC-70%RH

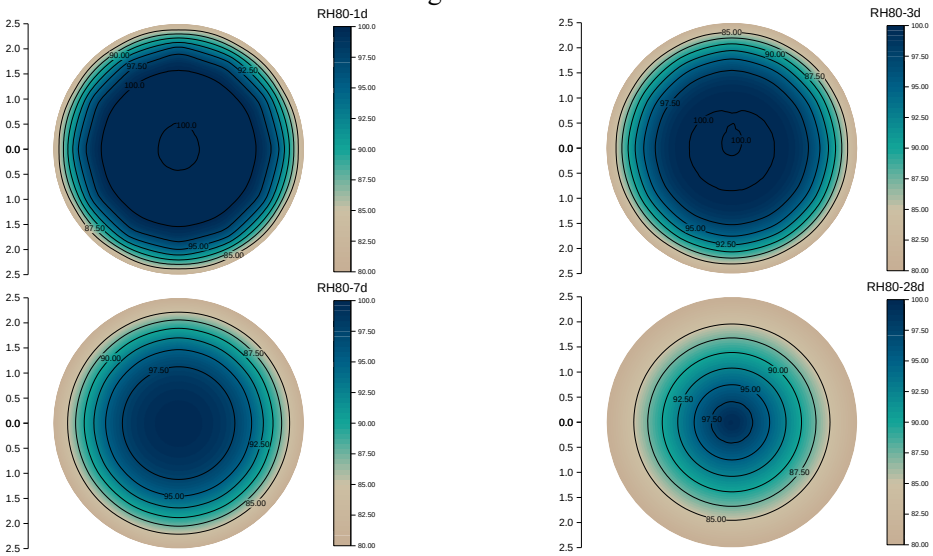


b. Curing at 18ºC-80%RH

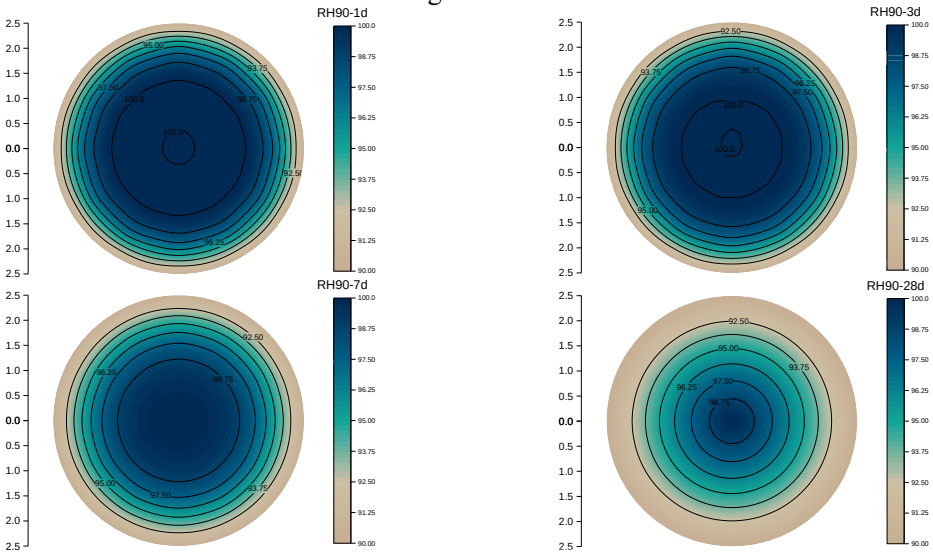


c. Curing at 18ºC-90%RH

Figure 4.9 Relative humidity distribution of specimen size Ø5cm (in %RH)

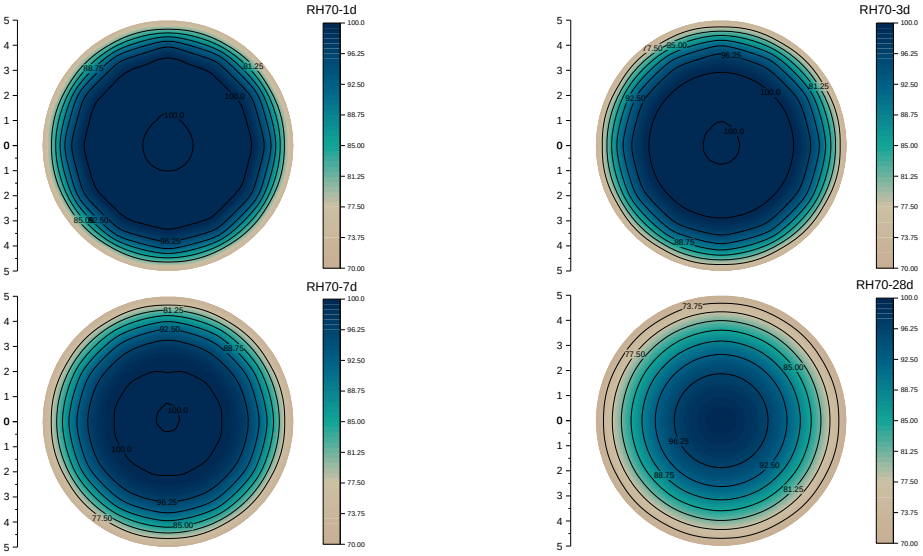


a. Curing at 18ºC-70%RH

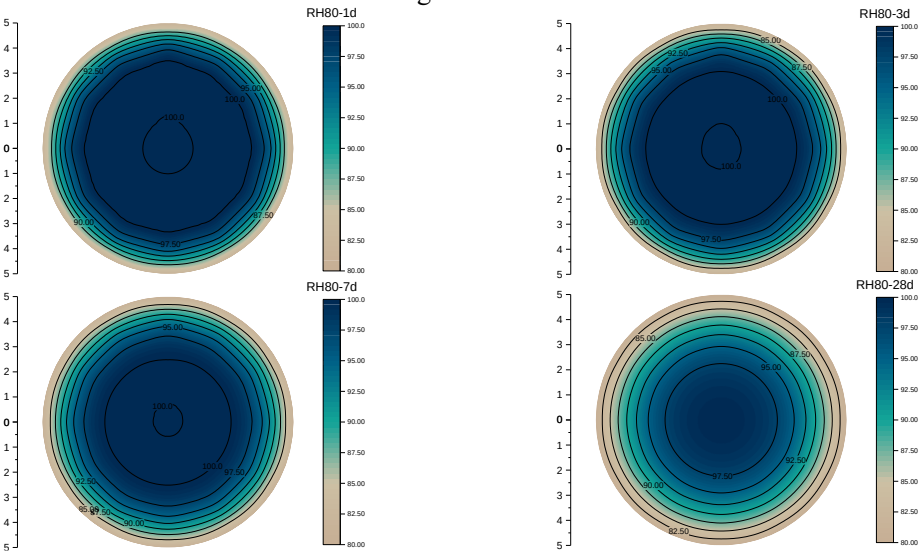


b. Curing at 18ºC-80%RH

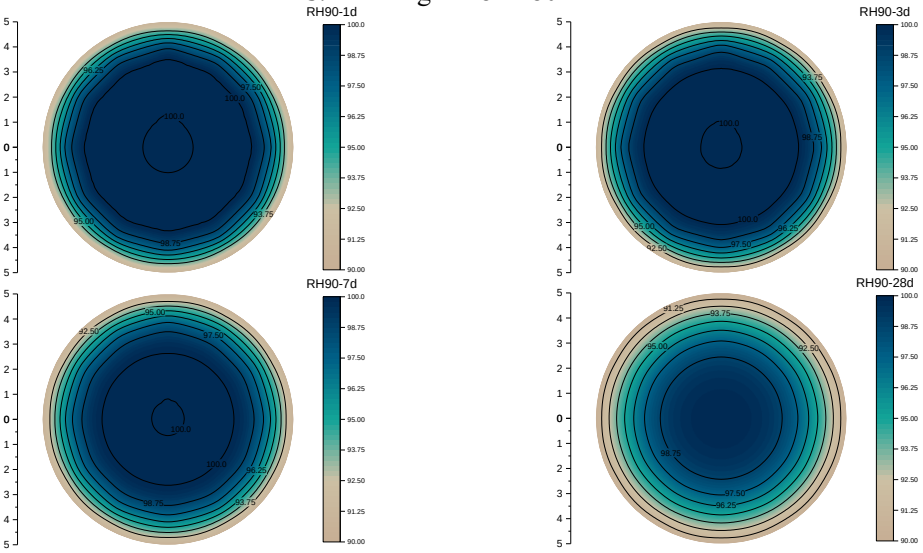


c. Curing at 18ºC-90%RH

Figure 4.10 Relative humidity distribution of specimen size Ø10cm (in %RH)

### 4.3.3 Distribution of equivalent age

Correspondingly, based on the relative humidity distribution on the cross-section of each curing condition and specimen size, the equivalent age distribution can be calculated through the proposed equivalent age function Eq. (3.13) that considered the influence of both temperature and relative humidity. First of all, under the condition of 18°C-100%RH, the corresponding equivalent ages of 1,3,7 and 28 days are predicted according to Eq. (3.13) as the results of 0.91, 2.73, 6.37 and 25.48 days, respectively. The predicted equivalent ages under saturated humidity(100%RH) are expected to be used for comparative analysis of the maturity distribution of each cross-section at unsaturated humidity(70%RH, 80%RH and 90%RH) with different specimens sizes.

Fig.4.11 to Fig.4.13 shows the equivalent age distribution on the cross-section of each size specimen curing at 18°C and different curing relative humidity. In Figure 4.11, the equivalent age distribution of $1cm^3$ size specimens are shown. When the curing age is 1day, the equivalent age distribution of section under different curing conditions is relatively uniform with a large area in the center part that is equal to the equivalent age of 0.91day under 100%RH curing. At a low curing relative humidity of 70%(see Figure 4.11a), the gradient distribution of equivalent age caused by curing relative humidity becomes evident from the 3rd day of curing, which is mainly reflected in the span of the equivalent age at the edge to the center from less than one day to several days. This is because the relative humidity at the edge is close to the ambient humidity. When the relative humidity is lower than 80%RH, the hydration reaction stops happening, so the equivalent age at the edge will not continue to increase. However, there is sufficient moisture in the center for hydration to promote an increase in the equivalent age. The gradual loss of moisture with time leads to the relative humidity decrease of the central part, results in the growth speed of the equivalent age gradually slows down. This also results in the equivalent age of central area just slightly higher than 7 days after curing for 28 days. Similar equivalent age distribution tendency can be found on 80%RH and 90%RH of specimens, but it is worth noting that the hydration reaction of all the cross-section of specimens under 90%RH will continue, hence the degree of equivalent age is significantly higher than that under other conditions. Although 80%RH is the critical relative humidity for cement hydration, the hydration rate of cement is still very low when the relative humidity is in the range between 80%RH and 95%RH[18]. Therefore, it can explain why the maximum equivalent age of 7 days(6.04 days) and 28 days(7.36 days) is so closed in the cross-section of $1cm^3$ specimen when curing at 80%RH. In contrast, the maximum equivalent age of Ø5cm and Ø10cm specimens at different curing humidity are closed at corresponding curing days due to the highest internal relative humidity equals to 100%RH for all curing days.

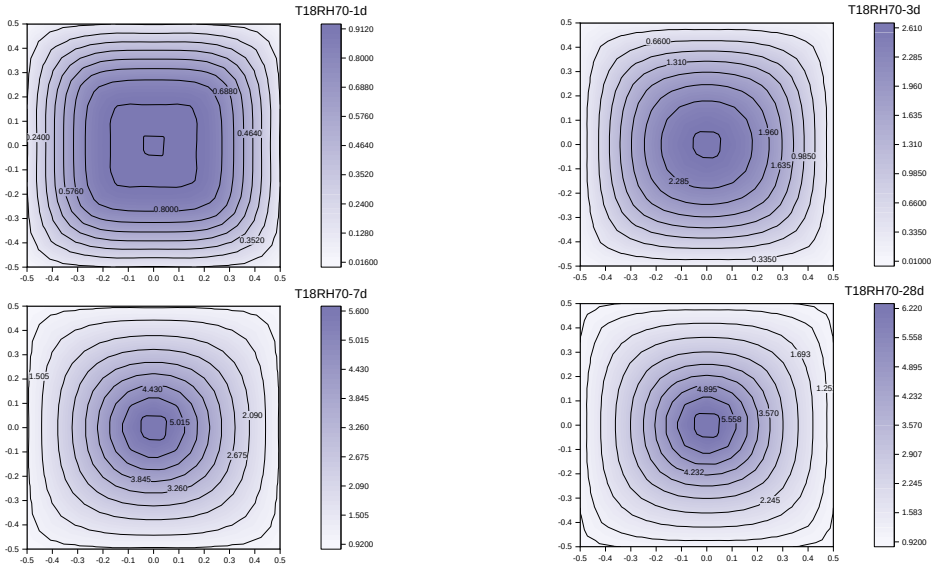


a. Curing at 18ºC-70%RH

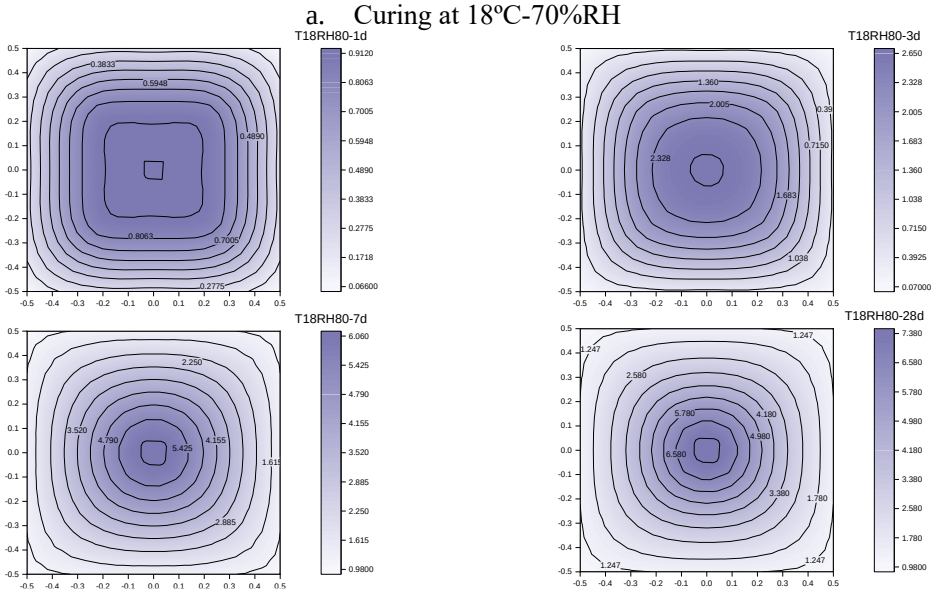


b. Curing at 18ºC-80%RH

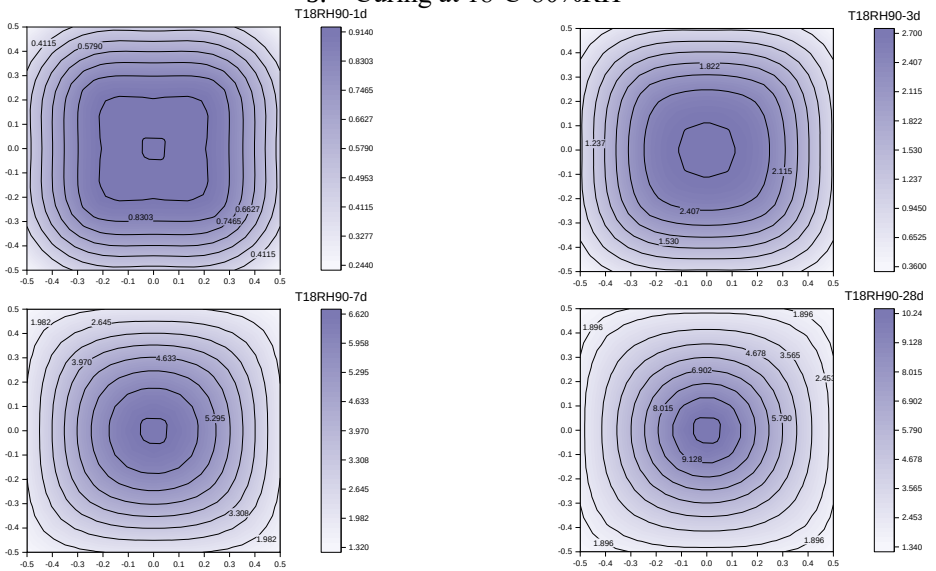


c. Curing at 18ºC-90%RH

Figure 4.11 Equivalent age of specimen size 1cm³ (in days)

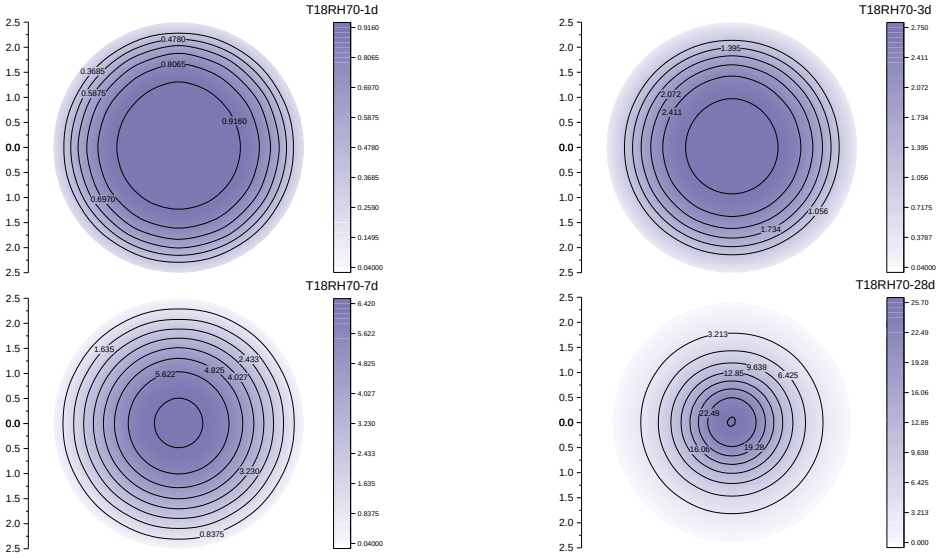


a. Curing at 18ºC-70%RH

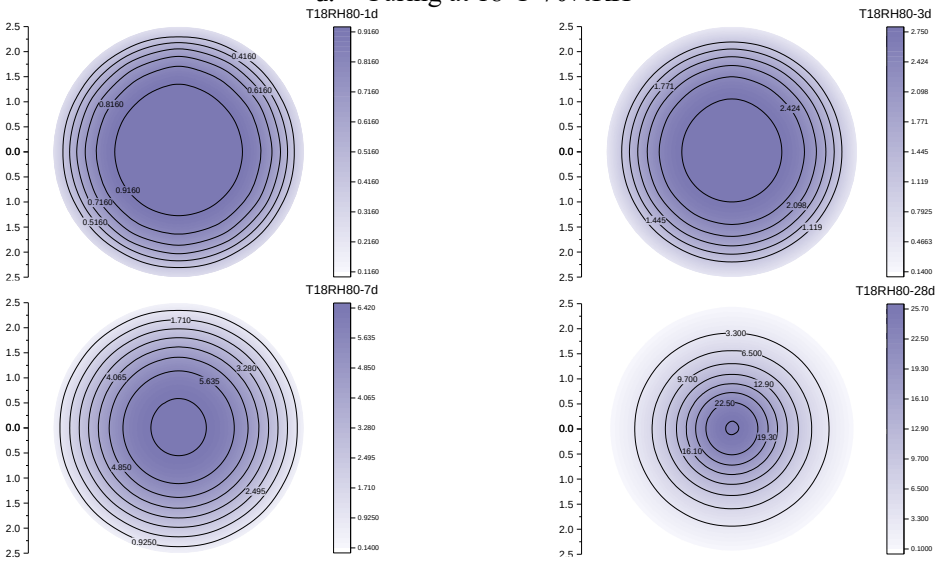


b. Curing at 18ºC-80%RH

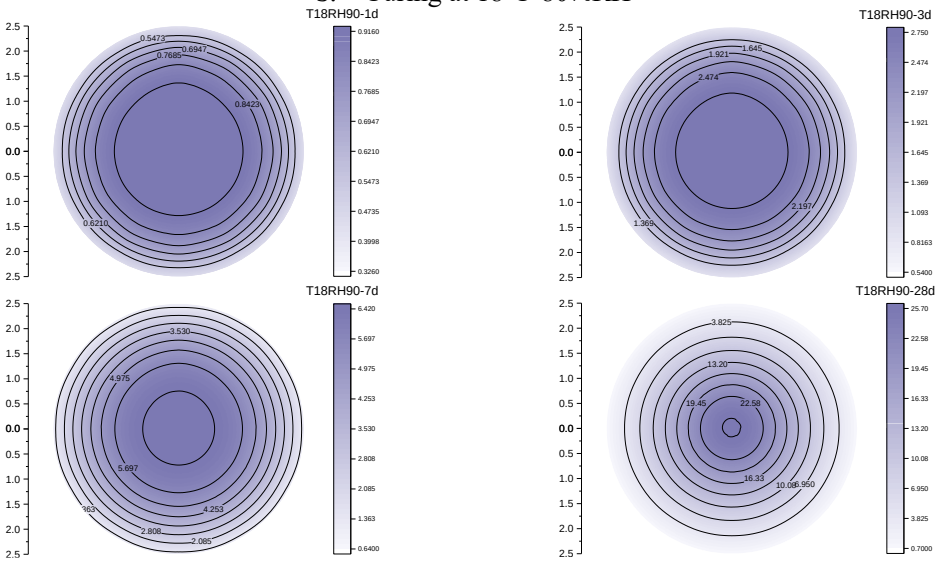


c. Curing at 18ºC-90%RH

Figure 4.12 Equivalent age of specimen size Ø5cm (in days)

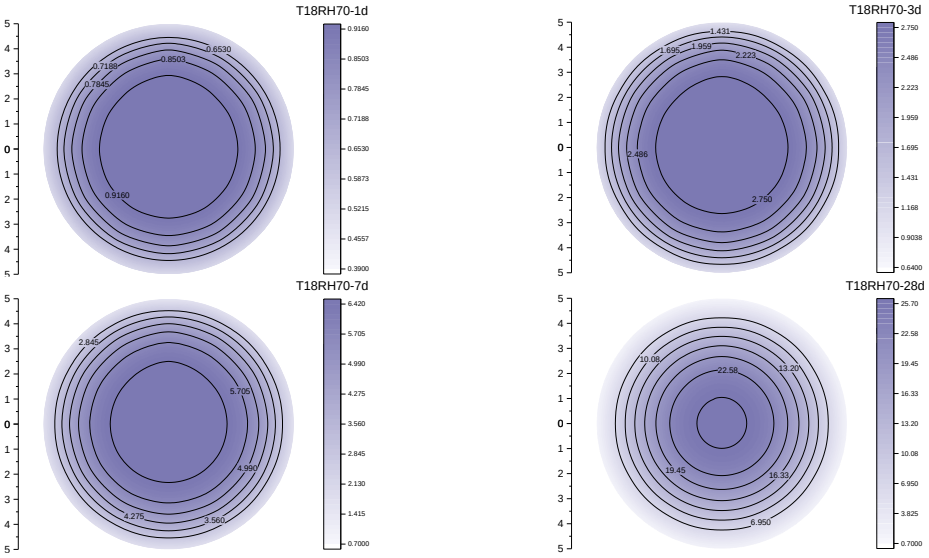


a. Curing at 18ºC-70%RH

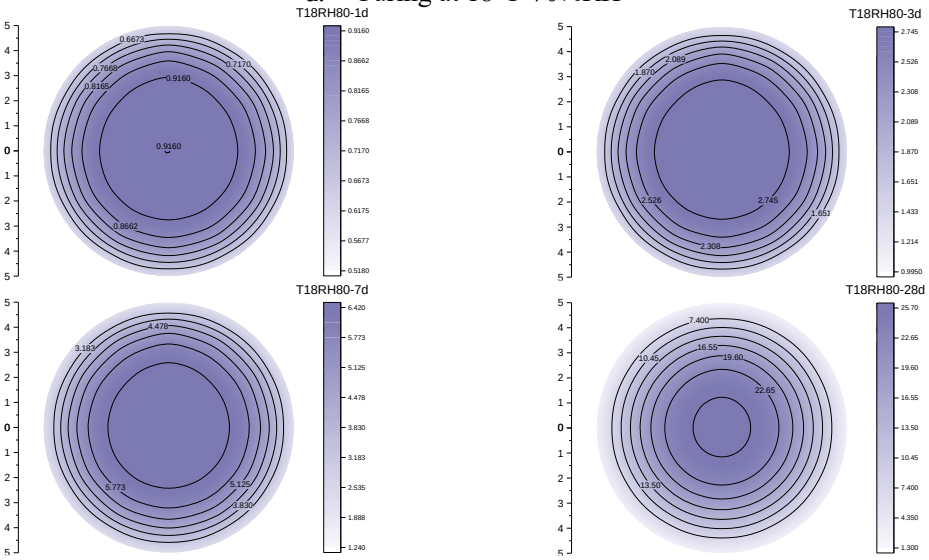


b. Curing at 18ºC-80%RH

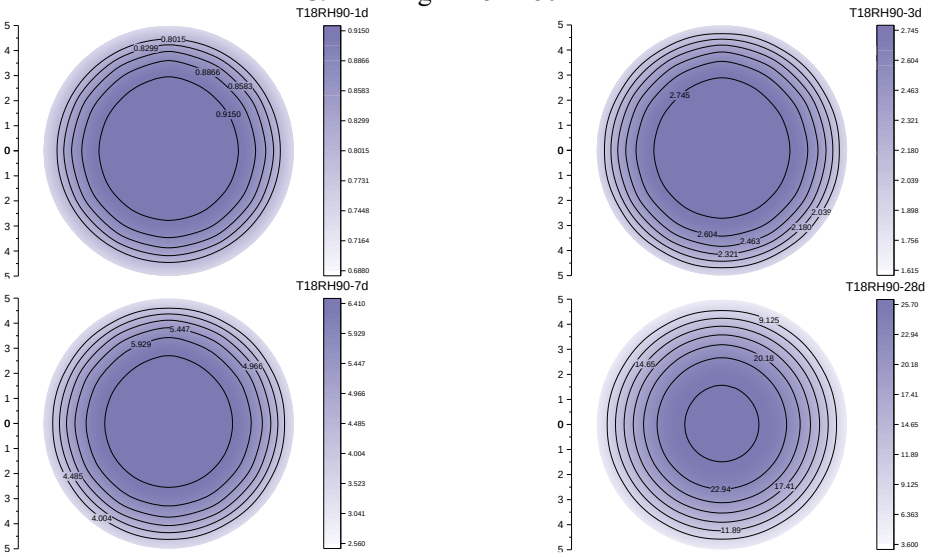


c. Curing at 18ºC-90%RH

Figure 4.13 Equivalent age of specimen size Ø10cm (in days)

As a conclusion, the equivalent age development versus actual curing age of each depth of Ø5cm specimen is shown in Fig. 4.14. Fig. 4.14a shows the position of each depth on the cross-section and Fig. 4.14b, c, d respectively shows the curing condition of 18°C-70%RH, 80%RH and 90%RH. A similar equivalent age development tendency can be found in the relative humidity condition of 70%RH and 80%RH within Fig. 4.14b and Fig. 4.14c. Thanks to the low curing relative humidity(70%RH and 80%RH), only slight difference on the equivalent age can be found at a depth of 1.5cm and 2cm, and almost the same level at 0.5cm and 1cm. This is because the simulation result of relative humidity of both conditions drop below or close to 80%RH at 0.5cm and 1cm depth. The relatively obvious development of the equivalent age can be found at each depth in the conditions of curing humidity for 90%RH. It is easy to understand that the curing humidity 90%RH is higher than the critical relative humidity 80%RH of cement hydration, so each internal depth will continue to hydrate throughout the whole curing process.

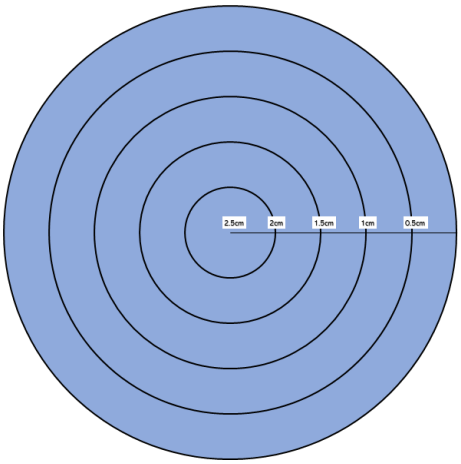


a. Depth schematic diagram of Ø5cm specimen

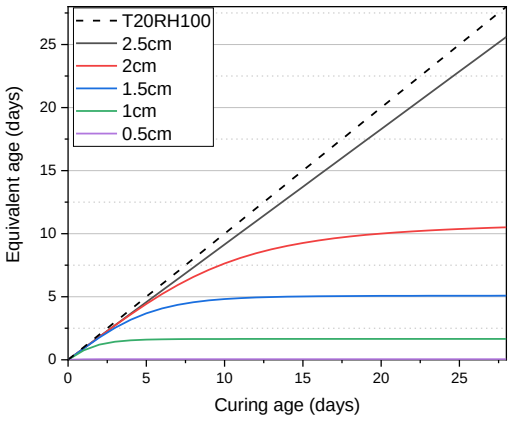


b. Curing at 18°C-70%RH

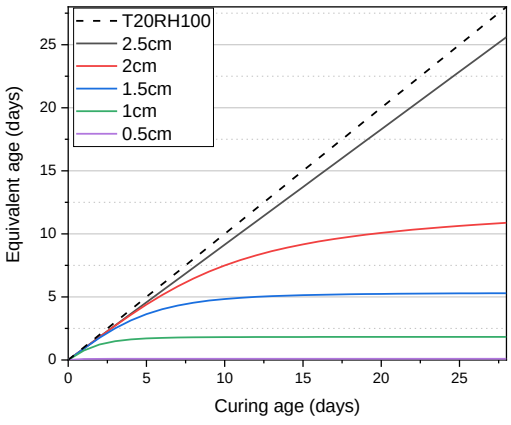


c. Curing at 18°C-80%RH

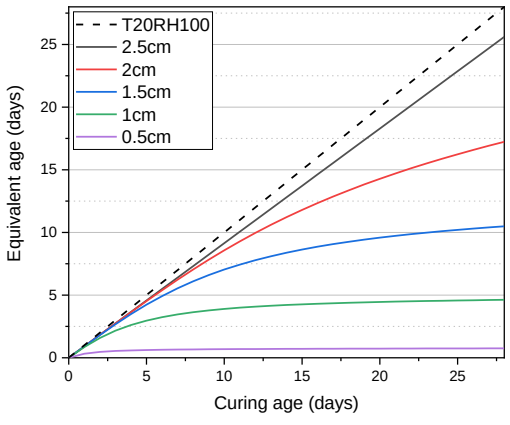


d. Curing at 18°C-90%RH

Figure 4.14 Equivalent age versus actual curing age of each depth of Ø5cm specimen

### 4.3.4 Distribution of compressive strength

Based on the equivalent age distribution of the specimens under different curing conditions, the strength distribution of each cross-section can be calculated according to Eq. (4.3). Fig. 4.15 to Fig. 4.23 have given the strength development of each piratical days of all the unsaturated relative humidity curing conditions(70%RH, 80%RH and 90%RH) and temperature conditions(10°C, 18°C and 40°C). In addition, according to the strength distribution results of each section, the corresponding average strength is calculated to present the predicted strength of each specimen. The calculation of average strength is carried out by integrating the strength of coordinate points on the cross-section with the center point as the origin of the coordinate. The specific calculation of the two different section shapes are based on the following equations.

For square section ($1cm^3$)

$$\bar{f} = \frac{1}{S}\iint f_{(x,y)}\, dx\, dy \tag{4.16}$$

For circular section (Ø5cm, Ø10cm)

$$\bar{f} = \frac{1}{S}\iint f_{(r,\theta)}\, dr\, d\theta \tag{4.17}$$

where，

$x$ is the distance from the center to the edge of the square section in the horizontal direction;

$y$ is the distance from the center to the edge of the square section in the vertical direction;

$r$ is the radius of the circular section;

$\theta$ is the angle;

$S$ is the area of the cross-sectional ;

$f_{(x,y)}$ and $f_{(r,\theta)}$ are the strength at the coordinates of $(x, y)$ and $(r, \theta)$;

$\bar{f}$ is the average strength.

The simulated cross-section in this study represents the cross-section at the middle position of the experimental specimen. When the specimen is under pressure on both sides, the position at top and bottom present a higher strength than the middle position of the specimen due to the hooping-effect. Therefore, the cross-section of the middle position of the specimen has a critical meaning to present the strength of the whole specimen. In addition, because the experimental body is affected by uniform distribution pressure, the average strength on the cross section calculated by integral can better reflect its strength grade.

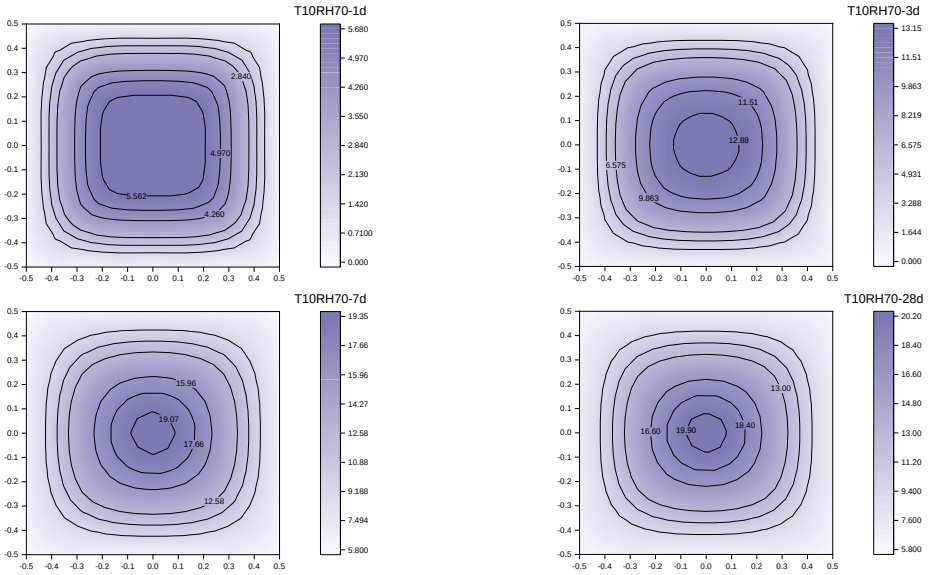


a. Curing at 10ºC-70%RH

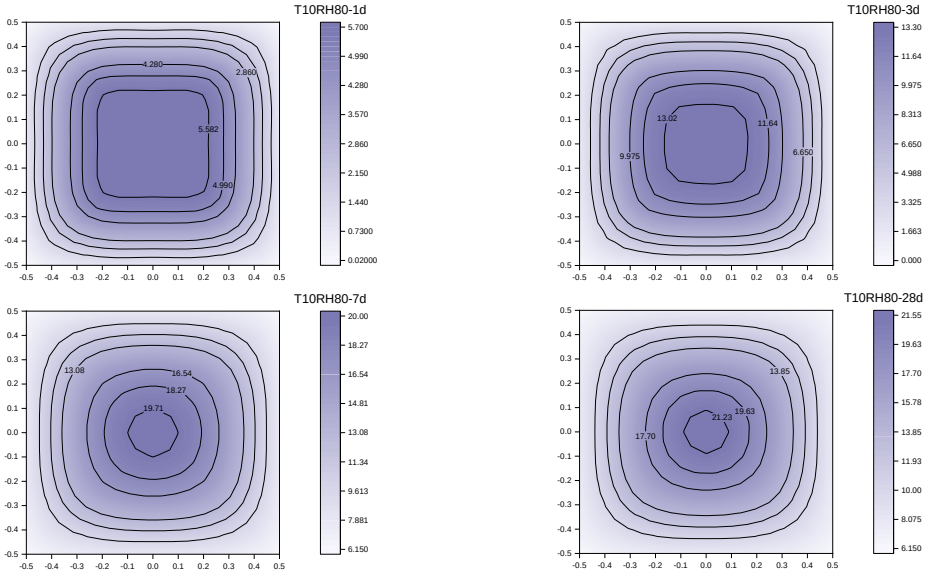


b. Curing at 10ºC-80%RH

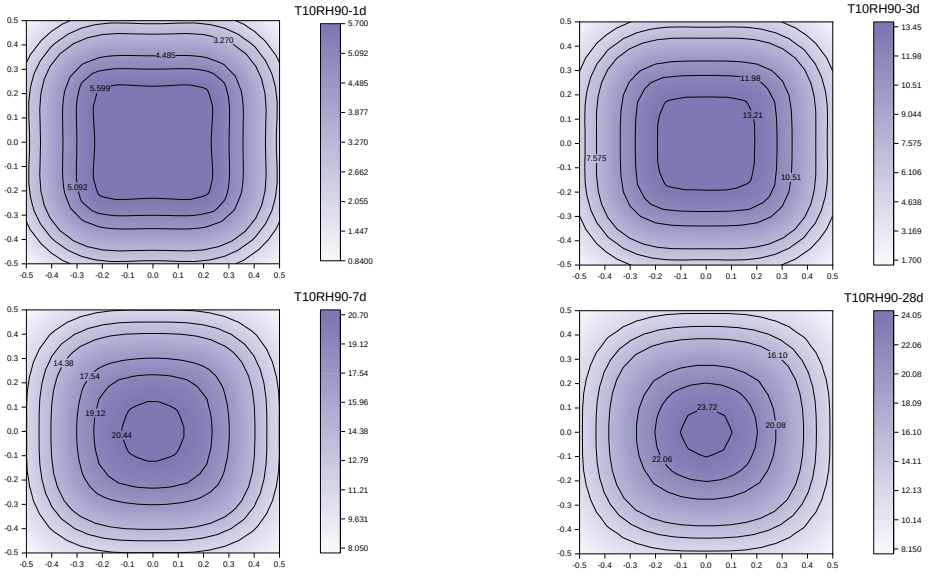


c. Curing at 10ºC-90%RH

Figure 4.15 Strength distribution of 1cm$^3$ specimen curing at 10 ºC

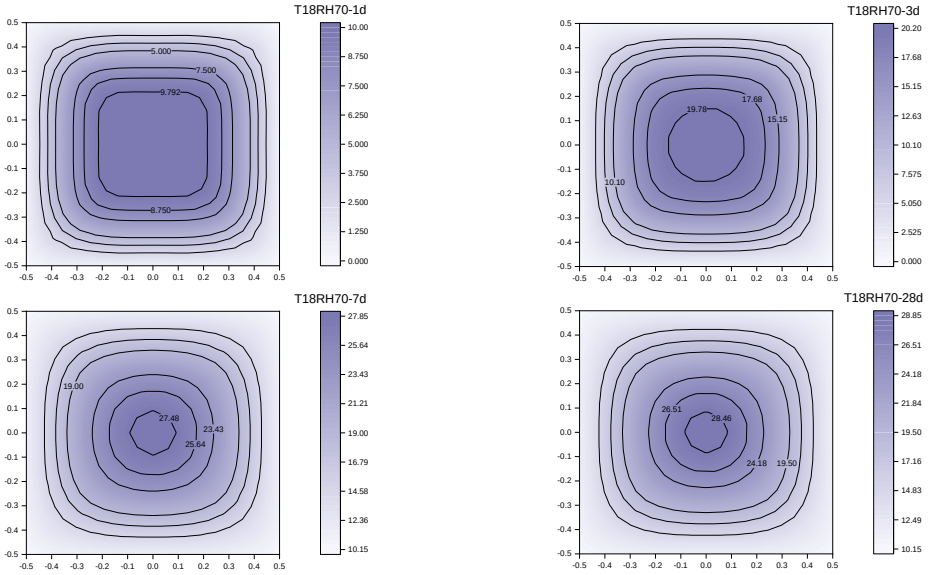


a. Curing at 18ºC-70%RH

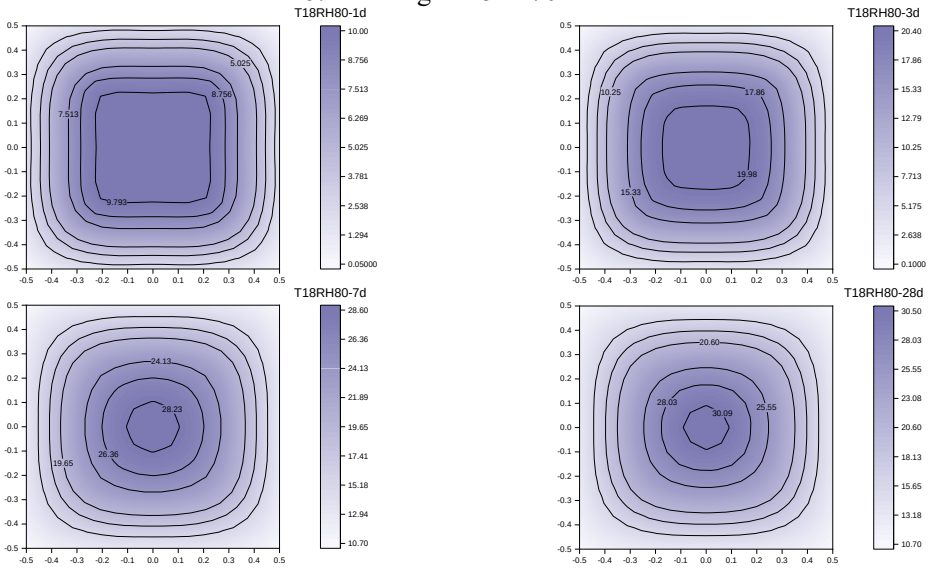


b. Curing at 18ºC-80%RH

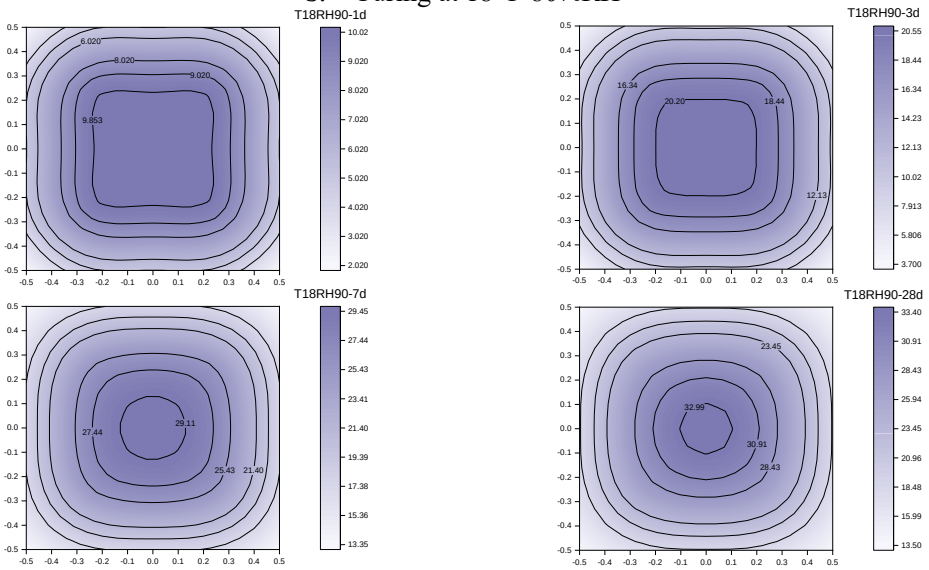


c. Curing at 18ºC-90%RH

Figure 4.16 Strength distribution of 1cm$^3$ specimen curing at 18 ºC

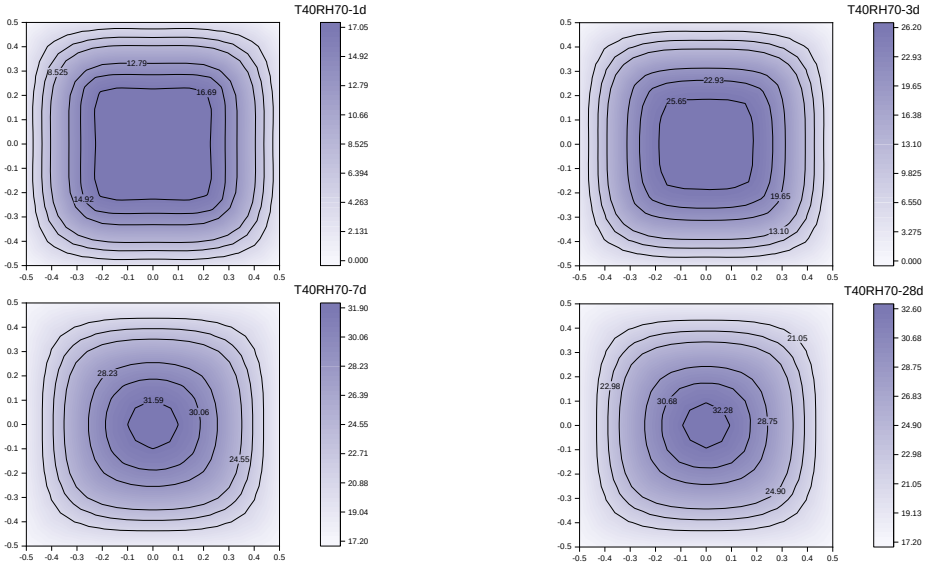


a. Curing at 40ºC-70%RH

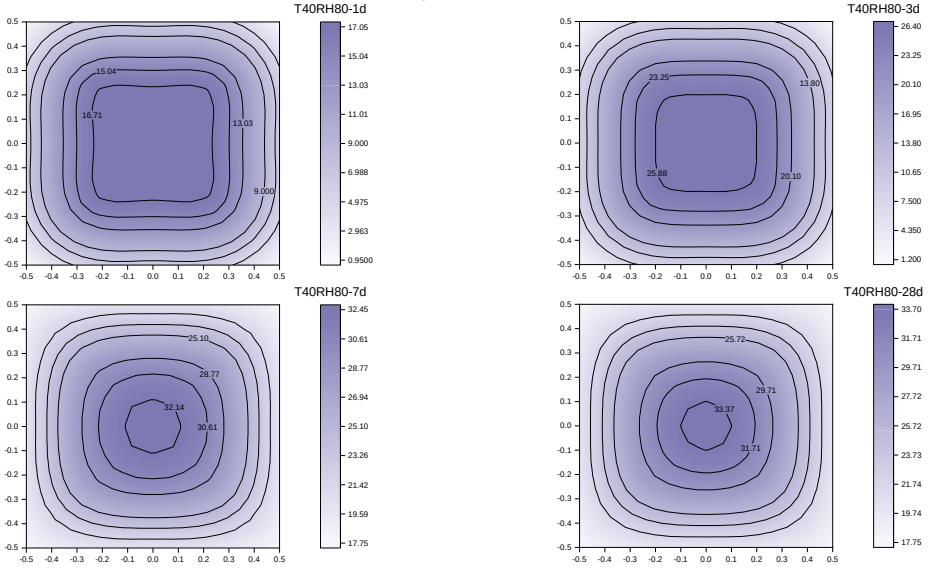


b. Curing at 40ºC-80%RH

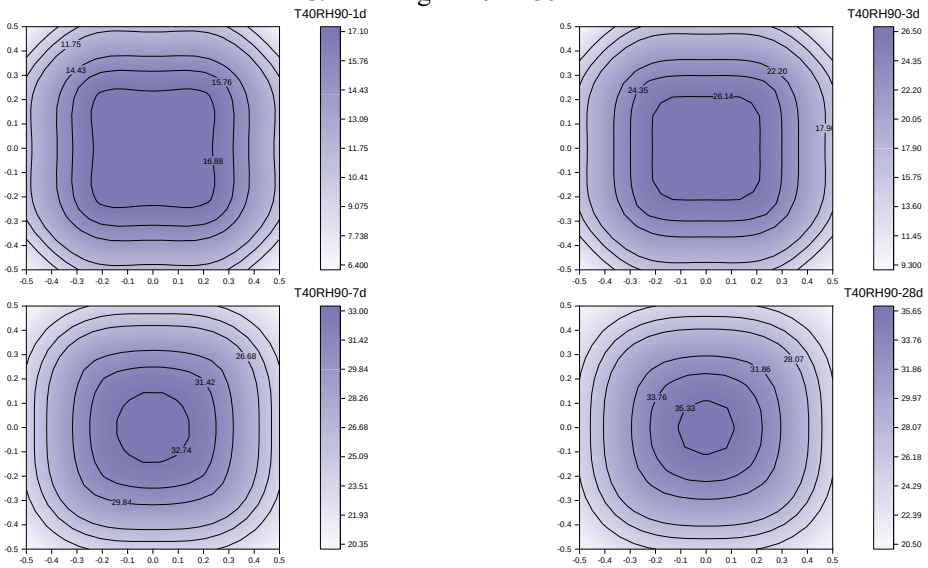


c. Curing at 40ºC-90%RH

Figure 4.17 Strength distribution of 1cm$^3$ specimen curing at 40 ºC

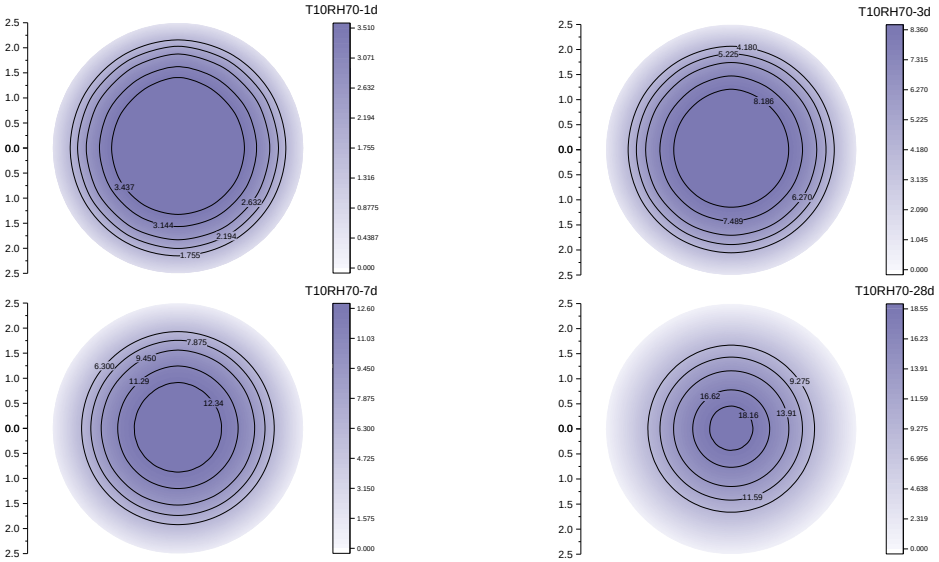


a. Curing at 10ºC-70%RH

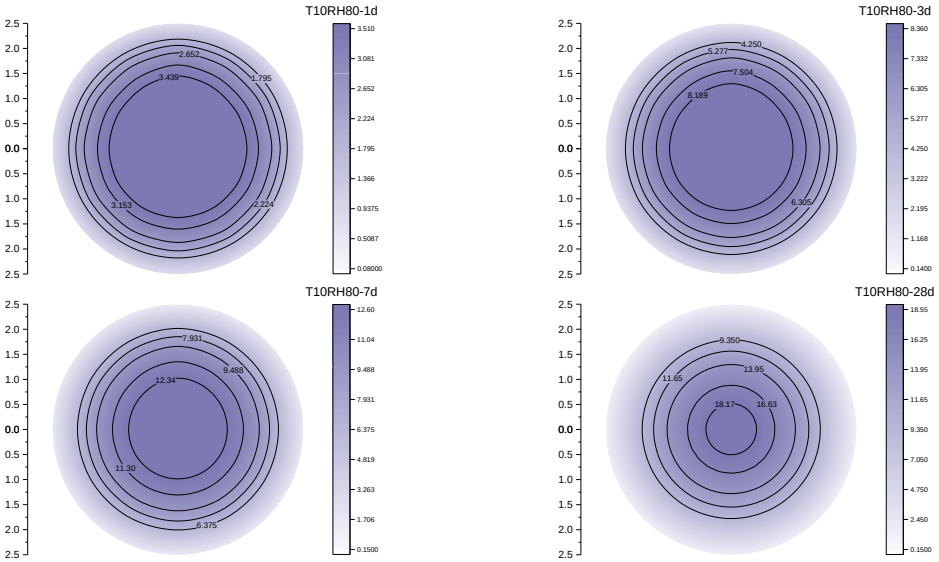


b. Curing at 10ºC-80%RH

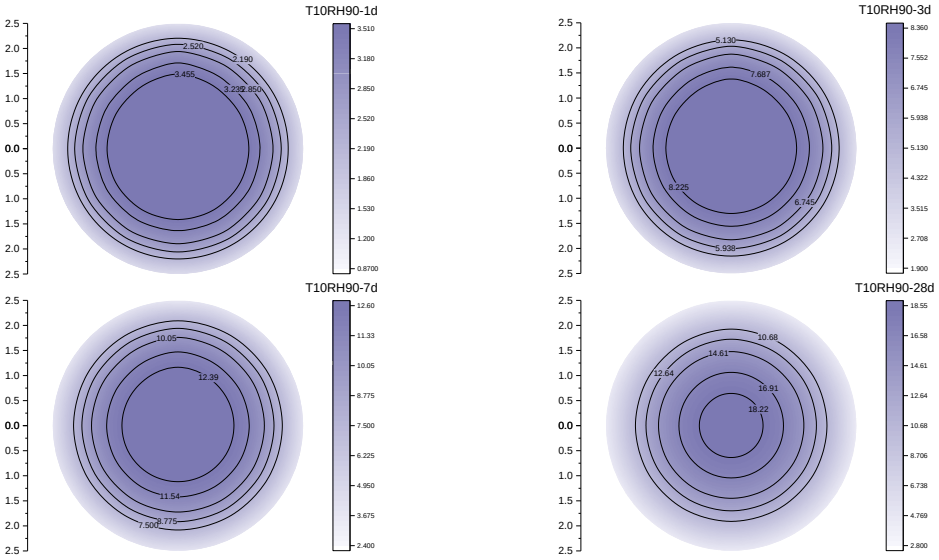


c. Curing at 10ºC-90%RH

Figure 4.18 Strength distribution of Ø5cm specimen curing at 10 ºC

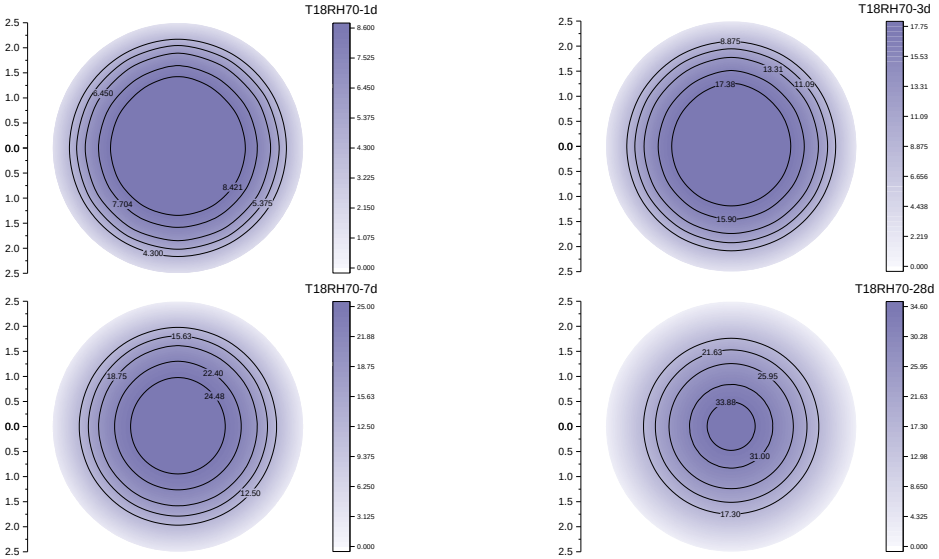


a. Curing at 18ºC-70%RH

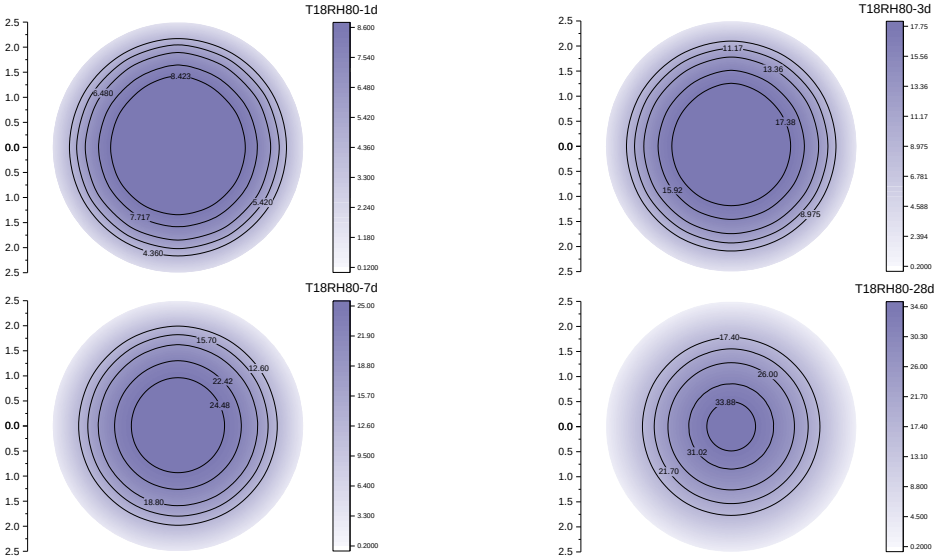


b. Curing at 18ºC-80%RH

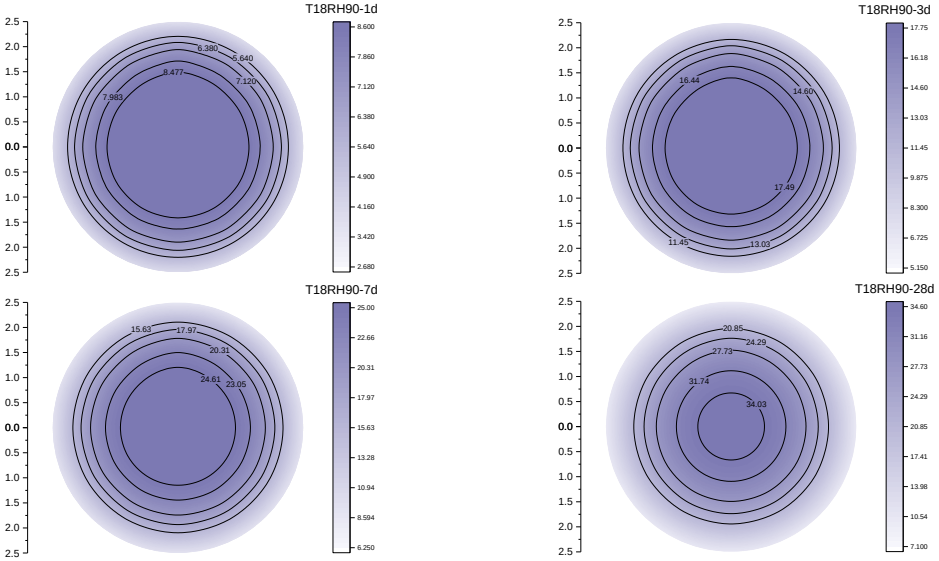


c. Curing at 18ºC-90%RH

Figure 4.19 Strength distribution of Ø5cm specimen curing at 18 ºC

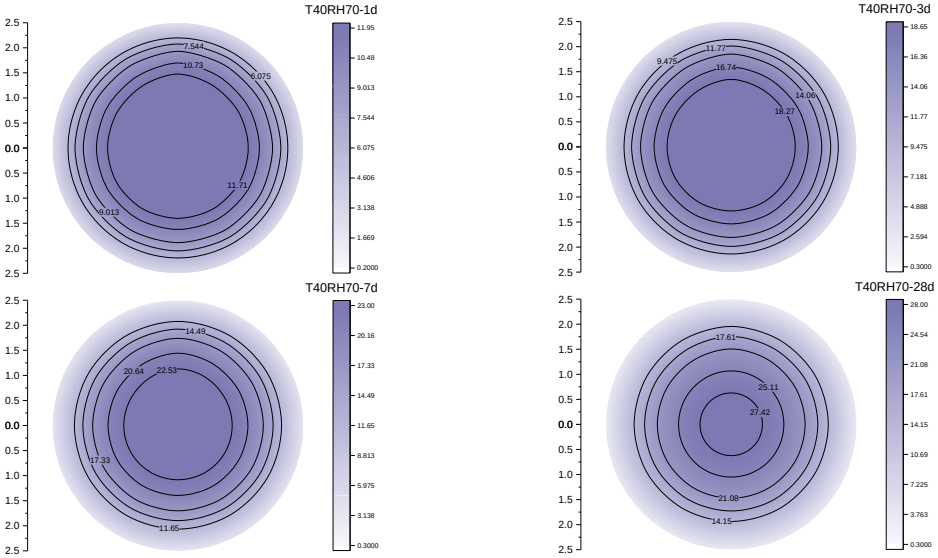


a. Curing at 40ºC-70%RH

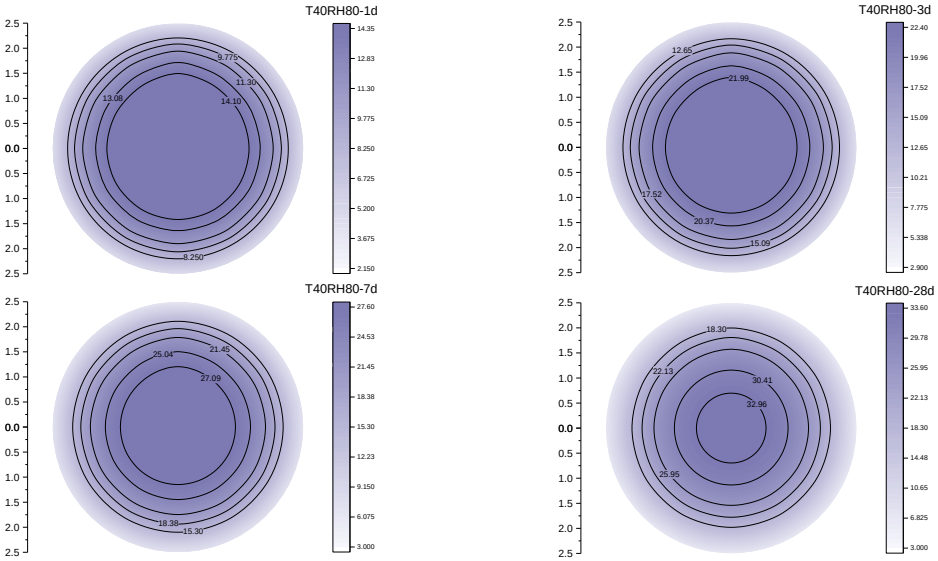


b. Curing at 40ºC-80%RH

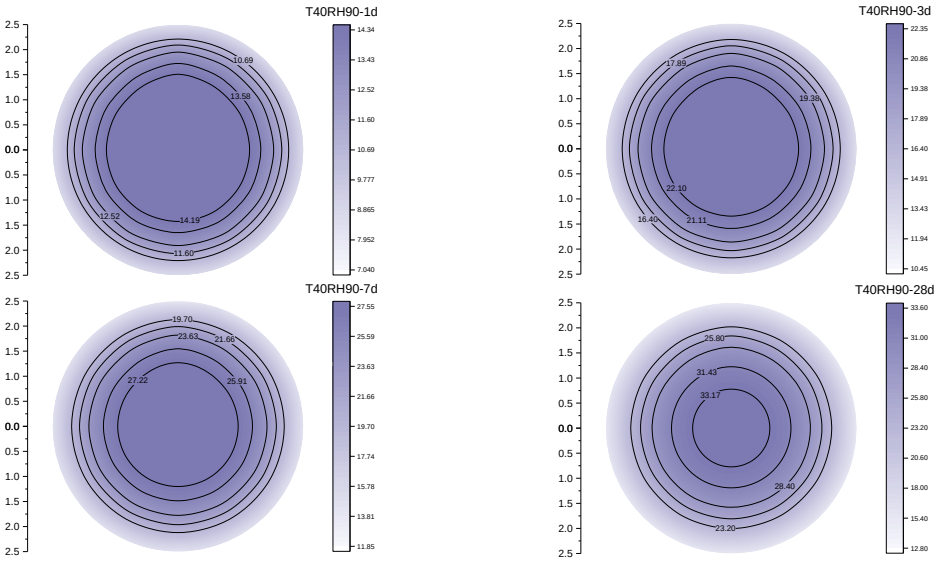


c. Curing at 40ºC-90%RH

Figure 4.20 Strength distribution of Ø5cm specimen curing at 40 ºC

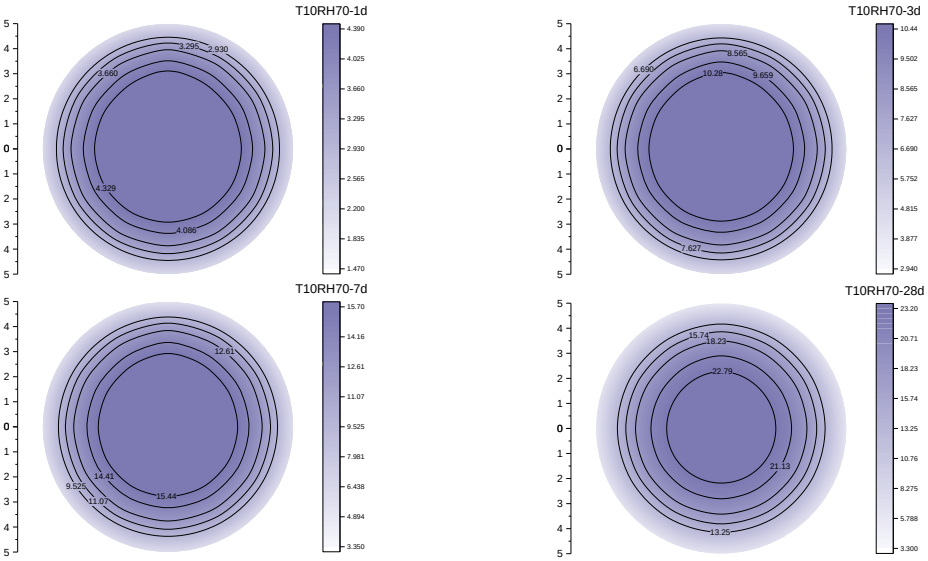


a. Curing at 10ºC-70%RH

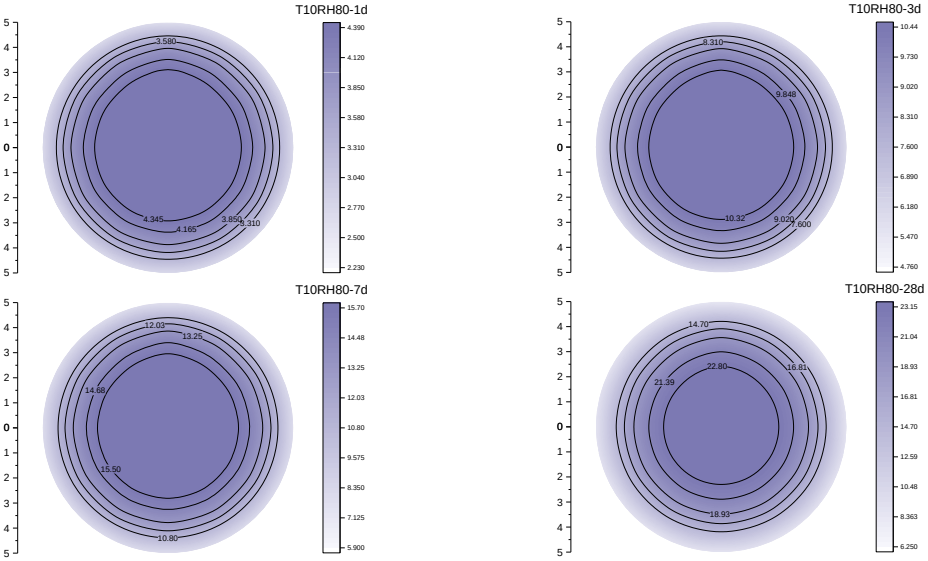


b. Curing at 10ºC-80%RH

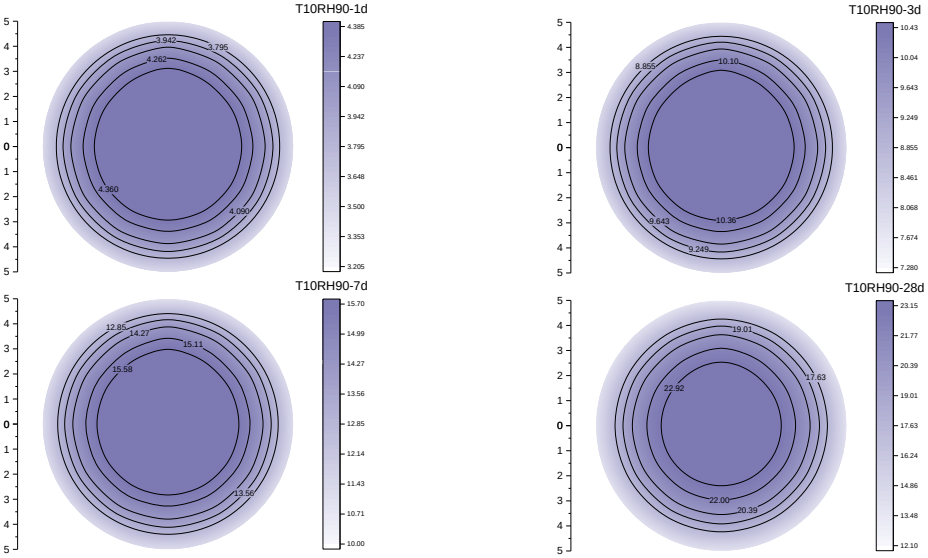


c. Curing at 10ºC-90%RH

Figure 4.21 Strength distribution of Ø10cm specimen curing at 10 ºC

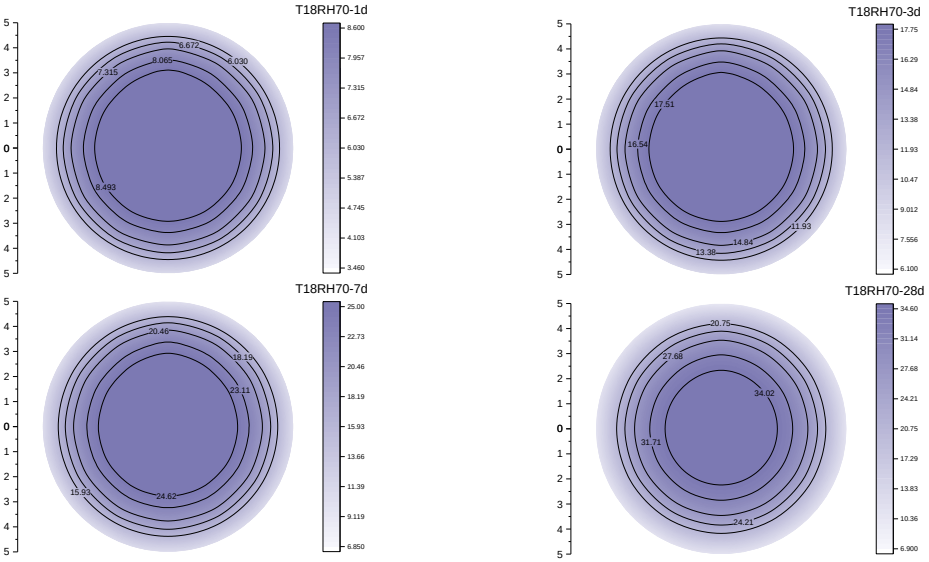


a. Curing at 18ºC-70%RH

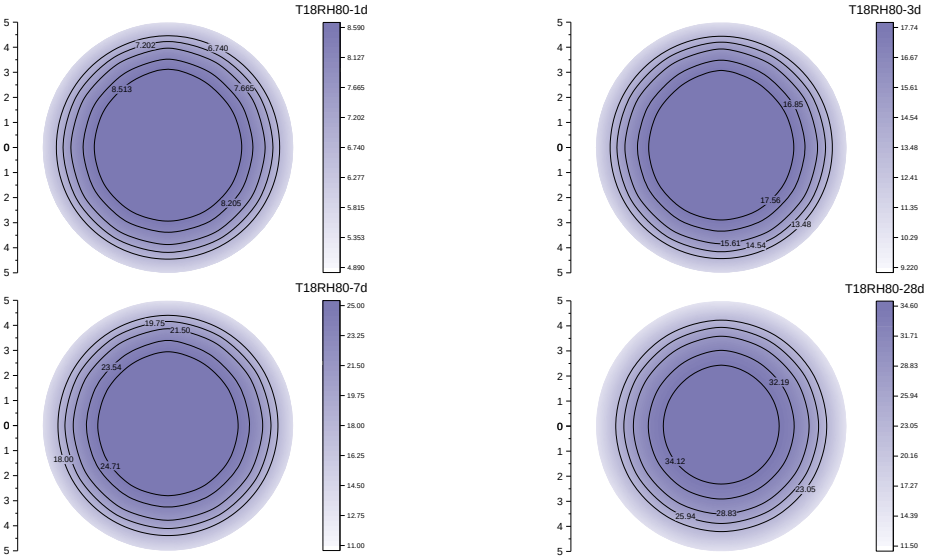


b. Curing at 18ºC-80%RH

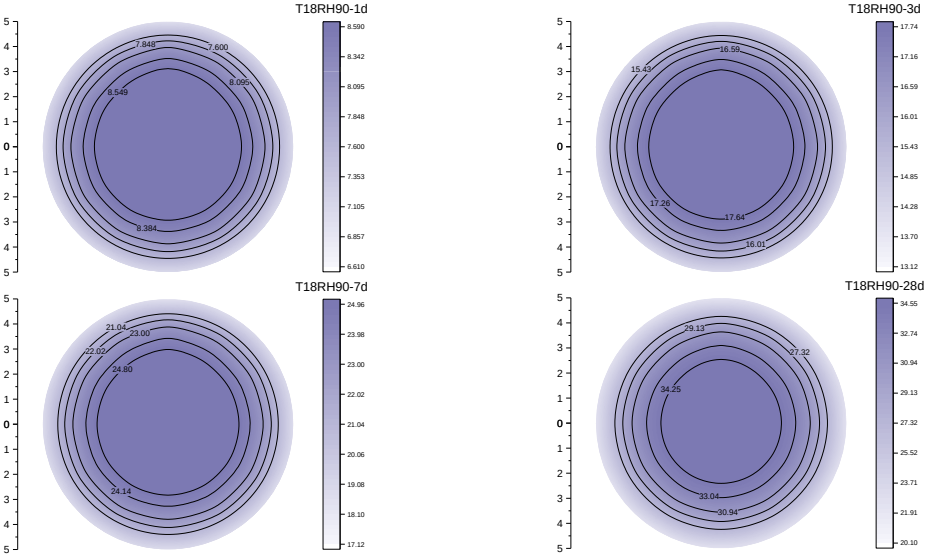


c. Curing at 18ºC-90%RH

Figure 4.22 Strength distribution of Ø10cm specimen curing at 18 ºC

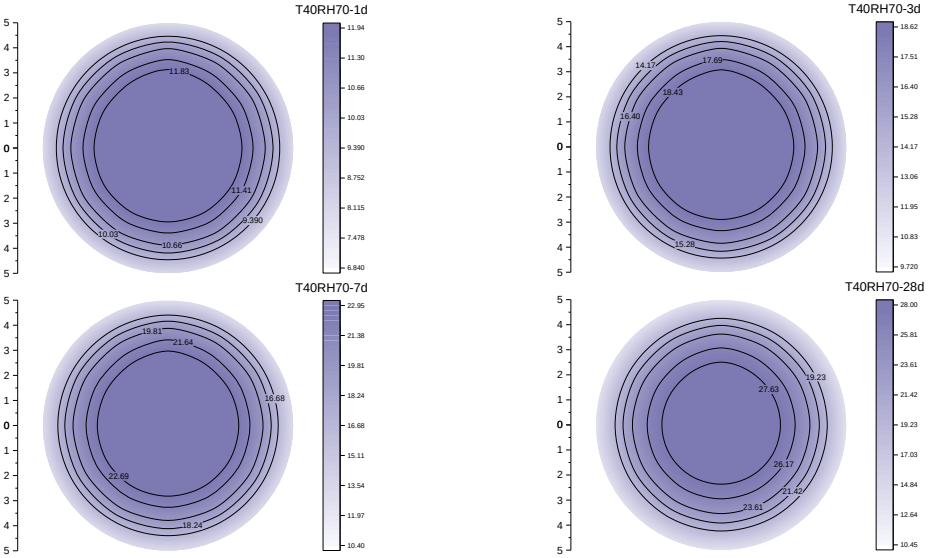


a. Curing at 40ºC-90%RH

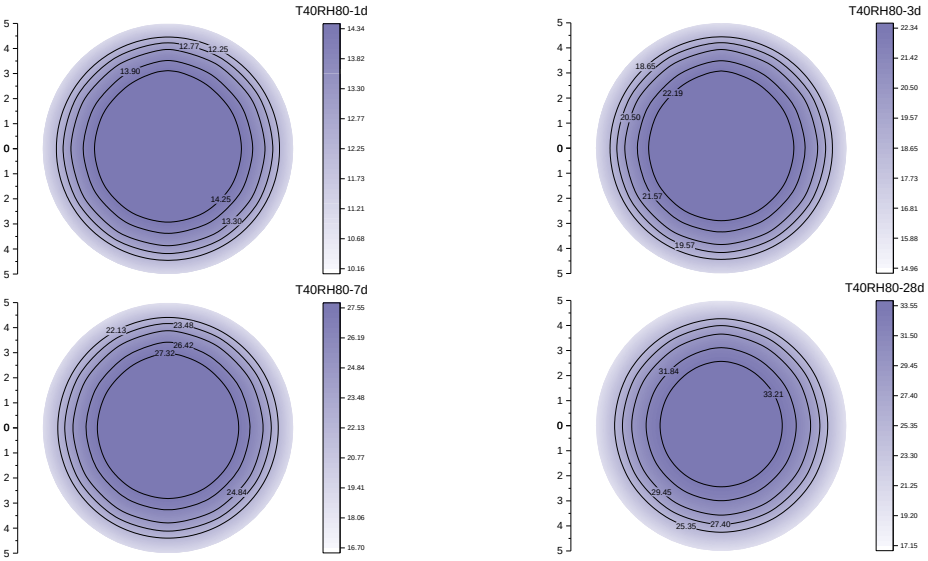


b. Curing at 40ºC-80%RH

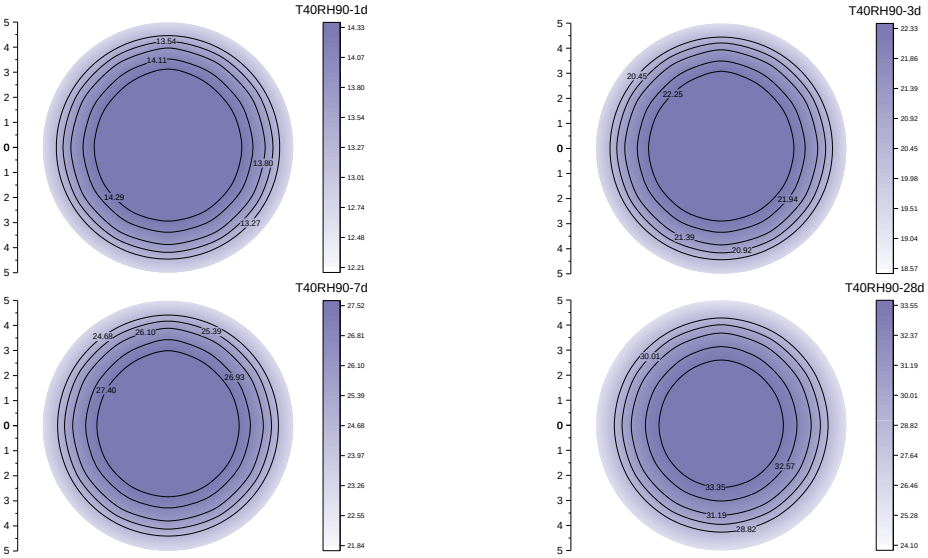


c. Curing at 40ºC-90%RH

Figure 4.23 Strength distribution of Ø10cm specimen curing at 40 ºC

In order to better demonstrate the accuracy of strength prediction, the average calculated strength of different sizes specimens were compared to the tested experimental strength. Fig. 4.24 to Fig. 4.26 respectively compared the strength of experiment and prediction for different curing relative humidity, temperature and specimen size.

In Fig. 4.24, predicted strength versus experimental strength of different curing relative humidity are shown. It is evident that the prediction accuracy under saturated relative humidity(100%RH) is significantly higher than that under unsaturated relative humidity (70%RH, 80%RH, 90%RH). This is because when relative humidity is the reference of 100%RH, the proposed equivalent age function only has one influence factor of temperature, in other words, there is no deviation introduced by relative humidity during calculation of strength prediction model. However, under the curing condition of unsaturated humidity, moisture evaporation causes a decrease of internal relative humidity, which leads to the interference of relative humidity on strength. A relatively close prediction accuracy was found under the three unsaturated humidity.

Fig. 4.25 shows the predicted strength versus experimental strength of different curing temperature. The accuracy of strength prediction at different temperatures is relatively close. However, it can be found that the proposed model slightly underestimates the experimental strength at temperatures of $18^{o}$ C and $40^{o}$ C. As discussed at the end of Section 3 of the determination of the diffusion coefficient, the simple diffusion method utilized in this study that neglected the temperature effect and led to a high relative humidity content at high temperature of the cross-section. Relatedly, the prediction result of equivalent age and strength is expected to be a higher value than tested. In contrast, the estimated strength is slightly lower than tested, see Fig. 4.25b and Fig. 4.25c. This may be caused by the proposed equivalent age function is highly sensitive with relative humidity. Although the critical relative humidity for cement hydration is 80%RH, the reaction rate of cement hydration is still very low when the relative humidity is in the range between 80%RH and 95%RH, see Fig. 3.7a, the rate of cement hydration is almost to 0 when relative humidity is around 95%RH. This also agree with the result of reference[18] that the hydration of cement shows an extremely low value when RH is below 95%RH. Considering the safety aspect, the lower evaluation strength will provide a safer guarantee for the actual project.

As shown in Fig. 4.26, it can be clearly found that the prediction results can well reflect the compressive strength results obtained in the experiment, and the accuracy of prediction is more precise in larger size specimens. This is mainly because the influence of environmental relative

humidity is lower on the bigger size specimen than that on the smaller one. Therefore, a more accurate calculated equivalent age and strength can be obtained in this case. The smallest specimen with a size of $1cm^3$ received a more scattered prediction result than the other two sizes, which may be because the ambient humidity would soon affect and cause the inside relative humidity to decrease, not only at the edge but also at the center of the section. In addition, the shape of the cube specimen is also subject to different humidity diffusion mechanism from that of the cylinder, especially in the four corners. Nevertheless, the ultimate application of this method is to evaluate the internal strength changes of massive slab of actual structures. The most basic 1-D diffusion model can well simulate the changes of internal humidity (like Ø5cm and Ø10cm applied in this research), so the practical application can be satisfied by the present method.

The maximum strength and minimum strength exist in the concrete specimen or structure, and the damage of the concrete is determined by the minimum strength. In other words, when the failure strength reaches its minimum allowable strength, the specimen will be cracked. The evaluation result of this study is the comparison between the average strength of the cross-section and the strength measured by the experiment (minimum strength). Therefore, some deviation may exist, but the coordination of the comparison results indicates that this deviation may be small or not evidence, the prediction results can generally reflect the experimental results.

Nevertheless, the internal microstructure of different specimens is complex and unsystematic, hence the actual relative humidity distribution is uneven. The simulation by diffusion model is only an idealized method to approach the relative humidity variation inside concrete. From an experimental viewpoint, the experimental deviation is also inevitable. All the operations are only theoretically close to the real value.

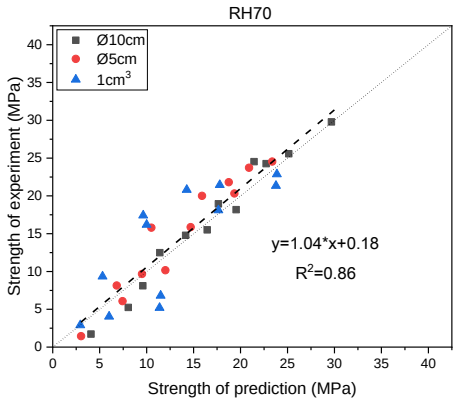


a. Curing at 70% relative humidity

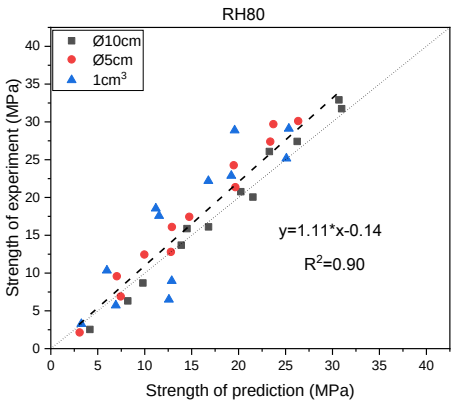


b. Curing at 80% relative humidity

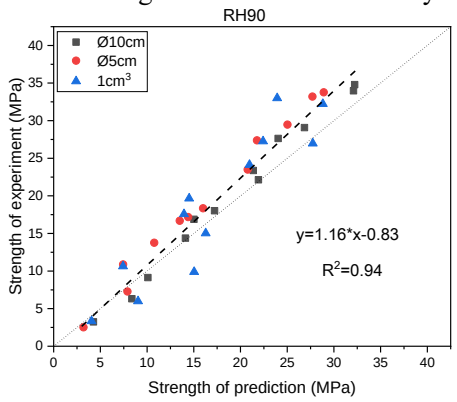


c. Curing at 90% relative humidity

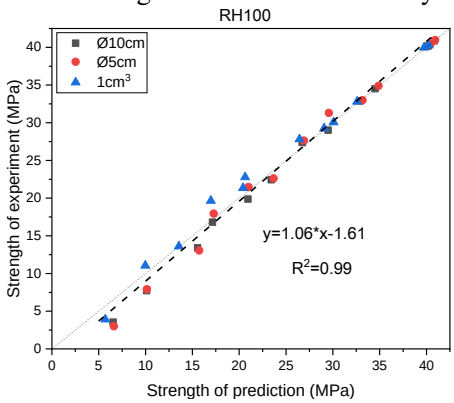


d. Curing at 100% relative humidity

Figure 4.24 Predicted strength versus experimental strength of different relative humidity

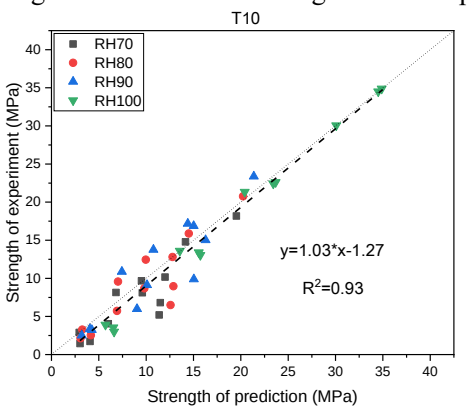


a. Curing at 10°C

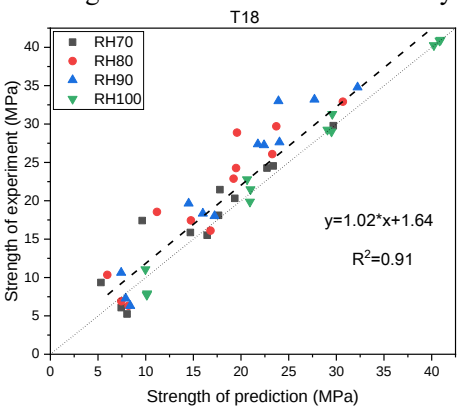


b. Curing at 18°C

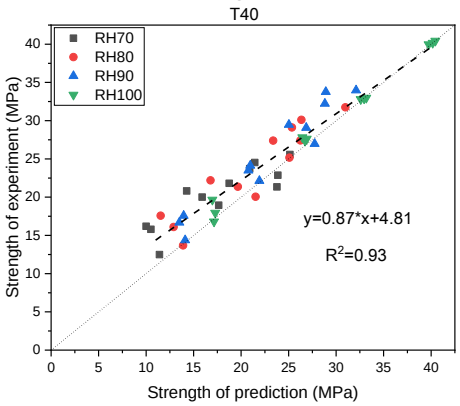


c. Curing at 40°C

Figure 4.25 Predicted strength versus experimental strength of different temperature

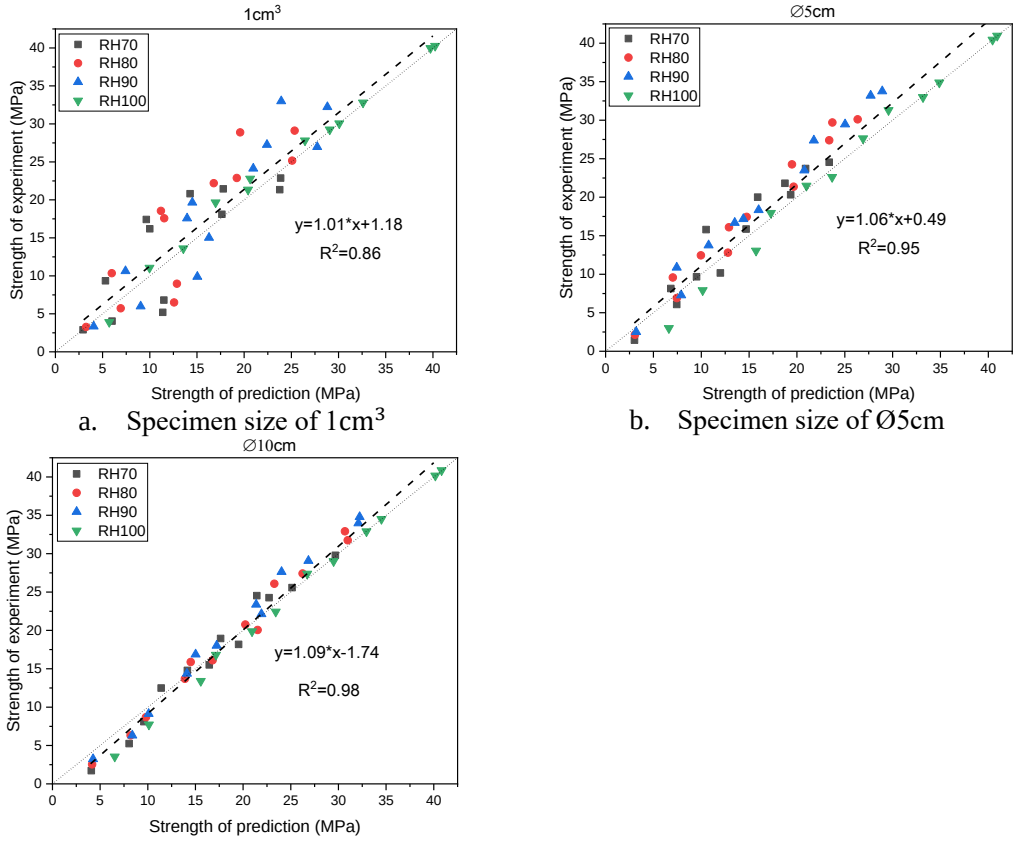


a. Specimen size of $1cm^3$ b. Specimen size of Ø5cm

c. Specimen size of Ø10cm

Figure 4.26 Predicted strength versus experimental strength of different specimen size

### 4.4 Conclusion

The compressive strength of specimens of different sizes was measured under different temperature and relative humidity curing conditions. Moreover, according to the 1-D and 2-D diffusion model, relative humidity distribution on the cross-section of each specimen is simulated. Based on the simulated relative humidity results on the cross-section, the equivalent age and strength of each cross-section are calculated by means of the equivalent age function proposed in Chapter 3 and the strength prediction model of fib model code 2010. Through the predicted and experimental results, the following conclusion can be obtained

1. The compressive strength of cement mortar is not only significantly influenced by temperature but also by relative humidity. A higher early-age strength is obtained when curing temperature is high, while a low relative humidity reduces the compressive strength of the mortars. Such a phenomenon is more evident at the later stage of curing.
2. With the curing time goes on, the humidity distribution of the internal section gradually decreases. Moreover, due to the small size of the specimens of $1cm^3$, the environmental humidity will soon affect the central position of the section. On the contrary, the humidity in

the cross-section of Ø 10cm is less affected by the environment relative humidity and relatively evenly distributed.

3. At a low curing relative humidity of 70%, the gradient distribution of equivalent age caused by curing relative humidity becomes evident from the 3rd day of curing. As the hydration reaction of all the cross-section of specimens under 90%RH will continue, so the equivalent age is significantly higher than that under other conditions. The equivalent age of the central area of Ø5cm and Ø10cm specimens at different curing humidity is equal to it at 100%RH curing.
4. The prediction accuracy under saturated relative humidity(100%RH) is significantly higher than that under unsaturated relative humidity (70%RH, 80%RH, 90%RH). Also, the proposed model slightly underestimates the experimental strength at temperatures of 18°C and 40°C. The prediction strength results can well reflect the compressive strength results obtained in the experiment, and the accuracy of prediction is more evident in larger size specimens.

Reference

[1] fib Model Code for Concrete Structures 2010, Ernst & Sohn, 2013.

[2] T. and T. Ministry of Land, Infrastructure, White Paper on Land, Infrastructure, Transport and Tourism in Japan, Http://Www.Mlit.Go.Jp/. (2009).

[3] Z.P. Bazant, L.J. Najjar, Nonlinear water diffusion in nonsaturated concrete, Mater. Struct. 5 (25) (1972) 3–20.

[4] Yunping Xi, Zdeněk P. Bažant, Hamlin M. Jennings, Moisture diffusion in cementitious materials Adsorption isotherms, Advanced Cement Based Materials, 1(6) (1994) 248-257.

[5] Jin-Keun Kim, Chil-Sung Lee, Moisture diffusion of concrete considering self-desiccation at early ages, Cement and Concrete Research, 29(12) (1999) 1921-1927.

[6] Feng C, Janssen H. Hygric properties of porous building materials (II): Analysis of temperature influence. Build Environ 2016;99:107-18.

[7] Patil PM, Roy S, Momoniat E. Thermal diffusion and diffusion-thermo effects on mixed convection from an exponentially impermeable stretching surface. Int J Heat Mass Tran 2016;100:428-429.

[8] Hasegawa S, Ashigaki Y, Senga M. Thermal diffusion effect of a regenerator with complex channels. App Therm Eng 2016;104:237-42.

[9] Drchalová J, Černý R. Non-steady-state methods for determining the moisture diffusivity of porous materials. Int Commun Heat Mass 1998;25:109–16.

[10] Kočí J, Kočí V, Ďurana K, Maděra J, Černý R. Determination of Moisture-Dependent Moisture Diffusivity Using Smoothed Experimental. AIP Conf Proc 2013;1558:2038-41.

[11] Xiao-Yong Wang, A hydration-based integrated system for blended cement to predict the early-age properties and durability of concrete (Ph.D thesis), Hanyang University, 2010.

[12] Su-Tae Kang, Jeong-Su Kim, Yun Lee, Yon-Dong Park, Jin-Keun Kim, Moisture diffusivity of early age concrete considering temperature and porosity, KSCE J. Civ. Eng. 16 (2012) 179–188.

[13] L. D'Aloia, G. Chanvillard, Determining the “apparent” activation energy of concrete: Ea—numerical simulations of the heat of hydration of cement, Cement and Concrete Research, 32(8) 2002 1277-1289.

[14] H. Kada-Benameur, E. Wirquin, B. Duthoit, Determination of apparent activation energy of concrete by isothermal calorimetry, Cement and Concrete Research, 30(2) (2000) 301-305

[15] Jin Keun Kim, Sang Hun Han, Kwang Myong Lee, Estimation of compressive strength by a new apparent activation energy function, Cement and Concrete Research,
31(2) (2001) 217-225.

[16] JIS A1108, Method of test for compressive strength of concrete, Japan Industrial Standards Committee, (2007) 269-279.

[17] P. Klieger. Effect of mixing and curing temperature on concrete strength. ACI J. Proce., 54, (1958) 1063-1081.

[18] Harmathy, T. Z., “Moisture Sorption of Building Materials,” Technical Paper, No. 242 March 1967, Division of Building Research, National Research Council, Canada, NRC 9492.

# Chapter 5 Strength prediction of different depths of surface layer concrete

### 5.1 Experimental process

Relative humidity inside concrete is measured by using a kind of temperature and humidity sensor produced by Sensirion with the model of SHT75. This capacitive sensor is able to effectively measure the temperature and humidity in the environment and transmit it to the data logger and the connected computer. Its accuracy on relative humidity is within ±1.8%. The waterproofing treatments is needed to be done before setting it into concrete. The plastic pipe with 8mm diameter is used for wrapping the body part of the sensor, and the top of the pipe is covered with a kind of fiber paper that only the water vapor can pass through. The connection between the fiber paper and the pipe is sealed with glue, shows in Fig. 5.1a. Concrete slab is utilized the same proportion with the compressive strength test in the previous chapter, cement mortar with the W/C=0.5. A concrete slab with 10cm depth is applied for the experiment, and only one surface is exposed to the air. Sensors are set at a depth of 0cm(surface), 1cm, 2cm and 4cm from the exposed surface. The schematic diagram of the experiment is illustrated in Fig. 5.1b. The test lasts for at least 500 hours from the starting time of casting. Because of the limitations of the processed sensor and the error of the sensor itself, the rising stage of humidity in the output data is omitted, and the humidity value exceeding 100% is processed as 100%.

Experimental analysis of the relative humidity distribution with time of different depths is conducted by three kinds of artificial curing environment: conventional drying curing, wind blowing curing, and surface heating curing.

- Conventional drying curing, general drying curing room condition with a temperature of 20 °C and relative humidity of 50%.
- Surface heating curing, a heat lamp is set above the exposed surface of mortar.
- Wind blowing curing, exposed surface is blown by an electric fan.

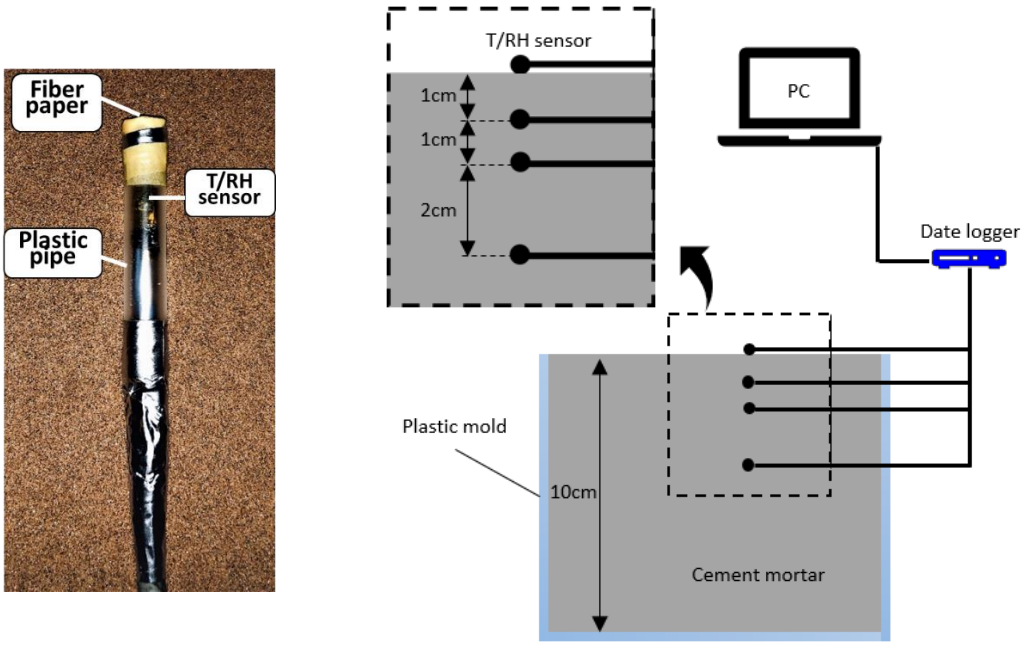


a. Processed sensor b. Experimental schematic diagram

Figure 5.1 Experimental system of RH measurement of surface concrete

## 5.2 Result and discussion

### 5.2.1 Measured temperature/relative humidity development

In order to correspond to the research results in the previous chapters, the experiment on the relative humidity change of surface concrete in this chapter still utilizes the pure cement mortar sample with the same mix proportion with the previous research. The purpose of the three different artificial curing methods is to find the development law of humidity development with time of surface layer concrete under different conditions. Experimental results are shown in Fig. 5.2. During the experimental process of this study, sensors are set before concrete casting, therefore, a rising range of humidity is measured. However, considering that the humidity is reduced from 100% through the theory of humidity development of concrete, so the rising range is omitted. That is to say, the initial values of sensors measured in Fig. 5.2 are the peak values of each sensor. As widely known that the relative humidity of concrete at an initial time is 100%, at this stage, the concrete system is considered as flexible liquid. Moreover, some of the initial value is not 100%, such as 1cm depth of conventional drying curing, 1cm and 2cm of surface heating curing, 2cm and 4cm of wind blowing curing, may be caused by deviation of sensor waterproof treatment. The sensors measured the humidity of the inner space of plastic pipe, and the hysteresis is existed for the reflection of the humidity of the concrete at each depth.

It is easy to find that the surface heat curing and wind blowing curing are effectively influenced the relative humidity development of surface layer of cement mortar. After 500 hours of testing, the surface humidity shows a rather difference of three groups. Which the surface humidity of surface heat curing and wind blowing curing are 25% and 46% at the later stable state, both are lower than the constant humidity of 50% of the curing room. The surface humidity of conventional drying curing at a stable state is about 55%. On another hand, the humidity of treated curing conditions at an initial decrease state shows more sharp than conventional drying curing. Fig. 5.2 a, b and c illustrates the time point of each condition when the surface humidity reaches a relative stable state ($\pm 1\%$ of stable humidity), which are the 99, 49 and 23 hours of conventional drying curing, surface heat curing and wind blowing curing, respectively. Which can be explained that the heating and wind blowing can accelerate the evaporation of the water from the surface. A similar phenomenon also can be found from the result of 1cm and 2cm depth relative humidity. For the further depth of 4cm, the lower influence of the surface condition is suffered, which leads that the closed values of relative humidity are measured of three conditions. As for the temperature, conventional drying curing and wind blowing curing show a similar temperature with a constant temperature of 20 °C of curing room, even though at different depth. Surface heating curing will lead a temperature gradient of depth, average values of 34.0 °C, 31.6 °C, 30.9 °C and 29.7 °C are measured for the depth of 0cm (surface), 1cm, 2cm and 4cm, respectively.

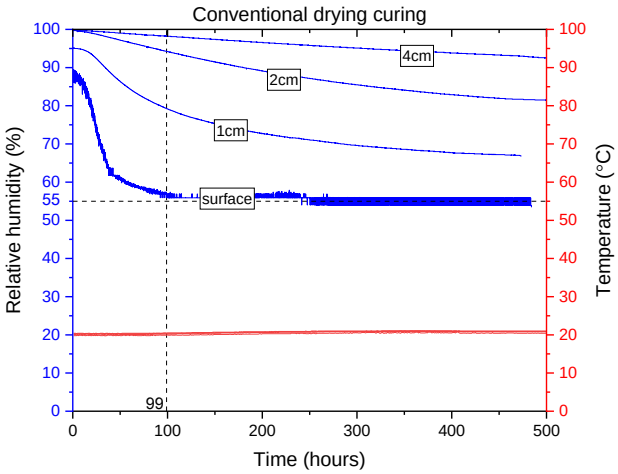


a. Curing condition of conventional drying

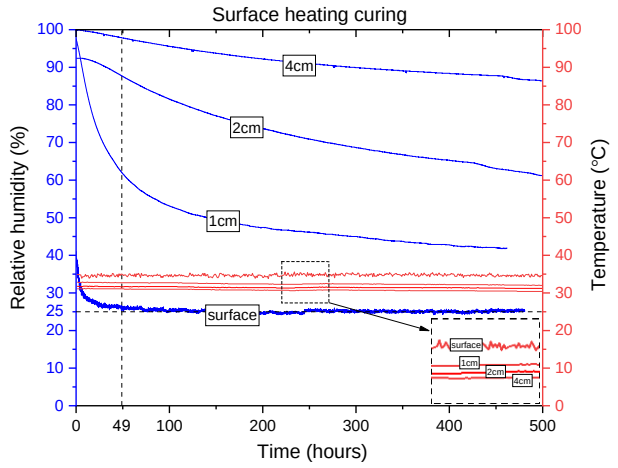


b. Curing condition of surface heating

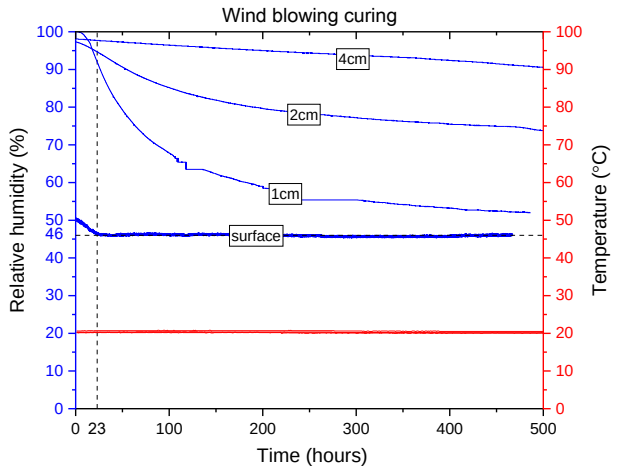


c. Curing condition of wind blowing

Figure 5.2 Measured relative humidity and temperature of three curing condition

### 5.2.2 Relative humidity reduction due to moisture diffusion

The finite difference method provides a very effective solution to the problem of internal humidity diffusion inside concrete. Based on the moisture diffusion Eq. (4.5), the numerical calculation of the moisture diffusion with time of different distances from the surface can be simulated.

However, the difficulty of this study is to determine the diffusion coefficient $D(H)$. Where the expression of $D(H)$ is shown as Eq. (6.3), the only unconfirmed parameter is $D_1$ in Eq. (4.7). $D_1$ is given as the maxim $D(H)$ at relative humidity equal to 100%, however, in this study, in order to explore the law of moisture transfer under different curing conditions, $D_1$ is determined by manual operation which can be called 'prediction-calibration'. Ultimately, values of 0.14*E-4, 0.22*E-4 and 0.2*E-4 were selected to apply to the curing condition of conventional drying, surface heating, and wind blowing, respectively. It is noted that the adopted value of $D_1$ in this study is several orders of magnitude higher than the empirical value of other studies, this may be caused by the experimented sample is used cement mortar and the measured value of relative humidity dropped dramatically at the surface layer also leading a high value of $D_1$. The diffusion coefficient calculated by Eq. (4.7) of each curing condition is figured in Fig. 5.5.

As for the boundary condition, the Dirichlet boundary condition is applied to the three different curing condition, nevertheless, the adopted relative humidity of boundary condition comes from not the ambient humidity in the laboratory, but the measured value of the surface sensors. The humidity values at a stable state of the surface sensors, 55%, 25%, and 46% are taken as the constant boundary humidity of the curing condition of conventional drying, surface heating and wind blowing, respectively. Which can be found whit the horizontal dotted line in Fig. 5.3.

Supposing that the solution domain of space is $0 < \mathrm{x} < \mathrm{L}$ and the solution domain of time is $\mathrm{t} > t_0$, so the initial conditions can be expressed as:

$$H = 100, \quad for\ t = t_0, 0 < x < L$$

$$H = 100, \quad for\ t > t_0, x = L$$

Meanwhile, the number of steps in space with 10, and the number of steps in time with 500 are selected for the simulation. The step length of both time and space are set as 1. Hence, it is easy to understand that the space steps mean the different depth from the exposed surface of concrete and each step presents 1cm distance, and the time steps mean the time from the diffusion starting and each step represents one hour.

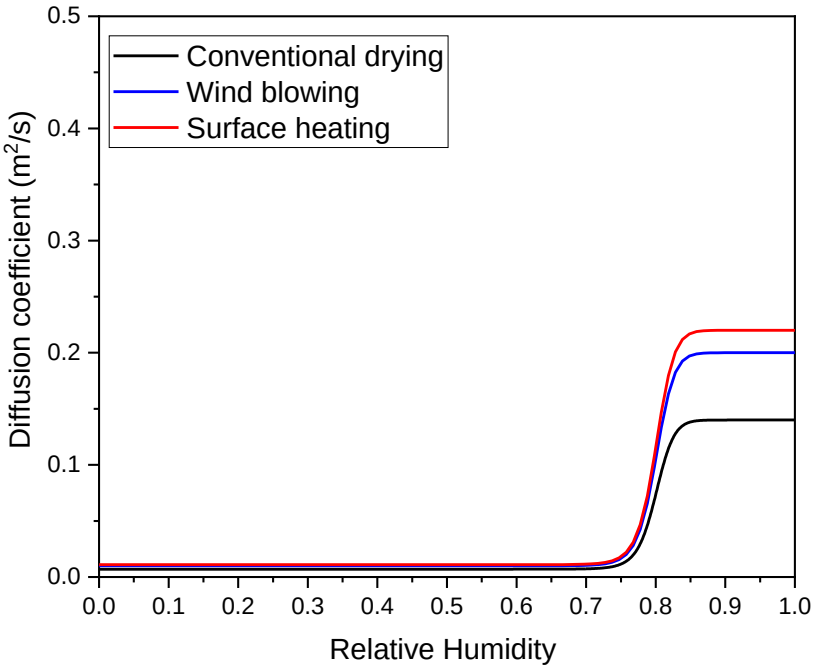


Figure 5.3 Diffusion coefficient of each curing condition (×E-4)

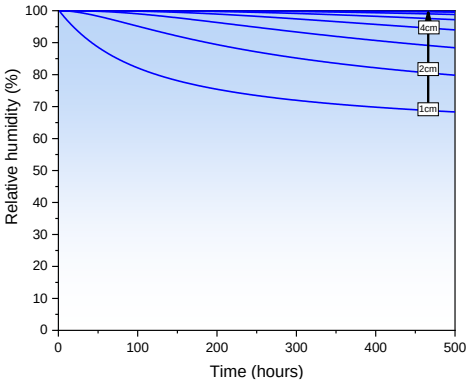


a. Conventional drying curing

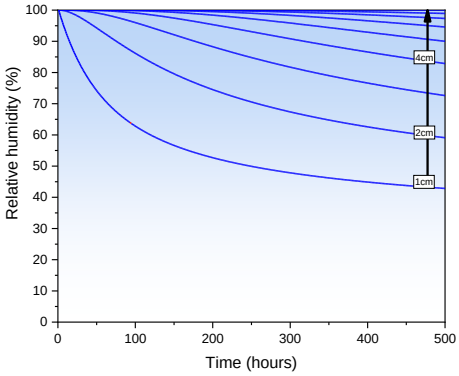


b. Surface heating curing

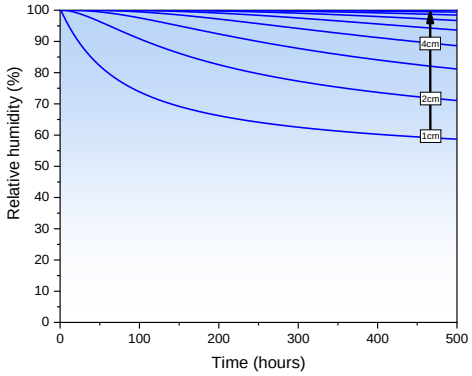


c. Wind blowing curing

Figure 5.4 Simulation result of relative humidity development with time of different depth

### 5.2.3 Comparison between experimental and simulation result

After the relative humidity distribution by moisture diffusion is simulated, the whole relative humidity reduction due to moisture diffusion can be calculated by a comprehensive consideration of both aspects. The comparison results of humidity development between the experimental and simulation of three curing conditions are shown in Fig. 5.5.

The utilized water transformation model can evaluate the water movement of surface concrete with high accuracy. Especially to the conventional drying curing, the relative humidity reduction is rather accurately between the experimental and estimated results, which with a reasonable condition without any influence on the exposed surface. Correspondingly, regarding to the curing condition with the surface treatment, the estimation results of the model can simulate the moisture development of concrete surface to a certain extent, but the accuracy is lower than that of ordinary dry curing. The reason may be the surface evaporation of water vapor and the transfer coefficient of water vapor inside concrete have not been precisely explicit. However, for this study, the development law of relative humidity in concrete is applied to the strength prediction of different positions inside concrete, so a relatively accurate tendency of humidity development is able to satisfy the requirements of the following research. Undeniably, more accurate studies of moisture transfer within concrete are needed in the future.

### 5.2.4 Strength development of each depths

Chapter 4 has figured out the expression of equivalent age and strength prediction model for position inside concrete, which considered both the influence of temperature (*T*) and internal relative humidity (*RH*), the compressive strength development inside concrete can be predicted by Eq. (4.3). Whereas the range of application of relative humidity with Eq. (4.3) is above 80%RH, equivalent age at RH below 80% is considered as 0. $f_{cm28}$ in Eq. (4.3) for the three curing condition is calculated based on the 28-day compressive strength under 18°C and 100%RH through equivalent age function in Eq. (4.9) with $RH$ equals to 100. Which $f_{cm28} = 41.59$ MPa is used for the calculation processes. In the process of calculation, the accumulative method is used to calculate the equivalent age, and the accumulative interval is adopted as 1 hour.

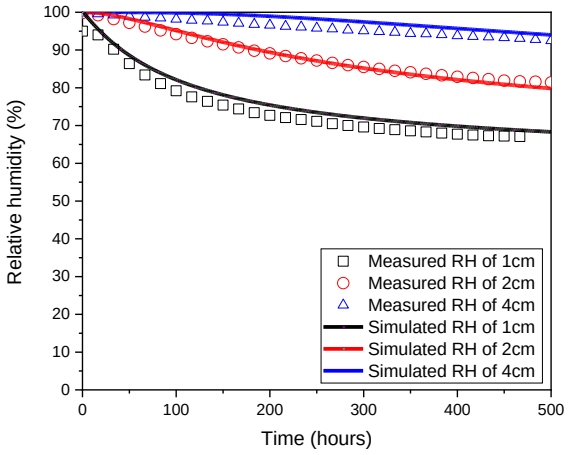


a. Conventional drying curing

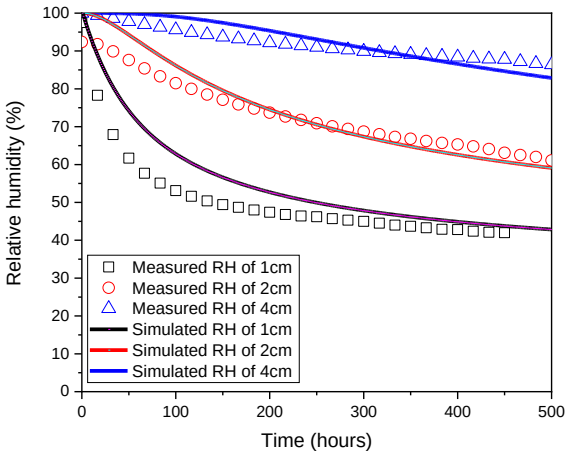


b. Surface heating curing

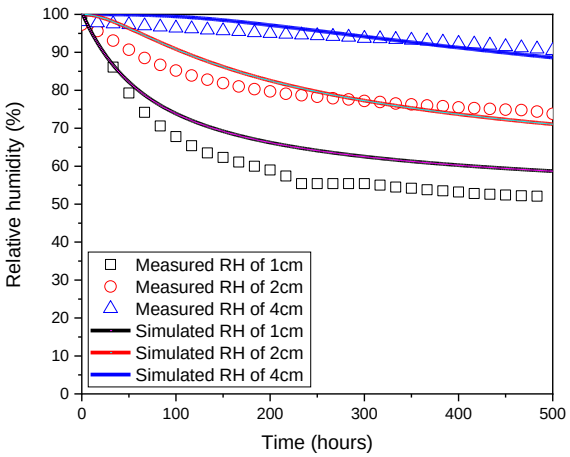


c. Wind flowing curing

Figure 5.5 Comparison between experimental and simulation result

Accordingly, based on the estimation results of humidity at different depths in Fig. 5.5 and Eq. (4.3), it is possible to simulate the development of strength at different depths. In order to better explain the influence of humidity change on hydration rate, a humidity influence coefficient $g_h$ is proposed here, and $g_h$ can be calculated as $g_h = e^{0.8484(RH-100)}$ according to Eq. (3.14). In Fig. 5.6 and Fig. 5.7, the development of humidity influence factors $g_h$, equivalent age and strength with time at depths of 1cm, 2cm and 4cm of each curing conditions' results are proposed.

For the development of relative humidity influence factor $g_h$ with time, the following patterns can be found. In the initial stage of curing, the value of $g_h$ is close to 1, which is due to sufficient internal moisture and the relative humidity is close to 100%. Then, $g_h$ decreased with the curing time going on. The faster the internal humidity decreases, the faster the $g_h$ decreases, t the speed will be the fastest at 1cm and the slowest at 4cm depth. Similar to the changing tendency with relative humidity inside concrete, $g_h$ change of conventional drying curing (Fig. 5.6a) of each depth is not so rapidly than the other two curing condition (Fig. 5.6b and Fig. 5.6c).

In each figure of Fig. 5.6 and Fig. 5.7, relative humidity of 100% is drawn as a reference. It can be found in Fig. 5.6d-5.6f that if there is no influence of relative humidity, the equivalent age shows a linear tendency at a constant curing temperature. The simulated equivalent age development with time of each depth and curing conditions grows with a reasonable tendency. High relative humidity leads to a high equivalent age at same curing condition. Moreover, as the $g_h$ of 1cm decreased most rapidly, the corresponding equivalent age value also grows slowly. Theoretically, the higher the temperature the higher the equivalent age is. For the curing condition of surface heating (Fig. 5.6e), the experimental result shows that the shallower the depth is, the higher the temperature will be. However, by integrating the influence of relative humidity, the result is still that the deeper the depth is, the larger the corresponding equivalent age will be. Even if the temperature is lower than the shallow depth. This indicates not only temperature, but also relative humidity has a significant effect on the equivalent age.

Fig.5.7 shows the simulated strength development with time of three different curding conditions and of the reference relative humidity of 100%. Since the hydration rate take as 0 when humidity drops to 80% due to Eq. (3.14), in the simulation results of strength, there will be some cases when the strength stops growing. As can be seen from Fig. 5.7b, the high curing temperature leads to a high rate of compressive strength development, which in turn leads to higher strength, even if the relative humidity drops rapidly. As for the conventional drying curing and wind flowing

curing in Fig. 5.7a and Fig. 5.7c, the same temperature of 20°C is applied in the simulation process. However, due to the rapid decrease of relative humidity caused by surface wind, the compressive strength at each depth is slightly lower than that of conventional drying curing. In addition, the development of compressive strength of wind blowing curing at the depth of 1cm and 2cm is stopped (when $h \leq 80\%$) during the simulation period (Fig. 5.7c), while only the compressive strength at the depth of 1cm stop developing of conventional drying curing (Fig. 5.7a).

At typical ages of 3days(72hours), 7days(168hours) and 14days(336hours), the results of strength are shown in table 5.1. As can be seen from the table, since the equivalent age of 1cm depth stops growing at a very early age, the strength under each condition also stops at a low strength and does not exceed 2MPa.

The strength at a depth of 2cm under each curing conditions can be found at nearly the same value for each typical age. At the age of 3days, 7days and 14days, the strength of 2cm depth of conventional drying curing can be reached about 67.2%, 49.9% and 41.7% of the reference strength; strength of same depth for surface heating curing and wind blowing curing can reach 48.3%, 37.5%, 32.6% and 49.3%, 35.8%, 29.9% of the reference strength at each curing ages.

At a depth of 4cm, relative high strength can be obtained due to the higher relative humidity content. At the age of 3days, 7days and 14 days, the strength of conventional drying curing can reach 99.5%, 95.7% and 86.4% of the strength of reference condition; the strength of surface heating curing can reach 95.5%, 84.8% and 74.0% of the strength of reference condition; the strength of wind blowing curing can reach 98.2%, 88.4% and 75.5% of the strength of reference condition. The results show that relative humidity has a serious effect on the internal strength of the surface layer of the concrete slab. It also fully reveals the necessity of sealing after concrete pouring during actual construction.

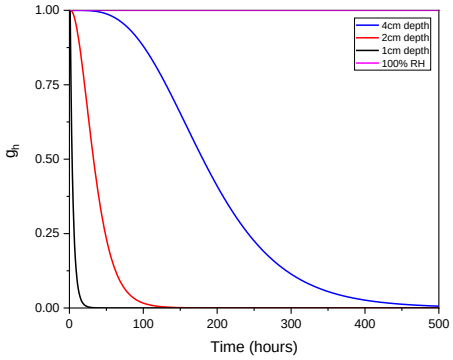


a. $g_h$ of conventional drying curing

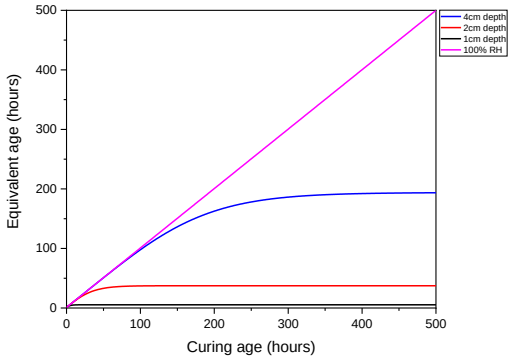


d. Equivalent age of conventional drying curing

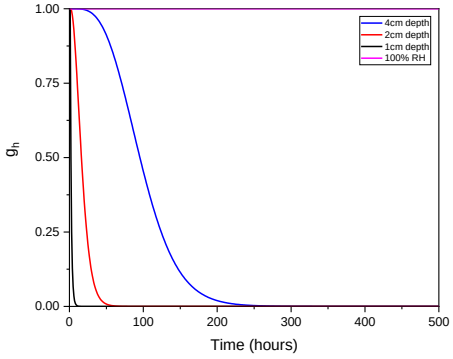


b. $g_h$ of surface heating curing

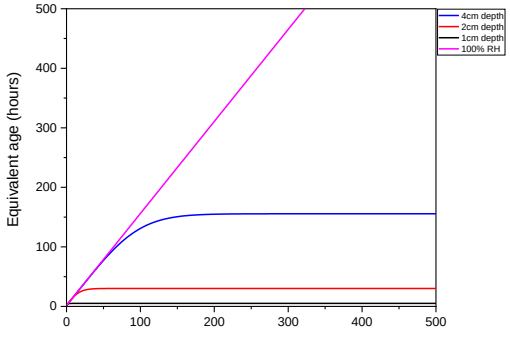


e. Equivalent age of surface heating curing

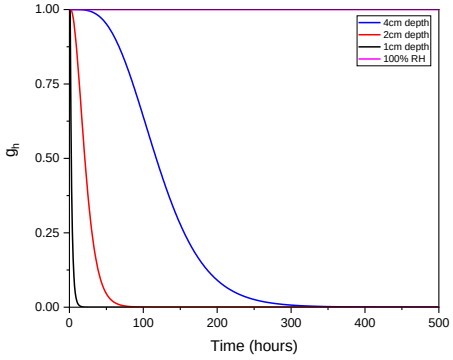


c. $g_h$ of wind flowing curing

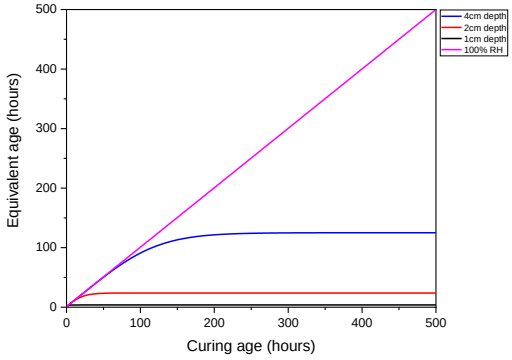


f. Equivalent age of wind flowing curing

Figure 5.6 Simulated $g_h$ and equivalent age development with time

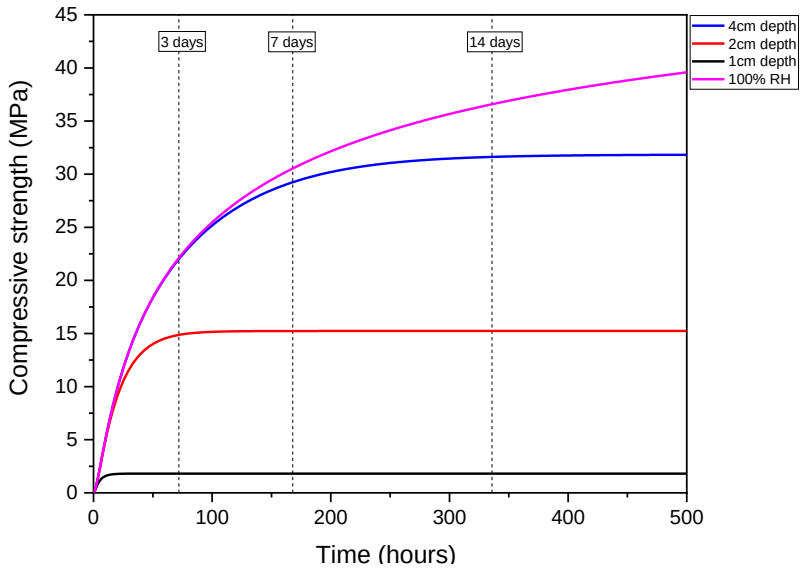


a. Conventional drying curing

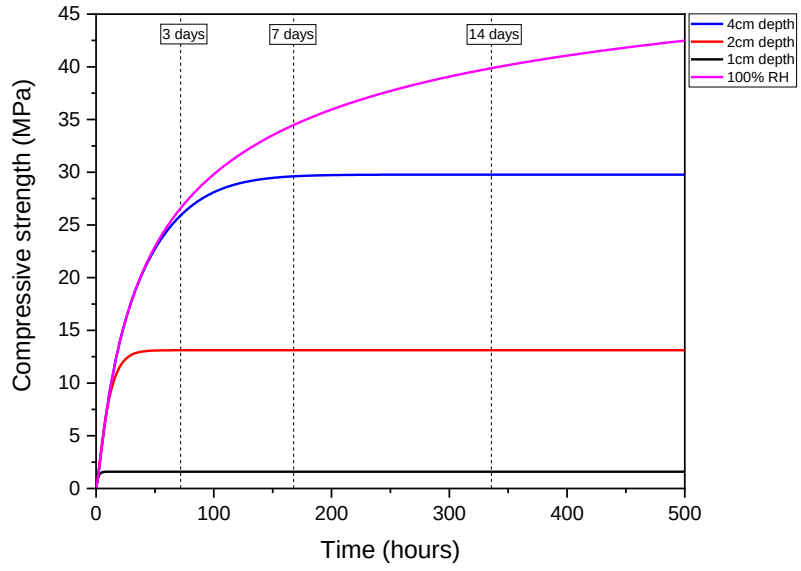


b. Surface heating curing

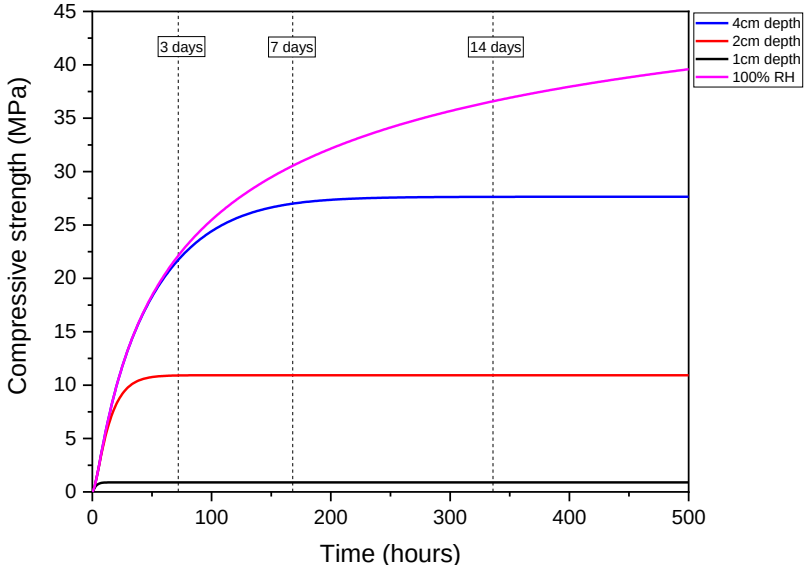


c. Wind flowing curing

Figure 5.7 Simulated strength development with time

Table 5.1 Strength of each depth at typical ages (MPa)

| | Conventional drying curing | | | | Surface heating curing | | | | Wind flowing curing | | | |
|---|---|---|---|---|---|---|---|---|---|---|---|---|
| | 100% RH | 4cm depth | 2cm depth | 1cm depth | 100% RH | 4cm depth | 2cm depth | 1cm depth | 100% RH | 4cm depth | 2cm depth | 1cm depth |
| 3 days (72hours) | 22.12 | 22.02 | 14.87 | 1.81 | 27.14 | 25.92 | 13.11 | 1.60 | 22.12 | 21.72 | 10.91 | 0.90 |
| 7days (168hours) | 30.54 | 29.24 | 15.23 | 1.81 | 34.93 | 29.61 | 13.11 | 1.60 | 30.54 | 27.00 | 10.93 | 0.90 |
| 14days (336hours) | 36.59 | 31.63 | 15.24 | 1.81 | 40.24 | 29.77 | 13.11 | 1.60 | 36.59 | 27.63 | 10.93 | 0.90 |

## 5.3 Verification of the proposed strength model of outdoor curing

The proposed strength prediction model with considering of relative humidity in the previous chapters is mainly based on the laboratory results. That is to say, the obtained model is performed at a controlled curing condition with temperature and relative humidity. In order to better implement the proposed strength prediction model into the actual construction project. An outdoor experiment with variable temperature and relative humidity is necessary.

### 5.3.1 Experimental process

The outdoor experiment is divided into two parts: temperature and relative humidity measurement and compressive strength test.

Temperature and relative humidity measurements are carried out on the ∅5×10cm specimen without demolding to make sure only one surface is exposed to the air. The measured depths are 1cm, 2cm and 4cm from the exposed surface. Also, ambient temperature and relative humidity are measured. Three different treatments of the ∅5×10cm specimen are applied to test the compressive strength --- specimens with and without demolding curing in the air and specimens with demolding curing in the water. All experiments are conducted outdoors, and curing area are treated to avoid the effects of rainfall on the surface of the specimen. Compressive strength is tested at the age of 1, 3, 7, 28 days. Fig. 5.8 shows the diagram of the experiment.

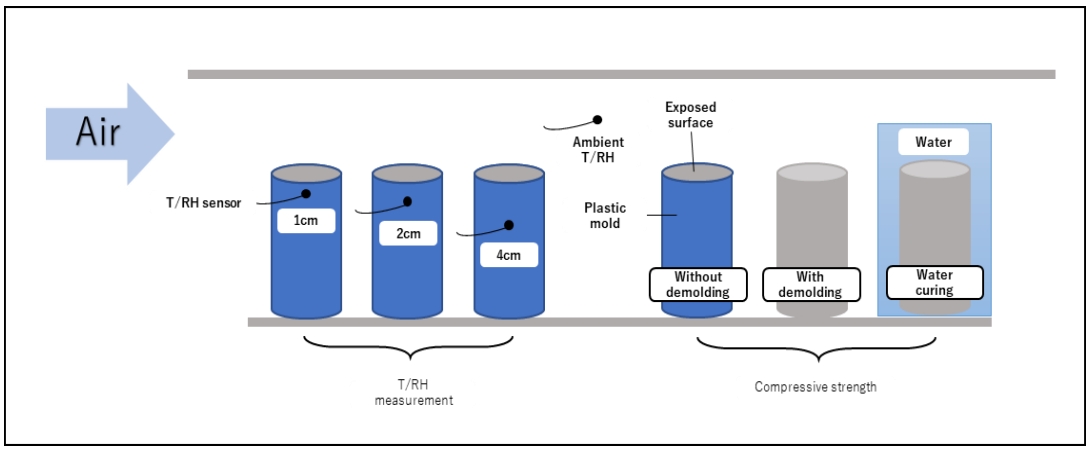


Figure 5.8 Diagram of the experiment of outdoor curing

### 5.3.2 Compressive strength

The compressive strength of three different kinds of outdoor curing condition is shown as Fig. 5.9, the scale on the X-axis is converted to hours. Tested results of compressive strength show a reasonable development tendency. Specimen with demolding shows the lowest strength, and the specimen of water curing shows the highest. The reason can be explained through the influence of humidity onto compressive which has already illustrated in Chapter 2. It is noted that the 28-day (672-hour) compressive strength of with and without demolding air curing is closed, and that of water curing is slightly higher.

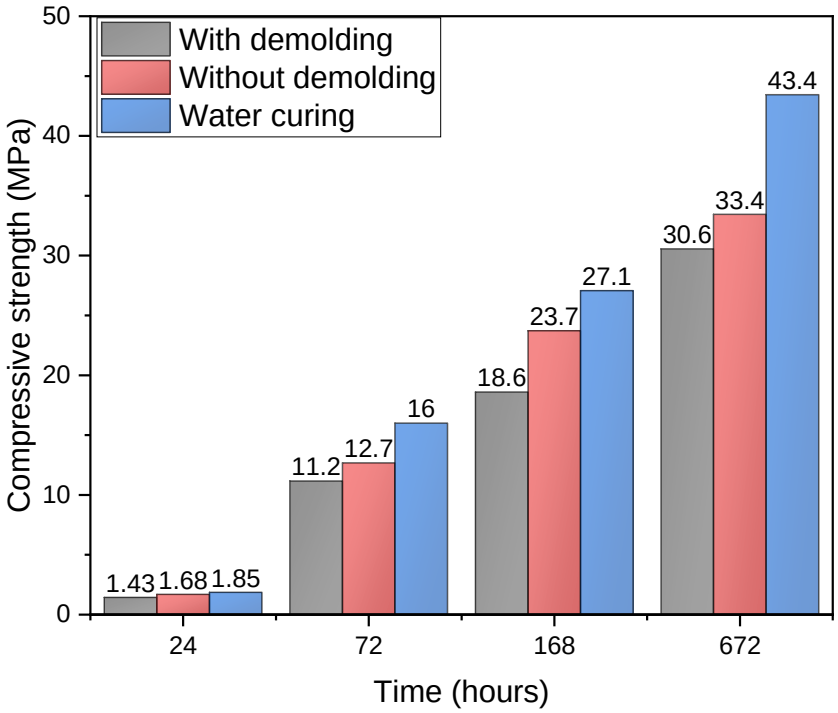


Figure 5.9 Tested compressive strength of outdoor curing

### 5.3.3 Strength of specimen without demolding and each depth

The recorded temperature and relative humidity history of each depth of specimens is shown as Fig. 5.10. The temperature history of each depths show almost the same value during the whole recording period. The relative humidity of each depths at early ages (less than 100 hours) shows an increased tendency and irregular values because of the waterproof treatment of the sensor and the sensitivity of the sensor itself. It is easy to know that there is no rising stage for the internal humidity of the new mixed cement mortar. Therefore, in the calculation process, the humidity in this rising stage is taken as the highest value of humidity of each depth to reduce the generation of errors. The humidity development trend becomes reasonable after 100 hours. The strength development of each depth is carried out by using the same applied model with Eq. (4.3) and the recorded temperature/relative humidity data in Fig. 5.10. The compressive strength of each depth and the tested compressive strength of water curing are given in Fig. 5.11. With the development of curing age, the strength of each depths grows with different trend due to the changing temperature and relative humidity.

It is clearly seen in Fig. 5.11 that even though the moisture value at the depth of 4cm is close to 100%RH, the strength evaluation results obtained by the model are still significantly lower than the strength of water-curing specimens. This indicates that the proposed humidity correction model is highly sensitive to relative humidity, and as long as the relative humidity is less than 100%, the corresponding equivalent age (or strength) will quickly decrease below the standard value. The same reason also leads to low strength values at 1cm and 2cm depths. The strength values of 1cm, 2cm and 4cm depth on the 28th day were 1.85MPa, 6.66MPa and 32.49MPa, respectively, which were 4.2%, 15.3% and 74.9% of the experimental strength of water curing at the 28 days. the strength development of exposed curing specimens shows a strength level similar to 4cm depth inside concrete.

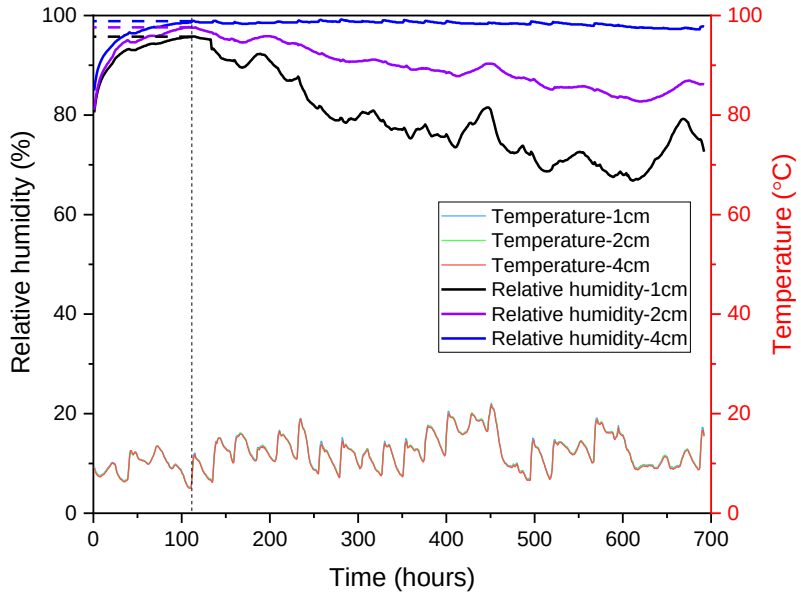


Figure 5.10 Temperature and relative humidity history of each depth

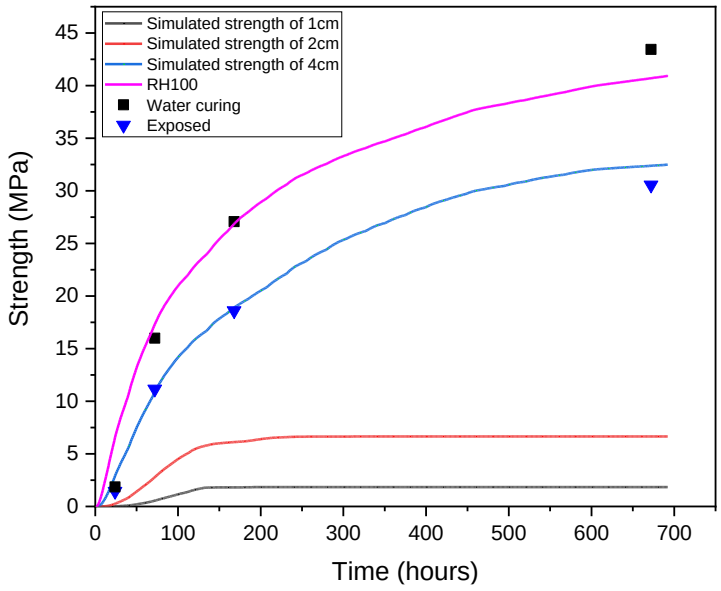


Figure 5.11 Comparison of predicted and tested strength of each depth

This research is a sub-project of 'smart sensor formwork system', provides an effective method to calculate the equivalent age at different temperatures and humidity, as well as the development of strength. The 'smart sensor formwork system' is a system in which the quality control of curing concrete is estimated and visualized using embedded various types of sensor onto formwork, and collecting T/RH history of the concrete surface via wireless network and estimating the strength development from concrete surface, see Fig. 5.12. The proposed proposal is highly sensitive to relative humidity and able to evaluate the equivalent age and strength development of concrete surface according varying temperature and relative humidity. In practical engineering, the development of temperature and relative humidity of concrete surface is obtained through smart sensor formwork system, and the development of temperature and relative humidity of surface layer concrete can be inferred and the strength development of surface concrete can be obtained based on the proposal in this study. Since the development of intensity is evaluated directly from the sensor data without measurement of specimen, the work efficiency is greatly improved. Both influence of temperature and relative humidity are taken into account to improve the accuracy of strength evaluation and the safety of construction are more ensured.

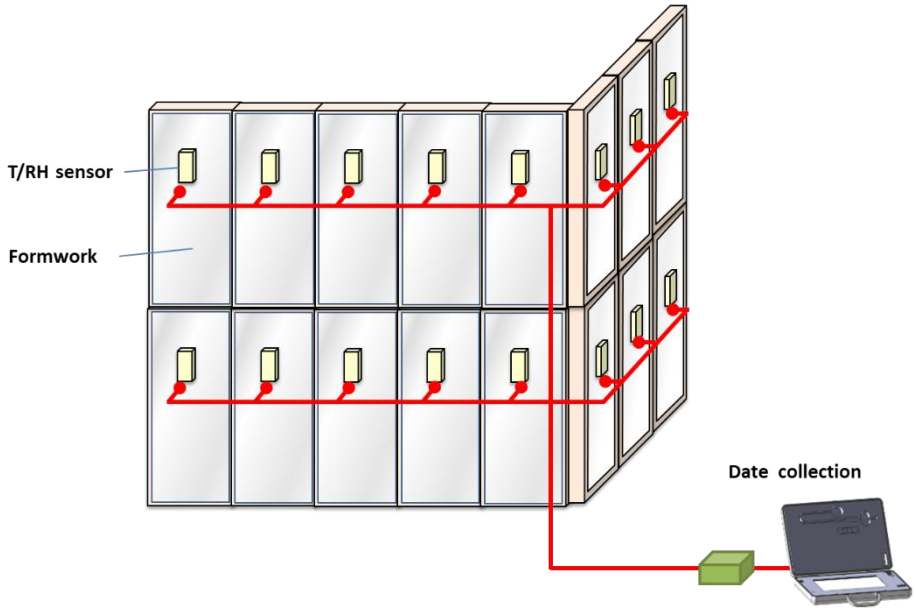


Figure 5.12 Schematic diagram of intelligent sensor formwork system

## 5.4 Conclusion

This chapter mainly focuses on the estimation of relative humidity development of surface layer of concrete. The finite difference method (FDM) introduced in Chapter 4 is used to solve the partial differential equation of moisture diffusion theory. The humidity change of different depths of the surface concrete was also measured by the temperature/humidity sensor to verify the simulation result. According to the relative humidity simulation results at different depths under three curing conditions, the relative humidity influence factors $g_h$ and compressive strength at different depths are simulated with the development of time. Based on the simulation and experiment results, the following conclusions can be summarized.

(1) The experiment is conducted by inserting the temperature/humidity sensors into different depth of the surface layer of concrete. Different curing treatments show different law of humidity development, both surface heating, and wind blowing can accelerate the loss of water in concrete, which is more evident in the near-surface layer of concrete.

(2) By comparing the simulated relative humidity reduction regarding moisture diffusion to the experimental results, it can be clearly found that the simulation of the model can accurately reflect the relative humidity development of surface layer of concrete.

(3) In the initial stage of curing, the value of $g_h$ is close to 1. The faster the internal humidity decreases, the faster the $g_h$ decreases and the decreasing speed will be the fastest at 1cm and the slowest at 4cm depth.

(4) The simulated equivalent age development with time of each depth and curing conditions grows with a reasonable tendency. High relative humidity leads to a high equivalent age at same curing condition. Not only temperature but also relative humidity has a significant effect on the equivalent age.

(5) Under three simulated conditions maintained in the laboratory, strength at a depth of 1cm would soon cease to grow and would be less than 10% of 100%RH strength. The strength at a depth of 2cm under each curing conditions can be found at nearly the same level for each typical age. But even so, due to sufficient water in the early ages, 2cm can still reach a tolerable strength value. At depth of 4cm, relative high strength can reach a considerable high level than that of the other two depths due to the sufficient relative humidity content during the whole curing period.

(6) For the outdooring curing specimens, even though the moisture value at the depth of 4cm is

close to 100%RH, the strength evaluation results obtained by the model are still significantly lower than the strength of water-curing specimens. And relatively low strength values s can be found at 1cm and 2cm depth. The strength values of 1cm, 2cm and 4cm depth on the 28th day were 1.85MPa, 6.66MPa and 32.49MPa, respectively, which were 4.2%, 15.3% and 74.9% of the experimental strength of water curing at the 28 days.

# Chapter 6 Conclusion

## 6.1 Conclusion

The initial maintenance of fresh concrete is of great significance to the quality of the constructions. The curing quality of initial concrete directly affects the strength and durability of concrete from surface to interior. To understand the curing of concrete, it is necessary to understand the hydration process of cement and its influence. The hydration process of cement is generally considered dependent on the main components of cement clinker, temperature and time. In the actual construction process, in order to ensure the continuity of the construction process of the building, when the hydration reaction is processing in the early curing stage, the demolding treatment is conducted. Water evaporates from the surface of the concrete, causing a difference in water pressure from the surface to the inside, and thus causing the moisture diffusion from the inside to the outside. This directly results from the outside of the cement hydration is not comprehensive, and lead to the strength and durability of low. For reinforced concrete structures, the poor quality of the concrete cover can lead to more carbon dioxide, salt and corrosion of the steel. Therefore, the early quality management of concrete surface layer plays a crucial role in the durability of concrete strength.

For the prediction models of concrete related to time-effect, the equivalent age function proposed in this thesis considering the influence of temperature and relative humidity also can be applicable, so as to get more accurate evaluation results.

This thesis based on the purpose of strength prediction of surface layer concrete, firstly proposed an equivalent age function that influenced by both temperature and relative humidity which could estimate the strength development at different curing temperatures and relative humidity conditions in chapter 3. Nevertheless, some drawbacks have been found of this proposed model, such as the proposed relative humidity modified function is obtained based on a constant condition of curing relative humidity, the applicability of such function in a changing environment needs more discussed. In addition, the application of the range of humidity also needs to be further discussed in the future. On the other hand, the propose of the thesis is for predicting the strength change in surface layer concrete, the humidity condition inside concrete is also different from the environment.

In order to well and reasonable estimate the strength development of surface layer concrete, a new humidity influence factor is proposed in chapter 4 based on the hydration rate of cement powder. This factor is proposed by referring the cement hydration rate and empirical function of other

researchers' and proposed by considering the safety of application to practical construction. After verification, the proposed model can thoroughly evaluate the strength growth of different humidity conditions. Such relative humidity modified model is also verified to the concrete slab based on the simulation result of humidity distribution with time. The internal strength of concrete in the outdoor environment was also predicted.

The detailed results of each chapter are included as follows.

Chapter 1 explains the background, purpose, and innovation of the research. And the overall structure of the doctoral thesis is also summarized.

**C**hapter 2 mainly aimed at the research content of the research of the thesis and summarized the previous research results which concern with. The aspects of the influence of relative humidity on hydration and strength, maturity method, strength prediction model and internal moisture transfer of concrete are mainly reviewed.

Chapter 3 based on the hydration degree of cement powder at different temperature and relative humidity, the hydration rate was calculated. Then the relationship between hydration degree and hydration rate can be illustrated. A hydration model was applied to obtain the rate constant at different relative humidity and temperature by regression analysis with the experiment result. Taking 20°C-100%RH as the standard condition, the change of rate constant under different temperature and humidity can be expressed by an exponential function, then the equivalent age equation under the action of temperature and humidity can be obtained. The hydration reaction of cement powder is evident under the curing condition of more than 80%RH by the experimental results. The hydration model can basically describe the nonlinear relationship between hydration degree and hydration rate under different temperature and relative humidity. The proposed exponential function can well fit the value of rate constant under different temperature and relative humidity, and then the modified equivalent age function can be proposed based on it.

In chapter 4, the compressive strength of specimens of different sizes was measured under different temperature and relative humidity curing conditions. Moreover, according to the 1-D and 2-D diffusion model, relative humidity distribution on the cross-section of each specimen is simulated. Based on the simulated relative humidity results on the cross-section, the equivalent age and strength of each cross-section are calculated by means of the equivalent age function proposed in Chapter 3 and the strength prediction model of fib model code 2010. The compressive strength of cement mortar is not only significantly influenced by temperature but also by relative humidity.

A higher early-age strength is obtained when curing temperature is high, while a low relative humidity reduces the compressive strength of the mortars. Such a phenomenon is more evident at the later stage of curing. With the curing time goes on, the humidity distribution of the internal section gradually decreases. Moreover, due to the small size of the specimens of $1\,cm^3$, the environmental humidity will soon affect the central position of the section. On the contrary, the humidity in the cross-section of Ø 10cm is less affected by the environment relative humidity and relatively evenly distributed. At a low curing relative humidity of 70%, the gradient distribution of equivalent age caused by curing relative humidity becomes evident from the 3rd day of curing. As the hydration reaction of all the cross-section of specimens under 90%RH will continue, so the equivalent age is significantly higher than that under other conditions. The equivalent age of the central area of Ø5cm and Ø10cm specimens at different curing humidity is basically equal to it at 100%RH curing.

The prediction accuracy under saturated relative humidity(100%RH) is significantly higher than that under unsaturated relative humidity (70%RH, 80%RH, 90%RH). Moreover, the proposed model slightly underestimates the experimental strength at temperatures of 18°C and 40°C. The prediction strength results can well reflect the compressive strength results obtained in the experiment, and the accuracy of prediction is more evident in larger size specimens.

Chapter 5 mainly focus on the estimation of relative humidity development of surface layer of concrete. The finite difference method (FDM) introduced in Chapter 4 is used to solve the partial differential equation of moisture diffusion theory. The humidity change of different depths of the surface concrete was also measured by the temperature/humidity sensor to verify the simulation result. According to the relative humidity simulation results at different depths under three curing conditions, the relative humidity influence factors $g_h$ and compressive strength at different depths are simulated with the development of time. The experiment is conducted by inserting the temperature/humidity sensors into different depth of the surface layer of concrete. Different curing treatments show different law of humidity development, both surface heating, and wind blowing can accelerate the loss of water in concrete. Which is more evident in the near-surface layer of concrete. By comparing the simulated relative humidity reduction regarding moisture diffusion to the experimental results, it can be clearly found that the simulation of the model can accurately reflect the relative humidity development of the surface layer of concrete. In the initial stage of curing, the value of $g_h$ is close to 1. The faster the internal humidity decreases, the faster the $g_h$

decreases, and the decreasing speed will be the fastest at 1cm and the slowest at 4cm depth. The simulated equivalent age development with time of each depth and curing conditions grows with a reasonable tendency. High relative humidity leads to a high equivalent age at same curing condition. Not only temperature but also relative humidity has a significant effect on the equivalent age. Under three simulated conditions maintained in the laboratory, strength at a depth of 1cm would soon cease to grow and would be less than 10% of 100%RH strength. The strength at a depth of 2cm under each curing conditions can be found at nearly the same level for each typical age. But even so, due to sufficient water in the early ages, 2cm can still reach a tolerable strength value. At depth of 4cm, relative high strength can reach a considerable high level than that of the other two depths due to the sufficient relative humidity content during the whole curing period. For the outdooring curing specimens, even though the moisture value at the depth of 4cm is close to 100%RH, the strength evaluation results obtained by the model are still significantly lower than the strength of water-curing specimens. And relatively low strength values s can be found at 1cm and 2cm depth. The strength values of 1cm, 2cm and 4cm depth on the 28th day were 1.85MPa, 6.66MPa and 32.49MPa, respectively, which were 4.2%, 15.3% and 74.9% of the experimental strength of water curing at the 28 days.

**6.2 Furfure research**

Although this thesis presented a method to predict the development of internal strength, the result is carried out by the internal temperature and humidity changes obtained through the sensors pre-embedded inside concrete. For the purposes of engineering, this is obviously time and effort consuming. Therefore, it would be the right research direction to deduce the internal temperature and humidity development by placing the sensor on the concrete surface. And sensors placed on the surface can be reused so that both economic efficiency and work efficiency will be greatly improved.

In addition, the influence of humidity on concrete strength in this study was carried out under the condition of specified water-binder ratio mortar under the specified environmental relative humidity, and whether the influence of environmental humidity on strength can replace the influence of real humidity inside concrete on strength remains to be verified. In addition, this experiment is conducted based on the experimental results of cement mortar. The results of strength development and humidity change are different from the results of concrete in practical construction. Therefore, in order to make the results closer to the practical construction, the same research on concrete needs

to be done. In the case of low water-cement ratio, the change of internal humidity caused by self-desiccation of cement hydration should be considered.

**Acknowledgments**

I would like to thank my supervisor Prof. Noguchi for his guide to my doctoral thesis. During every discussion with him, he would explain the research contents to me in detail in the form of charts with his excellent and professional knowledge. This easy to understand way dramatically speeds up our communication efficiency. He is also an easy-going person that supported my work all the time and never put any pressure on me. It is lucky I can research under the guidance of Prof. Noguchi. In the final revision stage of the Ph.D. thesis, Prof. Noguchi's revision advice much helped me to complete the revision smoothly, which made me respect and thank him more deeply.

Thanks to Prof. Maruyama who gave me a lot of meaningful suggestions on my thesis, I also learned a lot of thinking ways on how to do high-quality research. Also truehearted thanks to Assoc. Prof. Kitagaki with his enthusiastic help in learning and experiment.

I am also grateful to the members of my committee, Ass. Prof. Tomoyose, Mr. Yamamoto, Mr. Egashira, and Mr. Nishijima, for their patience and support in assisting with the laborious experiments I have been done through my research. Also sincerely thanks to Ass. Prof. Cai at Fukuoka University, who helped me so much on the paper revising and gave me a lot of concern in life and study.

I would like to thank my fellow doctoral students for their feedback, cooperation, and of course friendship. Many thanks to Chen, Wang, Cheng, Nakada, Sawa and so on, for there help with my experiment.

Last but not the least, I would like to thank my family and my wife for supporting me spiritually throughout writing this thesis and my life in general.